UNIVERSIDAD AUTÓNOMA DE MADRID

Departamento de Bioquímica

Characterization and regulation of K_v1.5-K_vβ1.3 complex.

ÁLVARO MACÍAS MARTÍNEZ

Madrid 2014

Departamento de Bioquímica
Facultad de Medicina
UNIVERSIDAD AUTÓNOMA DE MADRID

Characterization and regulation of K_v1.5-K_vβ1.3 complex.

Memoria presentada para optar al grado de Doctor con Mención Internacional por la Universidad Autónoma de Madrid presenta el Licenciado en Biología:

ÁLVARO MACÍAS MARTÍNEZ

Bajo la dirección de:

Dra. Carmen Valenzuela Miranda
Dra. Teresa González Gallego

Instituto de Investigaciones Biomédicas “Alberto Sols” (CSIC-UAM)
Madrid, 2014

El trabajo descrito en la presente Tesis Doctoral ha sido llevado a cabo en el Departamento de Modelos Experimentales de Enfermedades Humanas del Instituto de Investigaciones Biomédicas 'Alberto Sols' (CSIC-UAM) y ha sido financiado por los siguientes proyectos de investigación:

Mecanismos implicados en la regulación por kinasas del ensamblaje entre $K_v\alpha1.5$ y $K_v\beta1.3$. CICYT (SAF2007-65868). 2007-2010. Investigador principal: Carmen Valenzuela Miranda.

Red Temática de Investigación Cooperativa RECAVA. FIS (RD06/0014/0006). 2007-2010. Investigador principal: Lisardo Boscá Gomar.

Modulación adrenérgica de los canales $K_v1.5$-$K_v\beta1.3$ expresados en diferentes tipos de células cardiovasculares. CICYT (SAF2010- 14916) 2011-2014. Investigador principal: Carmen Valenzuela Miranda.

Red de Investigación Cardiovascular. FIS (RD12/0042/0019). 2012-2014. Investigador principal: Carmen Valenzuela Miranda.

Además, la realización de esta Tesis Doctoral ha sido posible gracias al disfrute de una beca predoctoral de la Junta de Ampliación de Estudios (JAE-Predoc), del Consejo Superior de Investigaciones Científicas.

A mi familia,
a ti que lees estas líneas
y sobre todo, a mis chicas,
Sonia y Emma,
mis pilares, mi equilibrio, mi todo.

"-¿Y piensas pasarte el resto de tu vida encerrado entre estas cuatro paredes, tomando notas y alimentándote a base de bocadillos?

-Tal vez algún día encuentre las respuestas que busco. Lo que si tengo muy claro, es que si no estoy aquí, nunca las encontraré. […] Si tengo que pasarme el resto de mi vida aquí encerrado para conseguir que una sola persona no sufra como mi madre sufrió por culpa de aquel maldito cáncer, o un solo niño no vea morir a su madre como yo vi morir a la mía, puedes estar segura de que aquí me quedaré.

[…]

-¿Realmente confías en conseguir algo positivo?

-Aún es pronto para saberlo. Cuando inicias una investigación de este tipo se te ofrecen mil caminos, y el problema estriba en que pronto o tarde tienes que decidirte por uno sin saber hacia dónde conduce. Tal vez no lleve a ninguna parte y hayas perdido media vida, pero ese esfuerzo nunca resulta totalmente inútil, puesto que sirve para indicar a los que vienen detrás que ésa era una vía sin salida. Los grandes descubrimientos suelen hacerse de ese modo: eliminando rutas erróneas hasta que se encuentra la correcta."

Alberto Vázquez-Figueroa
"El Señor de las Tinieblas", 2001

Agradecimientos

No me puedo creer que ya haya llegado este momento… escribir los Agradecimientos de mi Tesis Doctoral… Increíble!!!! Quién me iba a decir que iba a llegar este momento cuando estaba en el colegio, aunque, ya por aquel entonces sabía que algo relacionado con las Ciencias Naturales era 'lo mío'. Sonrío siempre al recordar una de mis mayores revelaciones y lo que sin duda alguna grabó en mí la idea de estudiar Biología, sin importarme mucho las garantías de futuro laboral que acompañaran a esa decisión… "comprender el mecanismo físico-químico que le permite al jabón quitar la grasa de las manos, pero al mismo tiempo ser compatible con el agua". Gracias a Antonio Pastor por haberme transmitido la ilusión por saber, por ir más allá, sin duda alguna a ti te debo ser Biólogo hoy en día. Recuerdo como mi padre, pensando en mi futuro, intentaba que estudiara otra carrera con más salida como medicina pero pocas cosas he tenido tan claras en mi vida, aunque me arrepintiese, necesitaba saber lo que era estudiar Biología.

Tras los años en la universidad, y coger experiencia en el trabajo de laboratorio, me llegó la oportunidad 'de refilón' de ampliar mis conocimientos en alguna materia y/o técnica que no pudiera aprender en el laboratorio que ya estaba. De este modo, me tropecé con el laboratorio de electrofisiología de la Dra. Carmen Valenzuela Miranda, y como aquello era algo que en la carrera siempre me había atraído y con la simple intención de saber un poquito más, decidí atreverme a ponerme en contacto con ella. Aún recuerdo la primera vez que entré en el C.S.I.C. y, aun tremendamente nervioso por el simple hecho de estar entre aquellas paredes y delante de 'Investigadores Científicos de verdad', Carmen me hablaba sobre su mundo (la electrofisiología cardiovascular) con esa naturalidad y esa pasión con la que sólo ella sabe hacerlo. Tras dejarme entrar en su casa, porque el laboratorio llega a convertirse en eso, consiguió que me enamorara de este campo y conseguimos una beca para poder hacer Mi Tesis. Mil gracias, Carmen, por dejarme seguir siendo 'El Lechón' del laboratorio, espero serlo siempre; por tu apoyo incondicional y confianza en mí, por enseñarme no sólo ciencia sino humanidad y respeto hacia los demás y hacia nosotros mismos, y por supuesto, por transmitirme el respeto y la admiración a este trabajo… gracias de corazón!!! Atrás quedan ya cuatro años y medio de congresos, risas, aprendizaje, momentos muy buenos y otros no tanto… gracias por todos ellos. También, por supuesto, a la Dra. Teresa González Gallego ('Doc!') porque los inicios nunca fueron fáciles y a ti te "tocó" estar codo con codo conmigo cuando siendo Lechón-Lechón entré en el labo. Gracias por tu entrega, por tu apoyo y por la pasión que demuestras en cada cosa que haces. Gracias a ambas por todo lo vivido en todos estos años, han hecho de mí una persona nueva. Espero, siguiendo el consejo de Valentín Fuster, seguir teniéndoos de tutoras, y amigas, el resto de mi carrera.

Por supuesto, a todas las componentes del laboratorio. A la Dra. Miren David, tú me ensañaste la perseverancia y el trabajo duro, a elaborar todos los controles posibles aunque eso suponga cuadruplicar (y en algunos casos mucho más) el volumen de trabajo, y por supuesto, el amor por el PowerPoint. Gracias por tu sentido del humor y por tus críticas siempre constructivas. A, la ya Doctora (qué fuerte), Cristina Moreno

Vadillo, juntos hemos vivido casi todo el camino de la Tesis, con momentos buenos y otros no tanto. Siempre hemos intentado conjugar el trabajo duro con el mejor ambiente y, a mi juicio, si no lo hemos conseguido hemos estado muy cerca. Ojalá el tiempo y la ciencia nos vuelvan a juntar en algún congreso en los que otros becarios nos señalarán con el dedo y dirán: Mira, no son ellos los del trabajo… Alicia y Ángela, las últimas en entrar al laboratorio pero que desde el principio conseguisteis integraros de un modo admirable. Gracias chicas por los momentos de risas, de mucho curro, las tertulias del café, por todo vuestro apoyo. Cada día estoy más contento, si es que influyó en algo, de haberos soltado el chaparrón de 'Lo bueno y lo malo de este laboratorio (por ser de electrofisiología)'. Gracias también a aquellas personas que pasaron por el laboratorio Gema, Ulyana, Carmen, Mariela o Najib, de todos he aprendido algo y habéis cambiado algo dentro de mí, gracias por dejarme compartir vuestro tiempo conmigo.

A todos y cada uno de los compañeros del Instituto con los que cada día he compartido uno de los mejores momentos del día… la hora de comer! Gracias a Mario (mi gordi), Antonio, María, Eva, Rafa, Ale, Ana Rosa, Blanca, Pepa, Toño, Miryam, Daniela… una gran familia científica. Aún tratando la ciencia como un tema tabú en la comida (que para eso es de descanso), habéis hecho que este camino sea muuucho más fácil. Gracias por todos esos momentos de risas hasta perder el aliento, el apoyo en los momentos de decadencia, por los chistes (unos buenos, y otros no tanto)… por todo. De verdad, esta Tesis tampoco habría sido posible sin vosotros.

A todo el laboratorio 1.9, gracias por dejarme ser uno más. Gracias a Jose (el otro macho alpha), Marina, Sandra, Elena, Diana… mi otro laboratorio. Gracias por enseñarme que ser grandes científicos y mejores personas no está reñido. Después de conoceros creo que otra ciencia es posible. Sois, todas (admítelo Jose, somos una más) y cada una de vosotras, extraordinarias.

A 'Los de la Complu', es decir, al grupo de los Dres. Francisco Pérez-Vizcaíno y Ángel Cogolludo, a Quique, Javi, Bianca, Laura, Carmen, Dani y Raquelle. Gracias por abrirme siempre las puertas de vuestra casa, por todas las colaboraciones realizadas, hayan llegado o no a buen término, porque siempre se puede contar con vosotros, pero sobre todo porque es un placer haber compartido celebraciones profesionales y personales.

A los Dres. Pilar de la Peña, Francisco Barros, Walter Stühmer y Luis A. Pardo, y a vuestros respectivos laboratorios, por supuesto. Gracias a todos vosotros por abrirme las puertas de vuestra casa y enseñarme tantas y tantas cosas, personales y profesionales. Espero poder seguir aprendiendo de vosotros siempre que me lo permitáis. De vuestros laboratorios me llevo muy buenos recuerdos y grandes amigos. A todos vosotros, Jorge, Araceli, Camilo, Joassia, Piotrek, Juan Carlos, Vincenzo, Ulrike, Diana, Adam, Estefanía,

Rayco,… espero veros pronto y recordar viejos tiempos. Gracias a todos por haberme hecho sentir como un miembro más de vuestra familia.

No puedo olvidarme de mis amigos de siempre, los de fuera del labo, los de toda la vida. Juanan y Alex, muy diferentes pero muy iguales a la vez, siempre dispuestos a hacer lo que sea necesario para introducir momentos relajados en los más tensos de la vida; gracias por hacerme la vida más agradable y por apoyar 'al niño' en todas las cosillas raras que hace. Gracias a Lyetor, grande y sabio, más de lo que piensa o sabe; gracias por hacerme sentir especial. Mis chicas Yoly, Virgy, Silvia y Sandra por aguantarnos a los chicos e interesaros desde siempre por mi evolución personal y profesional, sois muy grandes! Y como no, darles las gracias a los nuevos del grupo, los peques, Cristina, Luna, Sandra, Diego, Saúl y Nadia que inspiran cariño, ternura y que vemos en ellos el futuro de lo que somos nosotros. Esperemos que lo hagan un poco mejor.

Por supuesto a mis padres, Ramiro y Loli, mi apoyo en todos mis movimientos. Sin ellos, no sólo este trabajo, sino todas y cada una de las cosas que he hecho en mi vida, no habrían sido posibles. A mi hermana, Desi, que aunque con nuestras diferencias siempre ha estado, a su manera, apoyándome y aconsejándome en todo momento. Dani, el hermano que nunca tuve quien con una mirada y un abrazo en el momento justo a hecho más por mí, que mucha gente con todas las palabras del mundo. Y mis sobris, Andrea y Candela quienes algún día entenderán lo importantes que son para su 'Titi' quién espero algún día se convierta en su amigo y confidente. Mis abuelos, que me han dado todo sin pedir nada a cambio, y que dentro de lo que cabe, siempre han hecho todo lo posible por intentar entender esto tan raro a lo que me dedico; a ellos les debo mi infancia. Y Pilar, mi suegra, quien en todos estos años me ha demostrado su apoyo, comprensión, entusiasmo e interés por todo aquello que me rodea tanto desde un punto de vista personal como profesional; gracias por intentar siempre entender lo importante que es para mí.

Dejo para el final, a las personas más importantes de mi vida, Sonia y Emma: mi niñas, mi vida, mi equilibrio, mi todo. Gracias una vez más Sonia por saber esperarme, por apoyarme en todo (lo personal y lo profesional), por entender lo complicado de este mundillo que he elegido como profesión, por compartir conmigo buenos y malos momentos. A ti te debo poder estar escribiendo hoy estas líneas, tanto desde un punto de vista práctico como no tanto, puesto que si hoy soy Doctor, también te lo debo a ti y lo sabes. Gracias por formar un equilibrio, un equipo, un todo junto a mí, que espero dure toda la vida. Gracias por darme 10 minutos de vida más con cada una de tus sonrisas. Gracias por TODO. Gracias Emma por llenarnos de ilusión y amor con cada una de tus miradas, tus sonrisas, tus abrazos… ojalá algún día puedas llegar a sentir una pizca de lo que siento por ti. Aunque no quedarán escritos en ningún sitio, a ti te dedico todos y cada uno de los días de mi vida. Gracias equipo!!

Los canales de potasio dependientes de voltaje (K_v) son proteínas de membrana involucradas en diversos procesos fisiológicos y fisiopatológicos. De hecho, el funcionamiento electrofisiológico normal del corazón está determinado por la propagación ordenada de potenciales de acción (PA) generados en miocitos individuales. Por lo tanto, anomalías en la génesis, propagación, duración o configuración de estos PA constituyen la causa de arritmias cardíacas. Las corrientes de K^+ determinan la repolarización del PA cardíaco, el potencial de membrana, el ritmo cardíaco, la refractariedad del tejido cardíaco y, por tanto, constituyen importantes dianas moleculares para la acción de diversos moduladores de la función cardíaca. Los canales $K_v1.5$ son los principales responsables de la génesis de la corriente de salida ultrarápida de potasio (I_{Kur}) y, debido a que se expresan mayoritariamente en aurícula, la I_{Kur} determina la duración del PA auricular. Así, estos canales representan una diana farmacológica para el desarrollo de fármacos útiles en el tratamiento de arritmias supraventriculares. Estos canales se ensamblan con diversas subunidades $K_v\beta$. En particular, las subunidades $K_v\beta1.3$ modifican las características electrofisiológicas de los canales $K_v1.5$, induciendo una inactivación rápida y parcial, un mayor grado de inactivación lenta, un desplazamiento de la curva de activación hacia potenciales más electronegativos, y una disminución en la sensibilidad del canal al bloqueo inducido por fármacos. Tras inhibir la PKC con calfostina C los canales $K_v1.5$-$K_v\beta1.3$ generan corrientes de pequeña magnitud y sin inactivación rápida inducida por la $K_v\beta1.3$. En esta Tesis Doctoral hemos investigado los mecanismos subyacentes a este fenómeno utilizando técnicas electrofisiológicas y de imagen en sistemas heterólogos (células HEK293) y en tejidos nativos (miocardio de rata y humano). Los resultados obtenidos demuestran la existencia de un *canalosoma* funcional de $K_v1.5$, estrechamente regulado por PLC y PIP_2, y constituido por, al menos, $K_v\beta1.3$, el receptor de quinasas C activadas (RACK1), PKCβI, PKCβII, y PKCθ en células HEK293. En este *canalosoma*, las subunidades $K_v\beta1.3$ parecen tener un papel 'conector' entre $K_v1.5$ y RACK1 y, por tanto, con el resto de componentes del mismo. Un *canalosoma* $K_v1.5$ muy similar se encontró en ventrículo de rata pero no en aurícula. La inhibición de PKC inducida por calfostina C también modifica la inactivación dependiente de voltaje de los canales $K_v1.5$-$K_v\beta1.3$, así como sobre su farmacología que resulta ser más similar a la de $K_v1.5$. De hecho, los valores de IC_{50} para bupivacaína y quinidina fueron similares a los obtenidos para el bloqueo de $K_v1.5$. Dado que la inhibición de la PKC disminuye la magnitud de las corrientes generadas por los canales $K_v1.5$-$K_v\beta1.3$, estudiamos el reciclaje de los canales $K_v1.5$-$K_v\beta1.3$. Observamos que la inhibición de la PKC promueve una reducción de la densidad de canales $K_v1.5$ en membrana y un aumento de los canales internalizados sin modificar la cantidad total de los mismos. Experimentos en los que transfectamos Rab11 constitutivamente activo demostraron que PKC está involucrada en el reciclaje lento de los canales $K_v1.5$-$K_v\beta1.3$ mediado por Rab11. Por último, analizamos el papel funcional de la proteína Lgi1, que interfiere con la inactivación rápida inducida por $K_v\beta1$ sobre los canales K_v1 y que ha sido relacionada con ciertos tipos de epilepsia. Tras demostrar su expresión en el tejido cardíaco de rata, con un patrón de expresión similar a $K_v\beta1.3$, demostramos que Lgi1 anula la inactivación rápida inducida por $K_v\beta1.3$, tanto tras transfectar Lgi1, como tras añadirla a la solución interna de la pipeta; lo que se acompañaba de una disminución en la cantidad de canal en la membrana celular y de modificaciones del citoesqueleto. Además, demostramos que el patrón de expresión de Lgi1 es muy similar al de $K_v1.5$ en el ventrículo humano, lo que nos lleva a proponer a Lgi1 como un nuevo e importante modulador del complejo $K_v1.5$-$K_v\beta1.3$.

Voltage dependent potassium channels (K_v) are membrane proteins involved in several physiological and pathological events. In fact, the normal electrophysiological behavior of the heart is determined by the ordered propagation of action potentials generated in the individual myocytes. Therefore, abnormalities of the generation, propagation, duration or configuration of individual cardiac action potentials (AP) are the basis of cardiac arrhythmias. K^+ currents control the repolarization process of the cardiac AP, membrane potential, heart rate, myocardium refractoriness and, thus, they represent important molecular targets for the actions of neurotransmitters, hormones, drugs and toxins known to modulate cardiac function. Activation of $K_v1.5$ channels generates the ultrarapid outward potassium current (I_{Kur}) and because these channels are mostly expressed in atrial tissue, this current determines the atrial AP duration, representing a pharmacological target for the development of antiarrhythmic drugs useful in the treatment of supraventricular arrhythmias. $K_v1.5$ channels assembly with several $K_v\beta$ subunits ($K_v\beta1.2$, $K_v\beta1.3$ and $K_v\beta2.1$). In particular, $K_v\beta1.3$ subunits modify the electrophysiological characteristics of $K_v1.5$ channels, inducing a fast and partial inactivation, a greater degree of slow inactivation, a shift of the activation curve towards more negative potentials, and a decrease in the sensitivity of the channel to drug-induced blockade. Previous studies have shown that inhibition of PKC with calphostin C results in a small currents without the $K_v\beta1.3$-induced fast inactivation. In the present Doctoral Thesis the mechanisms underlying this phenomenon, using electrophysiological and imaging techniques, were investigated in both heterologous (HEK293 cells) and native systems (rat and human cardiac tissue). The results obtained revealed the existence of a functional $K_v1.5$ *channelosome,* tightly regulated by PLC and PIP_2, and conformed by, at least, $K_v\beta1.3$, the receptor for activated C kinase (RACK1), PKCβI, PKCβII, and PKCθ in HEK293 cells. In this *channelosome*, $K_v\beta1.3$ subunits seem to have a 'linker' role between $K_v1.5$ and RACK1 and, therefore, with the others components. Interestingly, a very similar $K_v1.5$ *channelosome* was found in rat ventricular but not in atrial tissue. PKC inhibition calphostin C-mediated also modifies the voltage dependent inactivation of $K_v1.5$-$K_v\beta1.3$ channels and in their pharmacology that appear to be similar to that displayed by $K_v1.5$ channels alone. Indeed, the IC_{50} values for bupivacaine and for quinidine were similar to those reported for $K_v1.5$ block. Since PKC inhibition results in a reduction of the current magnitude, the recycling of $K_v1.5$-$K_v\beta1.3$ channels was studied. We observed that PKC inhibition promotes a reduction of $K_v1.5$ density at the cell membrane and an increase in the channel internalized without modifying the total amount of the channel. Experiments in which Rab11 constitutively active was transfected, demonstrated that PKC activity was involved in the slow recycling of $K_v1.5$-$K_v\beta1.3$ channels Rab11-meadiated. Finally, the functional role of the Lgi1 protein was analyzed. Lgi1 interferes with the fast inactivation $K_v\beta1$-induced of K_v1 channels and mutations in this protein have been linked to certain types of epilepsy. After demonstrate its expression in rat cardiac tissue, with a similar expression pattern to $K_v\beta1.3$, we have shown that Lgi1 prevents the $K_v\beta1.3$-induced fast inactivation, either when Lgi1 was transfected or when the Lgi1 protein was added to the internal solution of the patch pipette with a decrease in the surface channel amount and cytoskeleton disorders. In addition, we show that the pattern of expression of Lgi1 is very similar to that shown by $K_v1.5$ in the human ventricle, leading us to propose Lgi1 as an important $K_v1.5$-$K_v\beta1.3$ modulator.

Figure list

Supplemental Figures

Table list

Abbreviations Index

5-HT_{1C}	5-HT (serotonin) receptor subtype, 1C
Å	Angstrom
O	Open state of the channel
Ab	Antibody
ADAM	A Disintegrin And Metalloprotease domain protein
AP	Action potential
Ba^{2+}	Barium ion
BSA	Bovine serum albumin
cAMP	Cyclic adenosine monophosphate
cDNA	Complementary desoxyribonucleic acid
Ca^{2+}	Calcium ion
CaMKII	Ca^{2+}/calmodulin-dependent protein kinase II
CMV	Citomegalovirus
C-terminus	Carboxyl terminal domain of proteins
CVD	Cardiovascular disease
DAG	Diacylglycerol
DMEM	Dulbecco´s Modified Eagle Medium
E_K	Equilibrium potential for K^+
FBS	Fetal bovine serum
FRET	Fluorescence Resonance Energy Transference
GΩ	Gigaohmn
HEK293	Human embrionic kindey cell line
IRES	Internal Ribosome Entry Sequence
IV	Current voltage relationship
I_{CaL}	Inward L-type calcium current
I_{CRAC}	Calcium release activated calcium current
I_{K1}	Inward rectifying potassium current
$I_{K,ACh}$	Inward rectifying acetylcholine-sensitive K^+ current
$I_{K,ATP}$	Inward rectifying ATP-sensitive K^+ current
I_{Kr}	Rapidly activating delayed rectifying potassium current
I_{Ks}	Slowly activating delayed rectifying potassium current
I_{Kur}	Ultrarapidly activating delayed rectifying potassium current
I_{Na}	Inward sodium current
I_{to}	Transient outward potassium current
IP	Immunoprecipitation
K^+	Potassium ion
K_{ATP}	ATP-sensitive potassium channel
kDa	Kilodalton
kHz	Kilohertz
K_v	Voltage dependent potassium channel
$K_v\beta$	Ancillary β-subunit of voltage-gated potassium channels
Lgi	Leucine-rich glioma inactivated protein
Ltk-	Leukocyte tyrosine kinase less mouse derived cell line
Mg^{2+}	Magnessium ion
mRNA	Messenger ribonucleic acid
Na^+	Sodium ion
N-terminus	Amino-terminal domain of proteins
P	P-loop
PBS	Phosphate buffer saline
PCR	Polimerase chain reaction
PIP_2	Phosphatidylinositol bisphosphate
PKA	Protein kinase A
PKC	Protein kinase C

PMA	Phorbol 12-myristate 13-acetate; protein kinase C (PKC) activator
Pro	Proline
PVP	Proline-Valine-Proline motif
QT	QT interval of the electrocardiogram
RT-PCR	Retrotranscriptase polimerase chain reaction
SCD	Sudden cardiac death
S.E.M.	Standard error of the mean
τ	Time constant
T1	Tetramerization domain
TEA	Tetraethylammonium
TIRF	Total Internal Reflection Fluorescence
TM	Transmembrane domain

1. INTRODUCTION

1.1 ION CHANNELS

Ion channels are part of the mechanism of cellular signaling of almost all live cells. Our ability to do gymnastic, to perceive a colorful world and to process language relies on rapid communication among cells. Such signaling, the fastest in our bodies, involves electrical fluxes produced when ion channels open and close. Ion channels are intrinsic membrane proteins acting as gated pores that regulate the movement of ions across cell membranes. Thus, they are part of the rapid communication mechanism of cellular signaling of almost all live cells. Fast electrical signaling is made possible by the homeostatic mechanisms that establish the standard environment and content of animal cells: high Na^+ [Na^+] and Ca^{2+} concentrations [Ca^{2+}] (but low [K^+]) in the blood and extracellular fluid, and high [K^+] (but low [Na^+] and [Ca^{2+}]) in the cytoplasm. Ion gradients are established following Goldman-Hodgkin-Katz equation (Goldman, 1943; Hodgkin & Katz, 1949) and maintained by active transporters and pumps, which prepare the way for rapid changes in membrane voltage produced by passive transport through ion channels. These pore-forming proteins allow ions to flow only "downhill", as dictated by their electrochemical gradients, but they do it rapidly (the rate of passage of ions through one open channel is often more than 10^6 ions per second) and selectively. Opening a Na^+ or Ca^{2+} selective channel permits Na^+ or Ca^{2+} to flow down its gradient into a cell, making the intracellular voltage more positive. Opening a K^+ selective channel permits K^+ to flow from the cell and restores the voltage to a more negative value. The dimensions of a typical cell and its membrane allow the voltage to be changed rapidly back and forth many times, with relatively small changes in concentration. This is essentially how all cellular electrical signaling is produced (Hille *et al.*, 1999).

Ion channels play a key role in the physiology of cells and defects in their function have profound physiological effects in excitable tissues (Hodgkin & Huxley, 1952). Moreover, ion channels play also crucial roles not only in excitable tissues, but also in other phenomena such as activation of immune cells (T-cells and macrophages), regulation of the cellular volume and function of the pancreatic β cells (Lewis & Cahalan, 1995; Villalonga *et al.*, 2010; Moreno *et al.*, 2013); blood pressure regulation (Joseph *et al.*, 2013), learning and memory (Need *et al.*, 2003); or cellular and tumor proliferation (Wang *et al.*, 2002). In fact, there have been described that some ion channels inhibit proliferation and, therefore, they are considered therapeutic targets in some types of cancer (Pardo *et al.*, 1999; Villalonga *et al.*, 2008). These relevant effects into the body functions convert ion channels into pharmacological targets in the treatment of several diseases (Wickenden, 2002a) such as cardiac arrhythmias (Tamargo *et al.*, 2004), epilepsy (Wickenden, 2002b), autoimmune disorders (Wulff *et al.*, 2003; Rangaraju *et al.*, 2009), cancer (Wang *et al.*, 2002), or diabetes (MacDonald *et al.*, 2003). All these process can be carried out, thanks to the intracellular communication among the different tissues of the body and, therefore, between cells or 'cell-cell signaling'. Indeed, channel mutations may results in the genesis of several pathologies named 'channelopathies'. In the last years, and helped by the last technological advances, the initial vision of the

ion channels has changed from static proteins, to another one much more dynamic, constantly modulated and tightly regulated by both intracellular and physiological processes.

1.2 VOLTAGE-GATED POTASSIUM CHANNELS

Voltage-gated ion channel protein superfamily, formed by more than 140 members, is one of the largest groups of signal transduction proteins (Hille *et al.*, 1999; Yu *et al.*, 2005). Among them, voltage-dependent potassium channels are the largest and most diverse family of ion channels and they are mainly characterized because "sense'' differences in the voltage potential across the cell membrane and open or close in response to changes in the membrane potential. The first K^+ channel to be identified came from the cloning of the *SHAKER* gene of *Drosophila sp*. which causes flies to shake when exposed to ether (Choe, 2002). However, ion channels have been found also in bacterial, archaeal, and eukaryotic cells (both plant and animal cells) since their amino acid sequences are very easy to recognize because K^+ channels contain a highly conserved segment called the potassium signature sequence [G(Y/F)GD] (Papazian *et al.*, 1987; Aiyar *et al.*, 1996). This sequence forms the structural element known as the **selectivity filter**, which prevents the passage of sodium ions, even when this ion is smaller, and allows potassium ions through the ion channel pore at rates approaching the diffusion limit.

The resolution of KcsA structure, a non-voltage-gated potassium channel in *Streptomyces lividans*, resulted in an essential advance in the knowledge and comprehension of the ion permeability mechanism across the ion channels (Doyle *et al.*, 1998), since it was obtained a detailed image of the potassium conductance mechanism (Morais-Cabral *et al.*, 2001; Zhou *et al.*, 2001). Based on their molecular architecture, different channel classes were distinguished (Figure 1) (Catterall, 1988; Sigworth, 1994; Snyders, 1999; Swartz, 2004). The simplest structural type of K^+ channels is visible in the 2TM/1P class, named after their typical composition of two transmembrane helixes (TM) and one P-loop (P), and is represented by the inward rectifier K^+ channels (K_{ir}) (Figure 1A). The second group is referred to voltage-gated K^+ channels (K_v), which are composed by six TM (S1-S6) and one P-loop, resulting in the 6TM/1P class (Figure 1B). The two-P K^+ channels family is constituted by the non-voltage-gated outward rectifier channels that have eight TM architecture containing two P-regions per subunit (8TM/2P, Figure 1C) and the class of the so-called "background" or "leakage" channels made up of two P-regions, hence structurally referred to as 4TM/2P type (Roden & George, Jr., 1997; Hille, 2001) (Figure 1D). KcsA belongs to the ion channels conformed by two transmembrane segments (2TM) and one P-loop (1P) or 2TM/1P channels, in which, the 2TM are related with the fifth and sixth transmembrane domains in K_v channels (Benavides-Haro *et al.*, 2003).

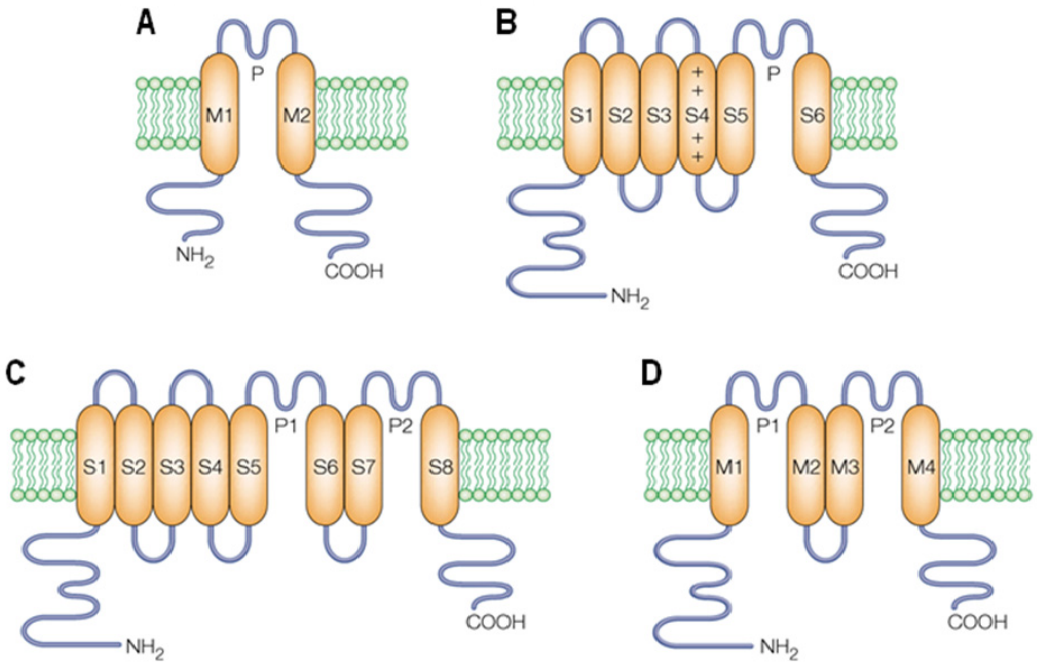

Figure 1: The four main classes of potassium channels. **A,** 2TM/P channels (which consist of two transmembrane (TM) helices with a P-loop between them), exemplified by inwardly rectifying K^+ channels and by bacterial K^+ channels such as KcsA. **B,** 6TM/P channels that are the predominant among ligand- and voltage-gated K^+ channels. **C,** 8TM/2P channels, which are hybrids of 6TM/P and 2TM/P, and were first found in yeast. **D,** 4TM/2P channels, which consist of two repeats of 2TM/P channels. 8TM/2P and 4TM/2P probably assemble as dimers to form a channel. 4TM/2P channels are far more common than was originally thought. These so-called 'leakage' channels are targets of numerous anesthetics. S4 is marked with plus signs to indicate its role in voltage sensing in the voltage-gated K^+ channels [taken from (Choe, 2002)].

To date, twelve different subfamilies of K_v channels subunits have been described (K_v1-12) (Goldstein *et al.*, 2001; Gutman *et al.*, 2005). K_v channels are formed by co-assembly of four α subunits, each containing six α-helical TM segments (S1-S6), with both N- and C-termini on the intracellular side of the membrane. Each subunit comprises two membrane-integrated functionally distinct modules; one forms the voltage-sensor (S1-S4) and the other the K^+ selective pore with the gate (S5-P-S6) (Figure 2A).

In the cytoplasmic side there is a specific sequence of amino acids in the N-terminus of voltage-gated K^+ channel proteins responsible for channel inactivation as well as for recognition between voltage-gated K^+ channel subunits. This sequence supervises the proper assembly of specific tetrameric channels (Li *et al.*, 1992) and it is called tetramerization domain, "T1" (Shen *et al.*, 1993) (Figure 2B). This domain determines the specificity of channel subunit assembly and also serves as a platform for binding of auxiliary K_v cytoplasmic β-subunits. The cytoplasmic C-terminus of *Shaker* K^+ channels has no obvious domain structure. By contrast, other K_v channels are characterized by the presence of a subunit assembly domain and/or a sensor domain in the C-terminus. These include K_v7 and K_v10-12 channels, as well as potassium channels gated by voltage and intracellular Ca^{2+} (e.g. KCa1 channels) and channels gated exclusively by intracellular ligands like Ca^{2+} (e.g. KCa2 channels) (Figure 2C). The auxiliary subunits known to be associated with this family (KCNE) are transmembrane proteins that appear to be intimately

associated with the pore domain and may displace the voltage-sensor domain or interact with it directly (Deal *et al.*, 1996; Kurokawa *et al.*, 2001; Yellen, 2002; Barros *et al.*, 2012).

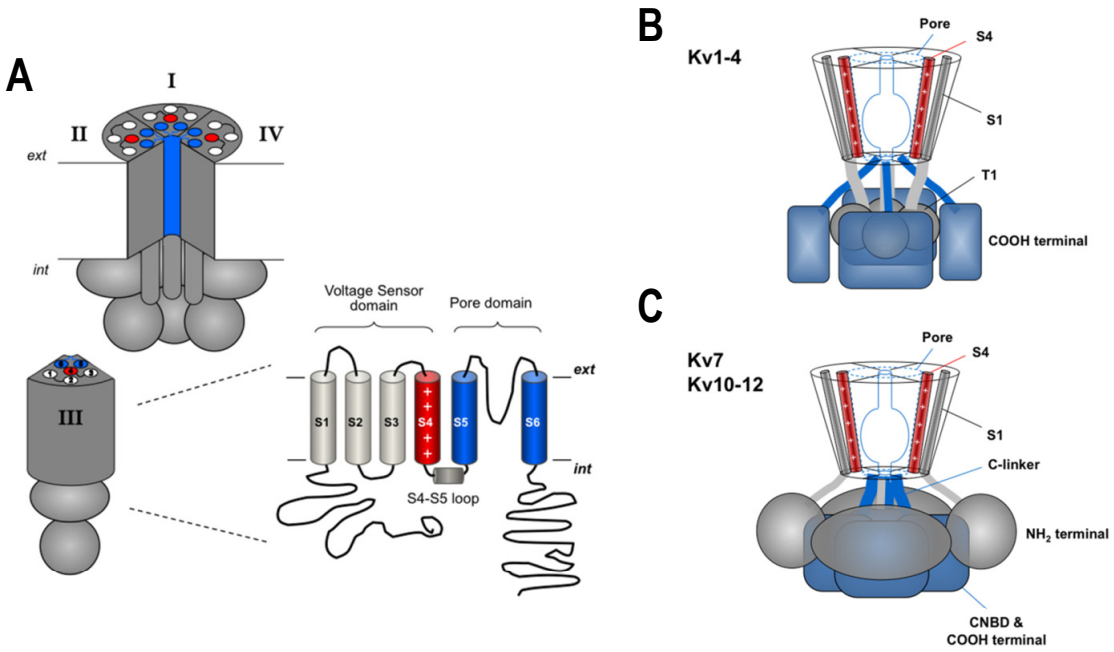

Figure 2: Summary of structural components of K_v channels. **A,** Schematic representation of the tetrameric organization of a K_v channel. A structural folding model of one of the four α-subunits is shown on the right. **B,** General organization of the K_v1–K_v4 channels group with the T1 "tetramerization domains" hanging centrally below the transmembrane core and attached to it through four linkers continued from the first transmembrane helices. In this case, the C-terminal structures probably track to the periphery surrounding T1 and extending to its bottom. **C,** General cytoplasmic architecture of the K_v7 and K_v10–K_v12 channels characterized by a C-terminus (i.e., the C-linker/CNBD region of the K_v10–K_v12 channels or the A–D helical regions of the K_v7 channels) forming a compact tetrameric structure in a central position immediately below the cytoplasmic pore opening. In this case the N-terminus probably surrounds the C-terminus and extends to its bottom establishing extensive contacts with its top and side surfaces. Note that in both models the initial N-terminal structures are likely to interact with the gate surroundings in the transmembrane core. S4 segment is also depicted as a reference [adapted from (Barros *et al.*, 2012)].

1.2.1. The voltage sensor

For K_v channels, very small changes in the voltage membrane of the cell (Sigworth, 2003) determine whether they are opened or closed, and therefore, they provide a way for the membrane voltage to feed back onto itself, a key property for generating electrical impulses (Hodgkin & Huxley, 1952). Although the role of the voltage sensor has been classically attributed to the S4 segment (Jiang *et al.*, 2003), different reports have revealed that the S1-S4 region acts as the voltage-sensor of K_v channels (Papazian *et al.*, 1991; Seoh *et al.*, 1996; Peyser & Nonner, 2012) (Figure 3). Thus, the S4 segment, which exhibits four-eight positively charged residues (Stuhmer *et al.*, 1989; Bezanilla, 2000) is the major component of the sensor for gating, although charged amino acids present in S1, S2 and S3 also contribute to this process. S3 is formed by two helixes referred to as S3a and S3b (Figure 3). In all crystal structures determined, S3b forms together with S4 a helix-turn-helix structure called the voltage-sensor paddle (Bezanilla & Stefani, 1998; Long *et al.*, 2005a; Chanda & Bezanilla, 2008). Depolarization of the cell membrane causes a physical outward movement of S4, which has been electrically monitored as the

gating current (Mannuzzu *et al.*, 1996; Bezanilla & Stefani, 1998), or also by means of fluorescence (Tao *et al.*, 2010). This movement induces further conformational changes that open the channel pore and permit selective K^+ permeation (Tristani-Firouzi *et al.*, 2002).

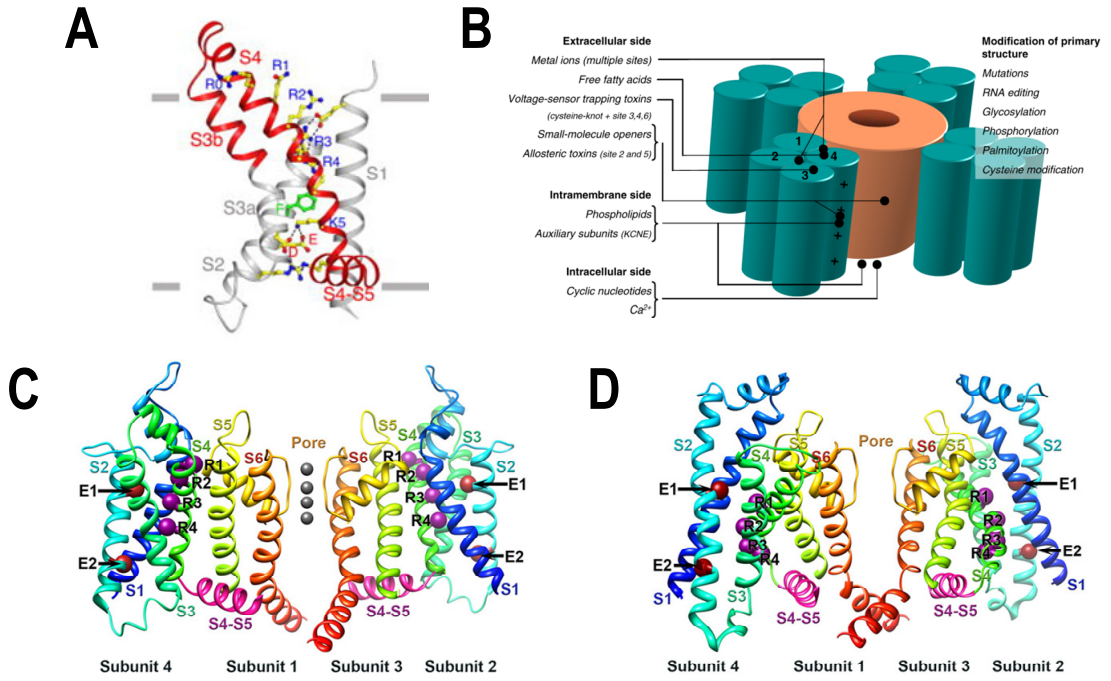

Figure 3: Schematic view of the voltage-sensor of K⁺ channels. **A,** View of the voltage sensor and S4-S5 linker helix of the open conformation from $K_v$chim. Side chains of the positively charged residues on S4 (labeled as R0, R1, R2, R3, R4, and K5) and the negatively charged residues forming ionizing hydrogen bonds (dashed black lines) with the positive charges, as well as those of the three residues (labeled F, E, and D) forming an occluded binding site in the voltage sensor, are shown as sticks and colored according to atom types (yellow, carbon; blue, nitrogen; red, oxygen; and green, phenylalanine) [taken from (Moreno, 2013)]. **B,** Scheme of the modulation of the K^+ ion channel. The pore-forming unit is shown in orange and the four surrounding VSDs in green with S1–S4 labeled in one subunit [taken from (Borjesson & Elinder, 2008)]. **C,** Structure of the of K_v1.2 channel, determined by x-ray crystallography [taken from (Long *et al.*, 2005b)]. The voltage-sensing and pore-forming modules of two subunits are indicated in a cross-section through the structure normal to the plane of the membrane. Note the labels indicating that the voltage-sensing module of subunit 4 interacts with the pore-forming module of subunit 1 (left) while the voltage-sensing module of subunit 2 interacts with the pore-forming module of subunit 3 (right). Transmembrane segments are colored: S1, dark blue; S2, light blue-green; S3, light green; S4, dark green; S5, yellow-green; S6, orange. The S4-S5 linker covalently connecting pore-forming and voltage-sensing modules are highlighted in magenta. Positions of the Cβ atoms of gating charge-carrying arginines in S4 (labeled as R1 through R4 and colored in purple) and negatively charged residues in S2 (labeled E1 (for An1) and E2 (for An2) and colored in brown) are shown in sphere representation. **D,** Rosetta membrane resting state model of K_v1.2 channel. The model is colored and labeled as in panel C. [C and D panels taken from (Catterall, 2010)].

1.2.2. The selectivity filter and the ion pore

The essential role of K^+ channels is selectively conducting K^+ ions across the cell membrane. The atomic radius of K^+ is 1.33 Å and that of Na^+ is 0.95 Å. Instead of this difference, K^+ channels has to be capable to select K^+ over Na^+ ions and these channels do it by a factor of more than 1000. Moreover, this

strong selectivity for K^+ is achieved without compromising the rates of conduction, which approach the diffusion limit. The K^+ channel pore is comprised of four usually identical subunits that encircle with four-fold symmetry a central ion conduction pathway (MacKinnon, 1991; Doyle *et al.*, 1998; Zhou *et al.*, 2001). The first K^+ channel to be crystallized was the bacterial KcsA channel (Figure 4). Each subunit contains two fully transmembrane α-helices termed inner (nearest the ion pathway) and outer (nearest the membrane) helixes (equivalent to S5 and S6 of K_v channels), and a tilted pore loop or 'P-loop' that runs half way through the membrane, pointing its C-terminus negative charge toward the ion pathway (MacKinnon, 1991). A stretch of eight amino acids within the pore loop is responsible for potassium selectivity (Heginbotham *et al.*, 1992). In addition, as it can be seen in the Figure 4, three ions appear in a queue within the pore, a result predicted more than 40 years earlier by Alan Hodgkin and Richard Keynes (Hodgkin & Keynes, 1955; Hille *et al.*, 1999). Near the midpoint of the membrane, the ion pathway is nearly 10 Å in diameter, forming a central water-filled cavity. Indeed, the design of the potassium channel includes this water-filled cavity to raise the dielectric constant at the membrane center, and oriented α-helices to provide favorable electrostatic interactions (Hille *et al.*, 1999). In this way, an hydrated K^+ ion remains suspended at the center of the cavity in the crystal structure (MacKinnon, 2003). Potassium channels remove the hydration shell from the ion when it enters the selectivity filter. The selectivity filter is formed by five residues (TVGYG-in prokaryotic species) in the P-loop from each subunit, which have their electro-negative carbonyl oxygen atoms aligned towards the center of the selectivity filter of the ion pore and form an anti-prism similar to a water-solvating shell around each potassium binding site. The distance between the carbonyl oxygen and the potassium ions in the binding site of the selectivity filter is the same as between water oxygen in the first hydration shell and a potassium ion in water solution, providing an energetically favorable route for de-solvation of the ions. On the contrary, passage of sodium ions would be energetically unfavorable, since the strong interactions between the filter and pore helix that would prevent the channel from collapsing to the smaller sodium ion size. The selectivity filter opens towards the extracellular solution, exposing four carbonyl oxygens to a glycine residue. The next residue towards the extracellular side of the protein is the negatively charged Asp80 (in KcsA). This residue, together with the five filter residues form the pore, connects the water-filled cavity in the centre of the protein with the extracellular solution. The result is that K^+ enters the channel easily, whereas Na^+ does not (Doyle *et al.*, 1998).

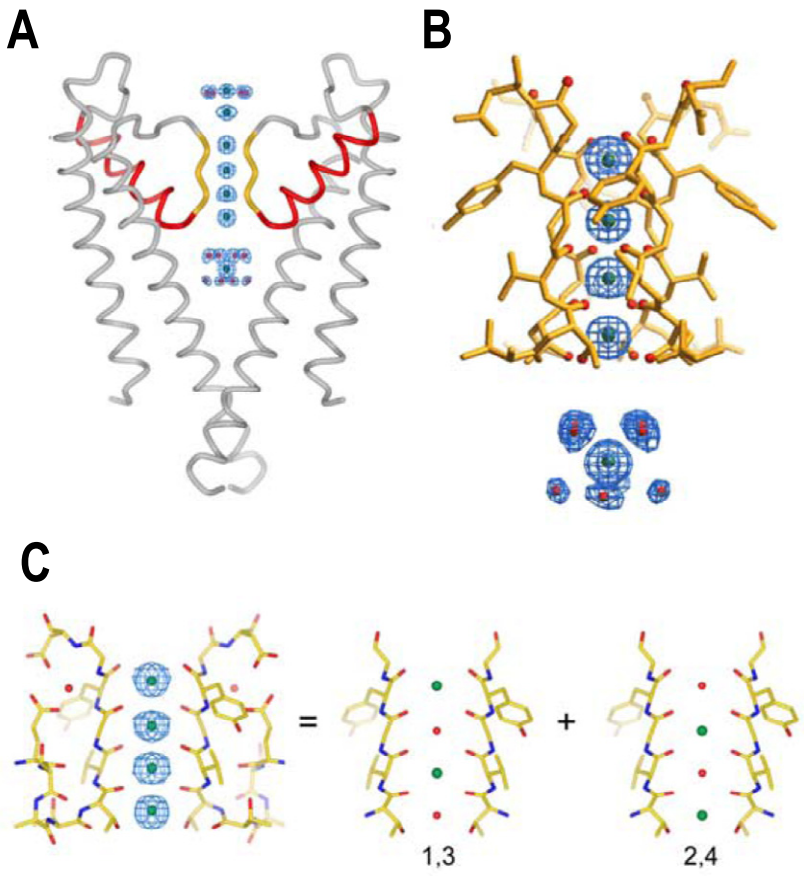

Figure 4: The ion conduction pore of K⁺ channels. **A,** Two of the four subunits from the KcsA pore are shown with the extracellular side on top. Each subunit contains an outer helix close to the membrane, an inner helix close to the pore, a pore helix (red) and a selectivity filter (gold). Blue mesh shows electron density for K^+ ions and water along the pore. **B,** Close-up view of the selectivity filter with dehydrated K^+ ions at positions 1 through 4 (external to internal) inside the filter and a hydrated K^+ ion in the central cavity below the filter. **C,** Electron density in the filter corresponds to two configurations of K^+ ions (green) alternating with water molecules (red): 1,3 contains K^+ at positions 1 and 3, 2,4 contains K^+ at positions 2 and 4 [taken from (MacKinnon, 2003)].

Potassium selectivity is determined by the selectivity filter, located in the extracellular third of the ion pathway, between the central cavity and the extracellular solution. The K^+ channel signature sequence amino acids [G(Y/F)GD] (Papazian *et al.*, 1987; Aiyar *et al.*, 1996; Doyle *et al.*, 1998), conserved in K^+ channels throughout the phylogeny, form the selectivity filter. Here, K^+ ions bind in an essentially dehydrated state, surrounded by eight oxygen atoms from the protein, four 'above' and four 'below' each ion. The arrangement of protein oxygen atoms surrounding each binding site in the selectivity filter mimics the hydrated K^+ ion observed in the central cavity. Potassium ions are therefore able to diffuse from water into the selectivity filter where the energetic cost of dehydration is compensated. Sodium ions, on the other hand, do not seem to enter the selectivity filter in crystal structures even when Na^+ is present in vast excess (Zhou *et al.*, 2001; Zhou & MacKinnon, 2003). It is also important to remark that the structure of K_v channels differs from that of the non-voltage-gated bacterial potassium channel KcsA due to a sharp-bend in the S6 helices (equivalent to the inner helices

of the KcsA channel). This bend occurs at a Pro-X-Pro sequence that is absolutely conserved in the K_v1-4 family of channels, but it was not found in KcsA (del Camino *et al.*, 2000; del Camino & Yellen, 2001).

1.3. MODULATORY SUBUNITS

The diversity of K_v channels structure and function is enhanced by heteromultimerization of different α-subunits and also by the effects of accessory β subunits (Tamargo *et al.*, 2004). Although the assembly of these regulatory subunits with the pore-forming α-subunit is not mandatory to form the ion channel, they form complexes with the α-subunit that modify their electrophysiological characteristics. Therefore, recapitulation of the physiological features of the native K^+ current frequently requires the introduction of the actions of accessory β-subunits. K^+ channel β-subunits represent a diverse molecular group, which includes cytoplasmic proteins (K_vβ1-3; the *K Channel Interacting Protein* or KChIP, mainly associated with K_v4 family; and the *K Channel Associated Protein* or KChAP) that interact with the intracellular domains of K_v channels; and transmembrane proteins, such as KCNE1 and KCNE2 subunits encoded by the *KCNE* gene family with 1TM; DPPX proteins or dipeptidil-aminopeptidases CD26-related also with only 1TM; and, on the other hand, proteins like *K^+ channel regulator protein 1* (KCR1) for K_v10.1 channels, or the sulfonylurea receptors (SUR) for the inward rectifiers Kir6.1-6.2, with 12TM (Tamargo *et al.*, 2004; Pongs & Schwarz, 2010). Moreover, coexpression of β subunits with α-subunits regulates cell surface expression, gating kinetics and drug-sensitivity of K^+ channels. Most K_vβ2 subunits assemble with α-subunits giving rise to a $\alpha_4\beta_4$ complex (Orlova *et al.*, 2003; Gonzalez *et al.*, 2010). However, it has been described that the K_vβ1 family (like the K_vβ subunit in which this Doctoral Thesis is focused) is consistent with the $\alpha_4\beta_n$ model (where n equals 0, 1, 2, 3, or 4) depending upon the relative concentration of alpha and beta subunits (Xu *et al.*, 1998). K_v channels play critical roles in the electrical responses throughout the cardiovascular system, being responsible for establishing the resting membrane potential and cellular repolarization in heart and peripheral vascular beds (Nelson & Quayle, 1995; Nerbonne & Kass, 2005; Jackson, 2005).

1.3.1. K_vβ subunits

The K_vβ subunits are cytoplasmic proteins with a molecular weight of ~40 kDa. The proteins β1, β2, and β3 are encoded by different genes, and additional variability is produced by alternative splicing of the *KCNAB1* gene on the N-terminal region, which generates the K_vβ1.3 subunit in which is based this Doctoral Thesis (England *et al.*, 1995a; Pongs *et al.*, 1999). These K_vβ subunits are aldo-keto reductase proteins forming a sensor of the redox state into the cell (Majumder *et al.*, 1995; Bahring *et al.*, 2001; Weng *et al.*, 2006). As it was confirmed by its crystal structure, K_vβ2 is an oxidoreductase enzyme

complete with a nicotinamide co-factor ($NADP^+$) in its active site which is structurally competent to mediate hydride transfer chemistry (Gulbis *et al.*, 1999). Therefore, these subunits may result relevant for the coupling between the cellular redox state and channel activity (Bahring *et al.*, 2001; Tipparaju *et al.*, 2005; Tipparaju *et al.*, 2007; Pan *et al.*, 2011). As stated above, $K_v\beta$ proteins follow the $\alpha_4\beta_n$ model (where n equals 0, 1, 2, 3, or 4) depending upon the relative concentration of alpha and beta subunits (Xu *et al.*, 1998). The C-termini of the $K_v\beta$ bind to the T1 domains of the α-subunits, which form a docking platform for these subunits (Gulbis *et al.*, 2000) (Figure 2). Along to modulating the channel activity at the cell surface, $K_v\beta$ subunits control the surface expression of the α-subunit (Shi *et al.*, 1996) as well as the inactivation kinetics of the channels which interact with. Indeed, some beta subunits modify the slow inactivation kinetic of those channels which interact with, from a slow inactivation to another much faster inactivation (Majumder *et al.*, 1995; Morales *et al.*, 1995; Uebele *et al.*, 1998).

Table 1. Biophysical properties and characteristics of $K_v\beta$ subunits [taken from (David, 2009)].

MODULATORY $K_v\beta$ SUBUNITS				
β subunit	***Gene and chromosome***	***Interacting channel***	***Expression***	***Functions***
K_v**β1**	KCNAB1; Chromosome 3; 3q26.1	$K_v\alpha1$	Heart Brain	Induces fast inactivation Increase the surface expression of the channel
K_v**β2**	KCNAB2; Chromosome 1; 1p36.3	$K_v\alpha1$ $K_v\alpha4$	Nervous system T-Lymphocytes	Increase the surface expression of the channel
K_v**β3**	KCNAB3; Chromosome 17; 17p13.1	$K_v\alpha1.2$ $K_v\alpha1.3$ $K_v\alpha1.4$ $K_v\alpha1.5$	Human heart Rat brain	Induces fast inactivation Increase the surface expression of the channel Enhances the slow inactivation of the channel

The interaction of K_v1 α-subunits and $K_v\beta$ subunit polypeptides is an early event in K_v1 biosynthesis, occurring in the endoplasmic reticulum (Shi *et al.*, 1996; Nagaya & Papazian, 1997). Despite dramatic differences in their effects on channel gating (Table 1), each $K_v\beta$ subunit displays robust trafficking effects. Indeed, $K_v\beta1.1$, β1.2, β2, and β3 subunits increase the membrane expression and the mature form of $K_v1.2$ when they are co-expressed (Shi *et al.,* 1996; Nagaya *et al.,* 1997).

Therefore, although some cytoplasmic K_v1 channel β-subunits modify the inactivation kinetics of the α-subunits, a more general and perhaps more important role is to mediate the biosynthetic maturation and surface expression of K_v channel complexes.

1.4 OTHER K^+ CHANNEL MODULATORY SUBUNITS

The *LGI1* gene (Chernova *et al.*, 1998), carries four and a half tandem repeats of a leucine rich repeat motif at the N-terminal end and is a secreted protein (Senechal *et al.*, 2005). Lgi1 acts through its cell receptors which have been defined so far as the disintegrin and metalloprotease (ADAM) members 22 and 23 (Kunapuli *et al.*, 2009) and the Nogo receptor 1 (Thomas *et al.*, 2010). ADAM 22/23 molecules do not carry metalloproteinase domains and appear to be involved in cell adhesion (Liu *et al.*, 2009). The Nogo-66 receptor family (NgR) consists in three glycophosphatidylinositol (GPI)-anchored receptors (NgR1, NgR2 and NgR3), which are primarily expressed by neurons in the central and peripheral mammalian nervous system and they are involved in neurodegenerative diseases (Borrie *et al.*, 2012).

It has been described that Lgi1 protein interferes with $K_v\beta1$-conferred inactivation of K_v1 channels, suggesting that can modulate the gating of K_v1 channels although the molecular basis of the Lgi1 effect on K_v1 channel inactivation is presently unknown (Schulte *et al.*, 2006). Even when $K_v\beta1.3$ and $K_v1.5$ subunits are expressed in human myocardium, none current with the $K_v1.5$-$K_v\beta1.3$ phenotype have been registered in any territory of the human heart. A possible explanation could be that a given protein present in this tissue modifies the $K_v\beta1.3$ activity. Lgi protein has four different isoforms (Lgi1-4) and it has been reported that they are expressed in the human heart (Gu *et al.*, 2002). In addition, Lgi1 mutations have been linked to certain types of epilepsy, some of them associated to autonomic symptoms (visceral/epigastric and cardiac palpitations) that occurred in 45% of patients (Ottman *et al.*, 1995). Also, it has been demonstrated that its differential expression in mice, reults in a model of cardiac hypertrophy (Mohamed *et al.*, 2012). Unfortunately, the role of Lgi1 at this level is unknown at the present time.

1.5 $K_v1.5$ CHANNELS

$K_v1.5$ channel is a '*Shaker-like*' K^+ channel (Papazian *et al.*, 1987), that was first cloned from human ventricle (Tamkun *et al.*, 1991) and then from atrium (Fedida *et al.*, 1993). $K_v1.5$ channels deserve special mention since their activation generates an atria-selective current of the human cardiac atrial repolarization (I_{Kur}) (Snyders *et al.*, 1993; Wang *et al.*, 1993; Fedida *et al.*, 1993; Mays *et al.*, 1995; Ravens & Wettwer, 2011), despite mRNA and protein expression of $K_v1.5$ has been described both in atria and

ventricle (Mays *et al.,* 1995) (Figure 5). This channel is encoded by the *KCNA5* gene; and, very recently, it has been proposed that both gain- and loss-of-function mutations in this gene enhance atrial fibrillation (AF) susceptibility (Christophersen *et al.*, 2013). Beside of the location of these channels at the intercalated disks (Mays *et al.*, 1995), a pattern which is disrupted after ischemic damage (Tamargo *et al.*, 2004), these channels have also been identified in vascular smooth muscle cells (Nelson & Quayle, 1995; Archer *et al.*, 1998; Cogolludo *et al.*, 2003), where they play a pivotal role in maintaining the resting membrane potential as well as in the response to hypoxia and different vasoactive agents, such as nitric oxide, endothelin-1, angiotensin-II or serotonin (Nelson & Quayle, 1995; Zhao *et al.*, 1997; Shimoda *et al.*, 1998; Hayabuchi *et al.*, 2001; Cogolludo *et al.*, 2003; Cogolludo *et al.*, 2006; Iwata *et al.*, 2014). In addition, they are expressed in many other tissues, including pulmonary arteries (Wang *et al.*, 1997), skeletal muscle (Matsubara *et al.*, 1994), brain (Swanson *et al.*, 1990), and immune cells (Jou *et al.*, 1998; Villalonga *et al.*, 2010). K_v1.5 are also involved in the maintenance of vascular smooth muscle tone, glucose-stimulated insulin release by β-pancreatic cell, cell volume regulation and cell growth (Hille *et al.*, 1999). Their important role in the cardiovascular system explains why K_v1.5 channels are potential targets for the development of new drugs useful in the treatment of several diseases like atrial fibrilation (AF) or chronic hypoxic pulmonary hypertension (Michelakis *et al.*, 2002; Pozeg *et al.*, 2003; Cogolludo *et al.*, 2006; Cogolludo *et al.*, 2009).

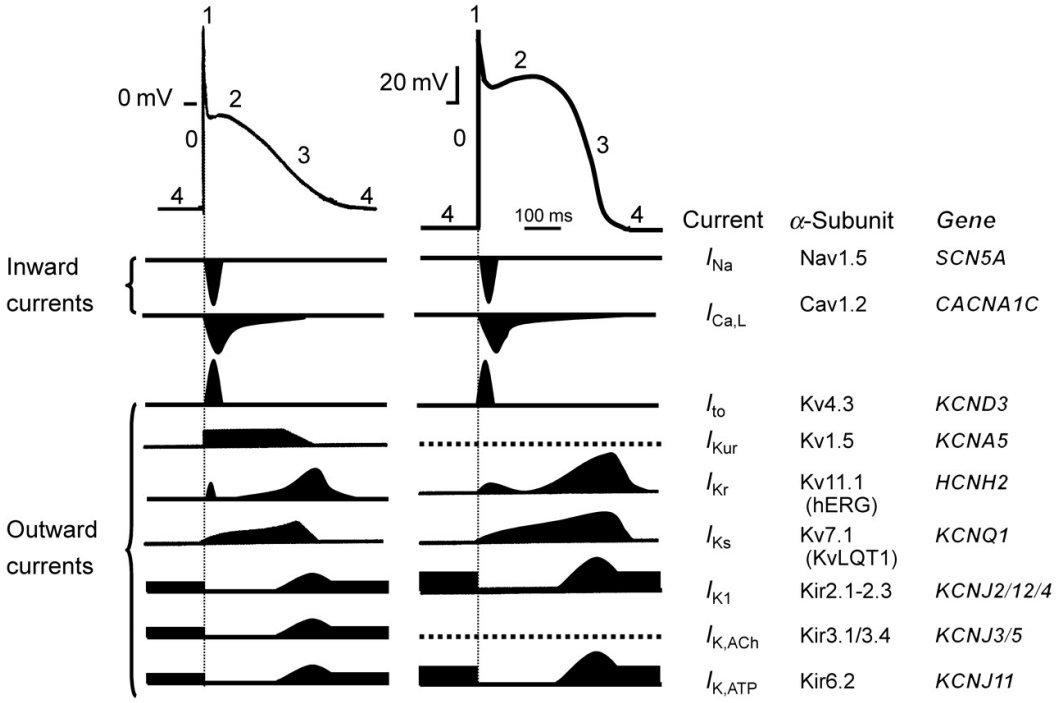

Figure 5: Inward depolarizing and outward repolarizing currents that underlie the atrial and ventricular action potential. Inward currents: I_{Na} sodium current; $I_{Ca,L}$ L-type calcium current; I_{to} transient outward current; I_{Kur} ultra rapidly activating delayed rectifier current; I_{Kr} and I_{Ks} rapidly and slowly activating delayed rectifier current; I_{K1} inward rectifier current; $I_{K,ACh}$ acetylcholine-activated potassium current. Note that I_{Kur} is present in atria only. Phase 0, rapid depolarization; phase 1, rapid early repolarization; phase 2, slow repolarization ('plateau' phase); phase 3, rapid late repolarization; phase 4, resting membrane potential [Adapted from (Ravens & Cerbai, 2008)].

Heterologous expression of $K_v1.5$ results in an outward current with a midpoint for activation potential of ≈0 mV (Snyders *et al.*, 1992; Snyders *et al.*, 1993; Fedida *et al.*, 1993; Valenzuela *et al.*, 1995a). $K_v1.5$ channels display outward rectification and very slow inactivation during strong depolarizations. At room temperature, current activates rapidly at potentials between 0 and +60 mV (τ_{act} <10 ms) and inactivates slowly and partially, i.e. by 10-20% after 250 ms at +60 mV. Temperature-dependent inactivation follows a bi-exponential slow time course with time constants of ≈240 and 2700 ms (Valenzuela *et al.*, 1996; Amos *et al.*, 1996; Macias *et al.*, 2010). $K_v1.5$ channel subunits can assemble as homo- or heterotetramers (Coetzee *et al.*, 1999; Villalonga *et al.*, 2010; Moreno *et al.*, 2013) through T1 domain as well as the first transmembrane segment (S1) (Babila *et al.*, 1994). In addition, they can associate with different β subunits, increasing the diversity of potassium currents in the human myocardium and other tissues (Coetzee *et al.*, 1999; Moreno *et al.*, 2013), which is further increased because the expression pattern of the channel subunits (α and β) is distinct between different tissues (myocardium *vs.* vascular smooth muscle) and between different regions within the same tissue (ventricular endocardium *vs.* ventricular epicardium) (Rhodes *et al.*, 1995; Shamotienko *et al.*, 1997; Martens *et al.*, 1999; Abbott *et al.*, 2007; Qin *et al.*, 2012). Even more, the expression pattern of both α and β subunits can be altered in different pathologies, which may lead to dramatic changes in the electrophysiological characteristics of a given K_v current. Gating kinetics, together with the relative expression levels of each K_v channel type in a particular cell, are determinants of the action potential characteristics. Therefore, in order to design more clinically useful drugs we need to understand how the alpha subunits generate K_v currents and how different effectors facilitate and influence subunit assembly and trafficking, as well as channel regulation (regulatory subunits, enzymes and other modulators) (Abbott *et al.*, 2007; David *et al.*, 2012).

1.5.1. $K_v1.5$ pharmacology

$K_v1.5$ channels deserve special mention in the cardiac pharmacology since their activation generates an atria-selective current (it is absent in ventricle). Thus, $K_v1.5$ channels are considered drug targets with antiarrhythmic potential (Ravens *et al.*, 2013). The anticipated antiarrhythmic mechanism of I_{Kur} blockers is the prolongation of the atrial action potential duration (APD) and effective refractory period (ERP) without any effect on QT-interval (Amos *et al.*, 1996; Li *et al.*, 1996; Caballero *et al.*, 2001; Matsuda *et al.*, 2001; Knobloch *et al.*, 2002; Brendel & Peukert, 2003). For these reasons, I_{Kur} has received a lot of interest as a potential drug target for the development of new antiarrhythmic drugs effective in the treatment of AF (Ford & Milnes, 2008; Tamargo *et al.*, 2009; Ravens, 2010; Ravens & Wettwer, 2011) and/or atria flutter without the risk of ventricular proarrhythmia (Brendel & Peukert, 2003). Indeed, numerous compounds have been screened for high $K_v1.5$ selectivity against all major cardiac ion channels, electrophysiologically characterized in isolated cardiomyocytes and cardiac tissue, and tested for their antiarrhythmic activity in various animal models of AF (Ravens *et al.*, 2013). The pharmacological

characterization of this channel revealed that I_{Kur} is almost insensitive to external TEA (Snyders *et al.*, 1993; Grissmer *et al.*, 1994), Ba^{2+} and class III antiarrhythmics of the methanesulfonanilide group (Grissmer *et al.*, 1994; Feng *et al.*, 1997), but is highly sensitive to 4-AP and internal TEA (Snyders *et al.*, 1993; Wang *et al.*, 1993; Grissmer *et al.*, 1994; Wang *et al.*, 1995). Despite these efforts, proof-of-concept of antiarrhythmic efficacy in human is still lacking. In order to fill this gap, a 'first-in-human' study was recently reported with the highly selective I_{Kur} blocker MK-0448 (Pavri *et al.*, 2012). However, the question of whether or not I_{Kur} block is effective in pharmacological conversion of recent onset AF into SR and/or reducing AF burden by maintenance of SR remains unanswered.

$K_v1.5$ channels are also very sensitive to block produced by antiarrhythmic drugs and local anesthetics which are weak bases that predominate in their cationic form at physiological pH. The neutral form of these drugs crosses the lipid membrane establishing an equilibrium between the external and the internal side of the cell membrane. These drugs dissociate (both at the external and at the internal side of the membrane) into their cationic forms establishing an equilibrium that will depend on the pH. The active form of these drugs is the cationic form that binds from the inside of the membrane to a receptor site located at the internal mouth of the ionic pore (Snyders *et al.*, 1992; Valenzuela *et al.*, 1995a; Valenzuela *et al.*, 1996; Franqueza *et al.*, 1997; Valenzuela *et al.*, 1997). It has been proposed that most of the critical residues for hydrophobic binding of quinidine in the $K_v1.5$ channel are aligned on one side of the putative S6, so that it is hypothesized that this region is the pore-lining one and is important in determining drug affinity and specificity (Snyders *et al.*, 1992). Stereoselective bupivacaine block of $K_v1.5$ channels (Valenzuela *et al.*, 1995b) is determined by a polar interaction with T507 and two hydrophobic interactions at positions L510 and V514 (Franqueza *et al.*, 1997). The length of the alkyl substituent at position 1 of bupivacaine-related local anesthetics determine their potency and stereoselectivity, likely because this alkyl chain interacts with a hydrophobic residue (L510) in the S6 of the channel (Longobardo *et al.*, 1998). In contrast, at low concentrations, uncharged-neutral as benzocaine (Delpon *et al.*, 1999; Caballero *et al.*, 2002), nifedipine (Zhang *et al.*, 1997), loratadine (Delpon *et al.*, 1997) and negatively charged drugs as angiotensin II type 1 receptor antagonists (Caballero *et al.*, 2000; Caballero *et al.*, 2001; Moreno *et al.*, 2003) modify the gating properties of $K_v1.5$ channels without obvious blockade. At higher concentrations, these drugs produce a voltage-dependent block, but their voltage-dependence is exactly a mirror image of that observed in the presence of cationic drugs (Fedida, 1997; Franqueza *et al.*, 1998; Caballero *et al.*, 2001). Furthermore, the residues in the S6 segment that determine the binding of quinidine and bupivacaine also determine the binding of neutral and acid drugs [benzocaine (Caballero *et al.*, 2002)] suggesting the existence of a common receptor site at the channel level (Decher *et al.*, 2004). The involved residues face towards the central cavity and overlap with putative binding sites for other blockers and K_v channels, like $K_v10.1$ and $K_v7.1$, suggesting a conservation of drug binding sites among different K^+ channel families (Tamargo *et al.*, 2004). However the pharmacology of these channels can be modified by the presence of variations in their structure like polimorfism (Drolet *et al.*, 2005; Simard *et al.*, 2005) or

their assembly with modulatory subunits, such as the $K_v\beta1.3$ subunit, which explains itself why in the presence of this modulatory protein the potency of bupivacaine and quinidine block of these channels is reduced, as well as the degree of stereoselective block (Gonzalez *et al.*, 2002; Arias *et al.*, 2007). It has been also reported that there exists an external binding site for the cationic form of bupivacaine, although its molecular nature is unknown (Longobardo *et al.*, 2000; Longobardo *et al.*, 2001).

1.5.2. $K_v1.5$ recycling

The complexes conformed by $K_v1.5$ and $K_v\beta$ subunits are assembled at an early stage of channel synthesis in the endoplasmic reticulum. Channel density at the cell surface, with or without β subunits, is a function of the equilibrium between trafficking to the surface and internalization dynein motor-dependent (Choi *et al.*, 2005). The fate of internalized $K_v1.5$ channels can be controlled by punctual residues located in the channel-pore domain (Manganas *et al.*, 2001), as well as by post-translational modifications including phosphorylation (Holmes *et al.*, 1996; Kwak *et al.*, 1999a; Kwak *et al.*, 1999b; Nesti *et al.*, 2004), sumoylation (Benson *et al.*, 2007), thioacylation (Zhang *et al.*, 2007), or modulation by PKA (Mason *et al.*, 2002) and PKC (Williams *et al.*, 2002).

The $K_v1.5$ channel recycling is highly controlled by specific Rab-GTPase. Thus, the internalization of the channel is carried out via Rab5 and it is rapidly targeted for recycling to the plasma membrane although a fraction of the channels are Rab7-targeted for degradation (Zadeh *et al.*, 2008). A fraction of $K_v1.5$ channels on the cell membrane is rapidly internalized with a half time of ≈10 min and some of the channels return quickly to the surface membrane with a half time of ≈30 min, and also with a slower recycling rate 2 h<τ<24 h, Rab4- and Rab11-meadiated respectively (McEwen *et al.*, 2007).

Specific concentration- and time-dependent internalization of $K_v1.5$ channels with possible permanent degradation of channels after long-term treatment, may also contribute to I_{Kur} reduction in therapy with conventional antiarrhythmic drugs, e.g. quinidine (Schumacher *et al.*, 2009). Surprisingly, within the $K_v1.5$ channel protein there is partial, but not complete, overlap in the binding sites required for quinidine-induced internalization and pore block and this fact highlight again the possibility for development of new agents that specifically enhance $K_v1.5$ channel internalization as an alternative and potentially beneficial new therapeutic strategy (Schumacher & Martens, 2010). Therefore, it would be of interest to determine how this system is used by the heart to modulate the expression of $K_v1.5$ and other ion channels as a mechanism to regulate cardiomyocyte excitability, and how other channels are affected by perturbations of retrograde trafficking. It is also possible that in certain disease states associated with channel remodeling, like atrial fibrillation and congestive heart failure, the trafficking or endocytosis mechanisms described above may be of key importance in determining the final population of surface-expressed channels. For example, it has been reported that microtubule abundance is increased in the myocytes of patients with congestive heart failure (Aquila *et al.*, 2004).

1.5.3. K_v1.5-mediated channelopathies

Although AF is not primarily considered an inheritable disease, recent epidemiological studies have provide evidence that gene polymorphisms may substantially enhance disease susceptibility (Gudbjartsson *et al.*, 2007; Kaab *et al.*, 2009; Ellinor *et al.*, 2010; Fedele *et al.*, 2013). A few cases of familial AF have been associated with genetic abnormalities relating to mutations in genes encoding for ion channels (Lubitz *et al.*, 2009). Patients with 'lone' AF lack heart disease or risk factors. Screening these patients for genetic aberration revealed a nonsense mutation in *KCNA5* in one patient with familial AF, which is absent in several hundred unrelated control individuals. When this mutation is heterozygously expressed, the defective gene encodes for a truncated K_v1.5 channel that fails to generate I_{Kur} (Olson *et al.*, 2006). Absence of I_{Kur} may excessively prolong atrial APD with an enhanced risk of early after-depolarizations that can trigger and/or maintain AF. Three further *KCNA5* loss-of-function mutations have been recently reported in 4 of the 120 unrelated AF families (Yang *et al.*, 2009; Christophersen *et al.*, 2013).

1.6 K_v1.5-K_vβ1.3 CHANNELS: CHARACTERISTICS AND MODULATION

Until now, a large number of β subunits, able to modify K_v1 channels, have been cloned from brain (Scott *et al.*, 1994; Rettig *et al.*, 1994; Heinemann *et al.*, 1995) and heart (Majumder *et al.*, 1995; Morales *et al.*, 1995; England *et al.*, 1995a; England *et al.*, 1995b). Based on the high homology between their sequence, these regulatory β subunits have been classified into three subfamilies: K_vβ1, K_vβ2 and K_vβ3 (England *et al.*, 1995b). The assembly between alpha and beta subunits is produced through specific domains at the N-terminus of the alpha subunit and the C-terminus of the β subunit. The sequences of the C-termini of β subunits are highly conserved, with the greatest differences in the N-termini (Yu *et al.*, 1996; Wang *et al.*, 1996; Sewing *et al.*, 1996). More specifically, until date three β subunits have been cloned from human myocardium: K_vβ1.2, K_vβ1.3 and K_vβ2.1, all of them cytoplasmic and with the ability of modulate K_v1.5 channels (Deal *et al.*, 1996). K_vβ1.2 and K_vβ1.3 are products of alternative splicing of the same gene (*KCNAB1*), with an identical C-terminus. The activation kinetics of channels formed by the assembly of K_v1.5 and K_vβ1.2 or K_vβ1.3 was not changed in comparison with that of K_v1.5 channels. However, K_vβ1.x change K_v1.5 current from a typical delayed rectifier to another with an incomplete fast inactivation superimposed to the slow inactivation characteristic of the K_v1.5 channels.

More specifically, K_vβ1.3 subunit interacts with K_v1.5 channel by two negatively charged residues on the core domain and three positively charged ones on the N terminus (Pan *et al.*, 2011). This interaction provides a number of functions to the channel, including a fast and partial inactivation

component, which is mediated by an equilibrium binding of the N-terminus of $K_v\beta1.3$ between PIPs and the inner pore region of the channel (Decher *et al.*, 2008) that overlaps with the bupivacaine and quinidine binding site of the channel (Decher *et al.*, 2005; Gonzalez *et al.*, 2010). An enhancement of the slow inactivation characteristic of $K_v1.5$ channel, a shift of the activation curve toward more negative potentials, functionally distinct from the inactivation (Uebele *et al.*, 1998); a 7-fold decrease in the sensitivity of the channel to the block induced by antiarrhythmic drugs and local anesthetics, and a decrease in the degree of stereoselective blockade (Gonzalez *et al.*, 2002; Decher *et al.*, 2005; Arias *et al.*, 2007). In addition, interaction of $K_v\beta$ subunits with $K_v1.5$ controls channel trafficking to the plasma membrane (Shi *et al.*, 1996; Accili *et al.*, 1997; Kuryshev *et al.*, 2001). $K_v1.5$ channels are highly regulated by the adrenergic system, which is differentially modulated by α and β stimulation (Li *et al.*, 1996) via PKC and protein kinase A (PKA), respectively (Murray *et al.*, 1994; Kwak *et al.*, 1999a; Kwak *et al.*, 1999b). PKC and PKA activities are also required for the $K_v1.5$ modulation by the auxiliary subunits $K_v\beta1.2$ and $K_v\beta1.3$ (Kwak *et al.*, 1999a; Kwak *et al.*, 1999b; Williams *et al.*, 2002), since their effects are abolished after removal of a consensus PKA phosphorylation site on the $K_v\beta1.3$ N-terminus (S24) or following incubation with calphostin C, a PKC inhibitor (Kwak *et al.*, 1999b).

1.6.1. PKC modulation of $K_v1.5$-$K_v\beta1.3$ channels

$K_v1.5$ has one consensus site for phosphorylation by PKC located on the extracellular S4–S5 linker and 4 consensus sites for PKA located in the N- and C-terminal domains. Isoproterenol increases I_{Kur} in human atrial myocytes and this effect is mimicked by direct stimulation of adenylate cyclase and suppressed by a PKA inhibitor peptide (Li *et al.*, 1996). In the presence of propranolol, phenylephrine inhibits I_{Kur}, an effect that is prevented by the PKC inhibitor bisindolylmaleimide. These results indicate that β-adrenergic stimulation enhances, whereas α-adrenergic stimulation inhibits I_{Kur} and suggest that these effects are mediated by PKA and PKC, respectively (Tamargo *et al.*, 2004), and therefore those kinase activities may have an important role in the treatment of cardiac diseases. In fact, cardiac hypertrophy is associated with an up-regulation of different PKC isoforms (Takeishi *et al.*, 1999; Kerkela *et al.*, 2002; Braz *et al.*, 2002; Hahn *et al.*, 2003). Similarly, δ-calmodulin kinase II (δ-CaMKII) expression increases during atrial fibrillation (Tessier *et al.*, 1999). Furthermore, one of the most effective treatments for atrial fibrillation is the oral administration of β-blockers (Kuhlkamp *et al.*, 2000), which induce a pharmacological remodeling that is capable of reversing the electrical dysfunction typically observed during atrial fibrillation (Workman *et al.*, 2003; Valenzuela, 2003). Regarding the PKA effect, it has been proposed that the coexpression of both in $K_v1.5$ and $K_v\beta1.3$ is required for the PKA-mediated increase in K^+ current (Ravens & Wettwer, 2011). Indeed, the enhancing effect on $K_v1.5$ inactivation by coexpression of $K_v1.5$ with $K_v\beta1.3$ is attenuated when $K_v\beta1.3$ is phosphorylated explaining the β-adrenoceptor-stimulated current increase (Kwak *et al.*, 1999a).

Stimulation of PKC has little effect on expressed $K_v1.5$ channels alone. However, co-assembly of $K_v\beta1.2$ with $K_v1.5$ enhances the response of the channel to PKC activation with a reduction in the K^+ current (Williams *et al.*, 2002). These results suggest that phosphorylation sites for PKC are probably located in the $K_v\beta1.2$ or in a residue of the channel exposed after the association with it. It has been also described that PKC inhibition by calphostin C reverses the $K_v\beta1.3$-dependent electrophysiological effects (Kwak *et al.*, 1999b). However, it has been described that this effect was not observed when several inhibitors PKC isoforms-specific were used, was not due to a dissociation of both subunits, and the channel conforms a protein complex with, at least, RACK1 and PKCβII (David *et al.*, 2012). However, the specific mechanism by which calphostin C produces an abolishment of the effect $K_v\beta1.3$-meadiated remains unknown.

1.6.2. PIP_2 effects on $K_v1.5$-$K_v\beta1.3$

Phosphatidylinositol 4,5-bisphosphate ($PtdIns(4,5)P_2$ or PIP_2) is the most abundant phosphoinositide localized at plasma membranes of eukaryotic cells (Logothetis *et al.*, 2010). PIP_2 is a well-recognized lipid precursor molecule that has garnered appreciation as a regulator of many physiological processes in both animal and plant cells for more than three decades (Michell, 2009). Since the mid-1990s, when three reports of PIP_2 regulation of K_{ATP} channel activity appeared (Furukawa *et al.*, 1996; Hilgemann & Ball, 1996; Fan & Makielski, 1997), there has been an explosion of reports demonstrating a dependence of the activity of most ion channels on the presence of phosphoinositides. In fact, co-expression of $K_v1.5$ channels and human thrombin or rat serotonin receptors, two receptors that increase phospholipase C (PLC) activity, inhibits $K_v1.5$ current amplitude without modifying the kinetics or voltage sensitivity of activation (Timpe & Fantl, 1994; Cogolludo *et al.*, 2006). Simultaneous injection of inositol 1,4,5-trisphosphate and superfusion of PMA reproduces the modulation of the $K_v1.5$ current suggesting that these receptors modulate $K_v1.5$ channels by increasing PLC activity.

PIP_2 antagonizes N-type inactivation of $K_v3.4$ by binding to its N-terminal domain and immobilizing the inactivation ball and that removes fast inactivation of $K_v1.1$ channels by immobilization of $K_v\beta1.1$ (Oliver *et al.*, 2004). In addition, $K_v\beta1.3$-mediated inactivation of $K_v1.5$ is mediated by an equilibrium binding of the N-terminus of $K_v\beta1.3$ between phosphoinositides (PIPs) and the inner pore region of the channel (Decher *et al.*, 2008).

Given the key role that membrane phosphoinositides play in regulating channel activity, it is important to highlight that fluctuations in intracellular PIP_2 levels due to Gq-coupled receptor stimulation might be relevant for the inactivation of K^+ channels and therefore, for electrical signaling in both heart and brain (Decher *et al.*, 2008; David, 2009). Thus, it is surprising that only a small number of channelopathies have been linked to phosphoinositides. And, for this reason, it has been proposed that channel-PIP_2 interactions should be tested mainly in those channels whose activity is PIP_2-dependent and in cases in

which ion channel mutations, important for that modulation lipids-mediated, can lead to channelopathies (Logothetis *et al.*, 2010).

1.7 PHYSIOLOGICAL ROLE: THE CARDIAC ACTION POTENTIAL

The normal electrophysiological behavior of the heart is determined by the ordered propagation of excitatory stimuli resulting in rapid depolarization and slow repolarization, generating action potentials (AP) in individual myocytes. At the most generic level, abnormalities of impulse generation, propagation, or the duration and configuration of individual cardiac action potentials form the basis of disordered cardiac rhythm. These concepts evolved during the twentieth century from clinical descriptions of arrhythmias, to descriptions of AP in specific regions of cardiac tissue, and led to the identification of specific whole-cell and single-channel ionic currents whose integrated activity generates action potentials. In the past decade, those genes whose expression generate specific molecular components, including pore-forming ion channel proteins, underlying individual ion currents in cardiac myocytes were defined. K^+ currents control the repolarization process of the cardiac action potential, determines membrane potential, the heart rate, myocardium refractoriness and, therefore, they represent important targets for the actions of neurotransmitters, hormones, drugs and toxins known to modulate cardiac function (Snyders, 1999; Coetzee *et al.*, 1999; Nerbonne, 2000; Ravens & Cerbai, 2008). The cardiac ventricular action potential exhibits five distinct phases (Figure 6): *Phase 0* corresponds to the rapid depolarization (or action potential upstroke) that ensures once the cell reaches the voltage threshold. At rest, the dominant membrane conductance is provided by the potassium channels. However, once the cell reaches a threshold level of approximately −65 mV, membrane sodium channels open. Hence, at threshold, the membrane rapidly switches from being mostly permeable to K^+ to being largely permeable to Na^+. The sodium current (I_{Na}) represents a very large and rapid transition. When the conductance to sodium suddenly increases, the large transmembrane gradient of Na^+ leads to a rush of ions into the cell in the form of an inwardly directed negative I_{Na}. Thus, the membrane rapidly depolarizes, and results in the upstroke of the action potential. In fact, given that during this phase the cell membrane is mostly permeable to Na^+, the membrane potential becomes transiently positive as it moves toward E_{Na} (approximately +40 mV). However, the increase in sodium conductance is very brief, and after a few milliseconds, the sodium channels enter in a nonconductive state. The membrane potential does not reach the sodium equilibrium potential, but stops at approximately ≈+30 mV and then begins to repolarize. *Phase 1* corresponds to the brief, rapid repolarization that is initiated at the end of the action potential upstroke and it is interrupted when the cell reaches the “plateau level” or phase 2. As shown in Figure 6, the end of the action potential upstroke is brought by the inactivation of the sodium channels. During the initial phase of repolarization of the action potential, or phase 1, potassium channels provide the dominant membrane conductance. Although there

can be important differences in the ionic currents that are activated at this stage, depending on the region of the heart from which the cells originate (and also depending on the animal species studied), in most cases the so-called "transient outward current" (I_{to}) provides most of the repolarizing charge. This rapidly activating potassium conductance turns on during the end of the action potential upstroke. When the sodium channels enter into their nonconductive state, repolarization begins in earnest, with the membrane potential heading toward the reversal potential for potassium. I_{to} inactivates also very rapidly, and its contribution to the repolarizing process during phases 2 and 3 of the action potential is smaller than that observed during phase 1. During the plateau or *Phase 2* repolarization progresses very slowly. Other voltage dependent membrane channels are also activated by cell depolarization, although they activate at a slower rate (Figure 6). Consequently, these channels provide a sizable current only several milliseconds after the end of the action potential upstroke. The two dominant currents during the phase 2 of the action potential are the inward calcium current (I_{Ca}) and the delayed rectifier potassium outward current (I_K), (including, the L-type calcium current and electrogenic sodium–calcium exchanger). The potassium current I_K includes, at least, two separate components: a rapid component (I_{Kr}) and a slow component (I_{Ks}). Note that, as it was stated above, the ultrarapid component (I_{Kur}) only appears in the atrial action potential as it can be observed in Figure 5. Given the concentration gradient for Ca^{2+}, opening of calcium channels leads to movement of calcium from the extracellular to the intracellular space (i.e., an inwardly directed, depolarizing current). Potassium ions, on the other hand, move in the opposite direction. The result is that, while the calcium channels remain open, repolarization by potassium currents is prevented by the presence of calcium current that is moving positive charges into the cell. Thus, during the plateau, the membrane potential depends on the balance between inward I_{Ca} and outward I_K currents. Although in some cells (e.g., Purkinje fibers, Figure 6) outward currents dominate and the plateau tends to have a consistently negative slope, in other cells there may be an actual slight depolarization before repolarization continues (in a "dome like" shape). Eventually a final phase of rapid repolarization, or *Phase 3*, ensures it. Inactivation of the calcium channels leads to the end of the plateau (Figure 6). Only potassium channels remain active; and consequently, the membrane potential returns relatively rapidly toward E_K. The delayed rectifier currents (I_{Kr} and I_{Ks}, and I_{Kur} in case) tend to close as the cell repolarizes, and thus the inward rectifier current (I_{K1}) predominates. Finally, *Phase 4* is the period between the last repolarization and the onset of the subsequent action potential. In atrial or ventricular myocytes, phase 4 corresponds to the resting membrane potential. In addition, there are differences in the expression patterns of the various voltage-gated K^+ current in cardiac cells isolated from different species, as well as in cells from different regions of the heart in the same species and these distinct K^+ current expression patterns contribute to regional differences in action potential waveforms (Figure 6). In atrial and ventricular muscle cells, the resting potential remains constant throughout the diastolic interval. In these cell types, the inward-rectifier current I_{K1} remains the dominant conductance at rest and it is largely responsible for setting the resting membrane potential. An additional small background conductance, with a more positive equilibrium potential, keeps the resting potential slightly more depolarized than the value estimated by the potassium

equilibrium potential. Atrial and ventricular myocytes remain at this level of potential until a new excitatory stimulus brings the membrane potential to threshold, thus eliciting a new active response. However, those cells which have spontaneous activity, require an hyperpolarization-activated inward current named 'funny current' or I_f current, also characterized by allowing both Na^+ and K^+ ions to pass through it. This current contributes to the spontaneous pacemaker activity in regions such as SA node, atrium, and AV node, and is believed to be a major factor in generating the pacemaker potential in Purkinje fibers (DiFrancesco, 2010).

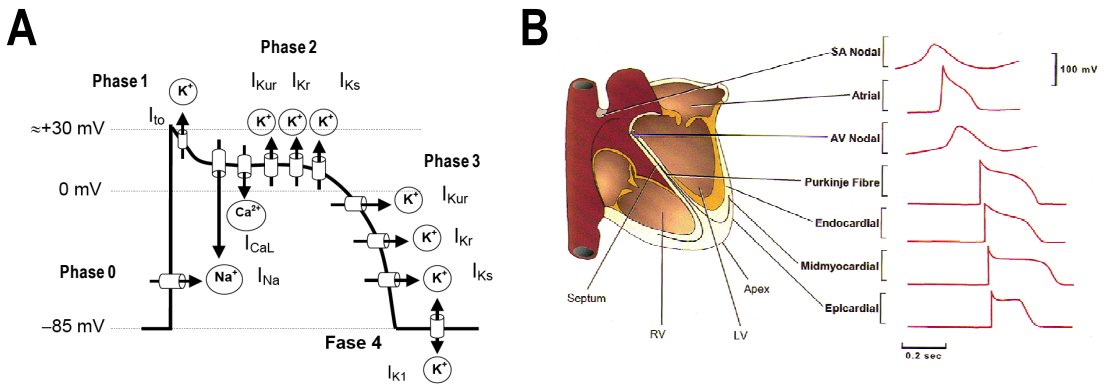

Figure 6: The cardiac action potential. **A,** Schematic representation of a Na^+-dependent action potential [taken from (David, 2009)]. **B,** Action potential waveforms are variable in different regions of the heart. Schematic representation of the heart; action potential waveforms recorded in different regions of the heart are illustrated. Action potentials are displaced in time to reflect the temporal sequence of propagation through the heart. SA, sino-atrial; AV, atrio-ventricular; RV, right ventricle; LV, left ventricle [taken from (Nerbonne, 2000)].

2. OBJECTIVES

The subcellular location of signal transduction proteins, enzymes, substrates and mediators has been revealed as an essential feature for an optimal, fast and efficient transmission of signals either from the extracellular or from intracellular medium. Thus, ion channels are present, in the different tissues, forming signaling complexes or *channelosomes*. In the past decade a myriad of protein-protein interactions involved in intracellular signaling have been described (Hubbard & Cohen, 1993; Mochly-Rosen, 1995; Burack & Shaw, 2000). The subcellular location of signal transduction proteins, enzymes, substrates and mediators has been revealed as an essential feature for an optimal, fast and efficient transmission of signals either from the extracellular or from intracellular medium (Pawson & Nash, 2003). Thus, ion channels present in the different tissues are forming signaling complexes or *channelosomes*. Inhibition of PKC prevented the $K_v\beta1.3$-induced fast inactivation (Kwak *et al.*, 1999b). We have recently demonstrated that only the inhibition of PKCβ isoforms was necessary to prevent the $K_v\beta1.3$-induced fast inactivation; supporting that each PKC isoform mediates unique subcellular functions (Dempsey *et al.*, 2000; Jaken & Parker, 2000) depending on the substrate that they phosphorylate (Carpenter et al., 1987; Parker et al., 1989). In this study, we show the existence of a $K_v1.5$ *channelosome* in rat ventricle, that is absent in atria, in which RACK1 acts as a link between $K_v1.5$ channels, the membrane and the cytoplasmic environment. This complex is formed by, at least, $K_v1.5$, $K_v\beta1.3$, RACK1, PKCβI and PKCβII. Interestingly, we also observed that PLC also modulates the $K_v\beta1.3$-induced fast inactivation (Disatnik *et al.*, 1994; David *et al.*, 2012). Thus, the variety of signal transduction proteins and enzymes linked to RACK1 (Schechtman & Mochly-Rosen, 2001) including PKCβ (Ron et al., 1994; Csukai et al., 1997) can be due to its ability to act as a scaffold protein not only for PKCβ isoforms, but also for PLC (Disatnik et al., 1994) and other regulators such as *Src* (Chang et al., 1998) and dynamin-1 (Rodriguez et al., 1999) among others. This can explain the diversity of responses generated by PKA and PKC on I_{Kur}.

RACK1 is a scaffolding protein and a member of the WD repeat family of proteins (Mochly-Rosen et al., 1995). Its role in the immune system, the heart and the brain and its contribution to disease states such as cancer, cardiac hypertrophy and addiction has been described (Pass et al., 2001; Korzick et al., 2001; Corsini et al., 2001; Al-Reefy et al., 2010). These proteins have a unique architectural assembly that facilitates protein anchoring and the stabilization of protein activity. A large body of evidence is accumulating which is helping to define the versatile role of RACK1 in assembling and dismantling complex signaling pathways from the cell membrane to the nucleus in health and disease (Ron et al., 2013). In many RACK1-associated pathological states, aberrant RACK1 signaling, which underpins the condition, arises from either increased or decreased expression of the scaffolding protein (Ron et al., 2013). Presumably, sub-optimal protein levels of RACK1 interfere with its compartmentalization and, in turn, hinder the formation of signaling complexes with correct stoichiometry at discrete intracellular locations. Thus, it is reasonable to hypothesize that the therapeutic potential of RACK1 could be realized by small molecules that selectively target RACK1 interacting proteins.

The *LGI1* gene (Chernova *et al.*, 1998), carries four and a half tandem repeats of a leucine rich repeat motif at the N-terminal end and is a secreted protein (Senechal *et al.*, 2005). Lgi1 receptors that have been defined so far, and depending on cell context, are the disintegrin and metalloprotease (ADAM) members 22 and 23 (Kunapuli *et al.*, 2009) and the Nogo receptor 1 (Thomas *et al.*, 2010). The ADAM 22/23 molecules do not carry metalloproteinase domains and appear to be implicated in cell adhesion (Liu *et al.*, 2009), which is consistent with the suggestion that LGI1 influences cell movement and invasion through reorganization of the actin cytoskeleton (Kunapuli *et al.*, 2010a). Lgi1 interferes with $K_v\beta1$-conferred inactivation of K_v1 channels, suggesting that Lgi1 can modulate the gating of K_v1 channels. The molecular basis of the Lgi1 effect on K_v1 channel inactivation is presently unknown (Schulte *et al.*, 2006). We know that, even when $K_v\beta1.3$ and $K_v1.5$ subunits are expressed in human myocardium, the current with the $K_v1.5$-$K_v\beta1.3$ phenotype had not been registered in any territory human heart (atrium or ventricle). One possible explanation could be that a particular protein present in this tissue effect modification activity $K_v\beta1.3$ subunit. Thus, we have studied the electrophysiological effects of Lgi1 on $K_v1.5$-$K_v\beta1.3$. We observed that Lgi1 prevents the $K_v\beta1.3$-induced fast inactivation and also that the current amplitude was smaller than under control conditions, effects that are due to a decreased expression of the channel in the cell membrane. Moreover, experiments from our laboratory demonstrate that Lgi1 is present in rat ventricle but not in atria, and also that $K_v1.5$ channel coimmunoprecipitates with Lgi1. Unfortunately, although it is known that Lgi1-4 isoforms are expressed in human heart, their roles at this level are unknown at the present time.

The **Hypothesis** of the present Doctoral Thesis is that $K_v1.5$ channels form signaling complexes in which $K_v1.5$-$K_v\beta1.3$ channels are regulated and physically linked to PLC, PKCβI, PKCβII and RACK1 (David *et al.*, 2012) and that modulation of the PKC or PLC activity may affect the electrophysiological and pharmacological properties of these channels.

The **Main Objective** of the present Doctoral Thesis is to analyze how the inhibition of PKC modifies the electrophysiological and pharmacological properties of $K_v1.5$-$K_v\beta1.3$ channels, as well as if Lgi1 is a new partner of the $K_v1.5$ *channelosome*.

In order to achieve this Objective, our **specific objectives** are to analyze:

1. The mechanisms by which PKC inhibition eliminates the $K_v\beta1.3$-induced fast inactivation.
2. The pharmacological consequences of PKC inhibition, by studying the effects of bupivacaine and quinidine on $K_v1.5$-$K_v\beta1.3$ channels.
3. The effects of the PKC inhibition on the traffic and recycling of $K_v1.5$ channels.
4. The role of Lgi1 on $K_v1.5$-$K_v\beta1.3$ channels.

3. MATERIALS AND METHODS

3.1. BIOLOGICAL MATERIAL

The experiments performed in this Doctoral Thesis were performed in HEK293 cells, rat and human cardiac tissue.

3.1.1. HEK293 cells: cellular culture

The HEK293 cell line was obtained from the American Type Culture Collection (RocK$_v$ille, MD, US) and cultured at 37ºC in DMEM supplemented with 10% FBS and antibiotics (1% v/v: penicillin G 100 U/mL and streptomycin 100 μg/mL, respectively; all from Gibco) in a 5% CO_2 humidified atmosphere. The culture cell medium was changed every 2-3 days, and the cells were briefly trypsinized every 4-5 days.

3.1.2. Rat samples

Rat heart samples were kindly provided by Dr. Ángel Cogolludo and Dr. Francisco Pérez-Vizcaíno (Universidad Complutense de Madrid), for immunoprecipitation experiments. Adults (8–12 weeks old) male Wistar rats, housed in a 12 h light–dark cycle animal facility and a temperature of 24±2°C, were used in this study. All procedures with animals were specifically approved by the "Ethics Committee for Animal Experimentation" of the Universidad Complutense de Madrid and carried out in accordance with the protocols issued which followed National (normative 1201/2005) and International recommendations (Directive 2010/63 from the European Communities Council). Special care was taken in all cases to minimize animal suffering.

3.1.3. Human samples

Slices of human heart samples embedded in paraffin were kindly provided by Dr. Javier Regadera (Universidad Autónoma de Madrid), for immunohistochemistry assays performed. Myocardial samples of individuals without cardiovascular histories were obtained from autopsy procedures at La Paz Hospital (Madrid). Fully written informed consent was obtained from the family of all donors. Gross and histopathological study of hearts did not show acute myocardial lesions. For histopathologic procedures, tissues were processed by fixing in 4% buffered formaldehyde and embedded in paraffin wax. Paraffin-embedded tissue sections were obtained from the archives of the pathology laboratories of the Hospital La Paz. The study protocol was approved by the respective institutional review boards and ethics committees.

3.2. cDNA CONSTRUCTIONS AND CELL TRANSFECTION

3.2.1. pBK-K_vβ1.3-IRES-K_v1.5-HA

This construction was made in order to be used in live cell imaging and in immunocytochemistry experiments, since we needed a construction which ensures that K_vβ1.3 subunit was present in all transfected cells and also that we can detect the presence of the channel in the membrane by the external side of the cell. Briefly, HA tag was digested with *BlpI* and *AflII* of a K_v1.5-HA construct kindly provided by Prof. DJ Snyders (University of Antwerpen, Belgium), and this cDNA fragment was exchanged, in the same position, within K_vβ1.3-IRES-K_v1.5 construction using the T4 DNA ligase (M1801, Promega) (see the scheme of this process in Figure 7).

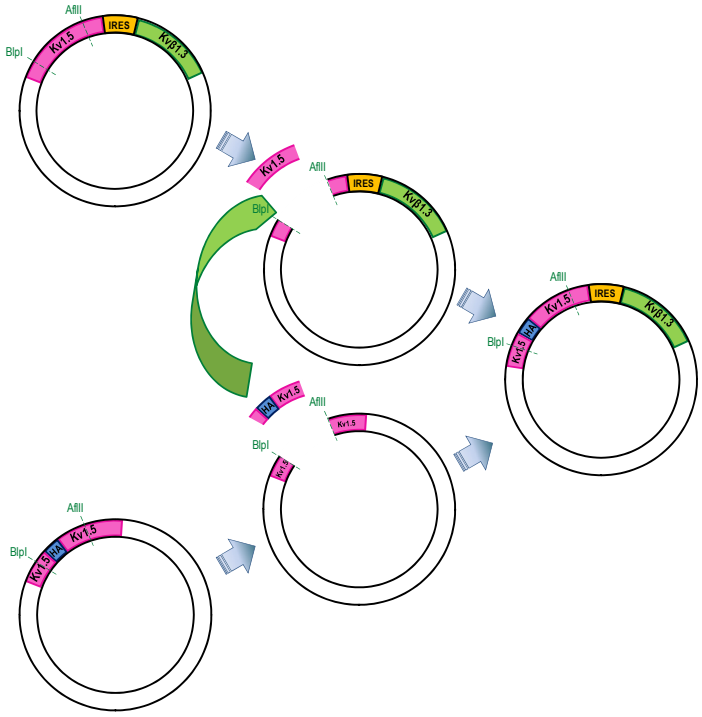

Figure 7: Scheme of the technique used to clone the pBK-K_vβ1.3-IRES-K_v1.5-HA construction. Firstly, it is necessary to have unique restriction points around de HA-tag in the donor vector and that, at the same time, this point only cut once in the acceptor vector. Once we got these restriction sites, and using these enzymes, we exchanged the insert of interest in the acceptor vector in order to get the final construction, K_v1.5-HA channel into the bicistronic construction.

3.2.2. pBK-K_vβ1.3-IRES-K_v1.5-FLAG

A FLAG epitope (DYKDDDDK) was inserted into the external side of the K_v1.5 (between S1-S2) of the K_vβ1.3-IRES-K_v1.5- cDNA construction. This construction was used for biotinylation experiments in order to increase the biotinylation efficiency. To insert this amino acid sequence between *BlpI* and *AflII*

sites in K_v1.5, flanked by single glycine codons, into the extracellular loop between S1 and S2 transmembrane segments of the channel [specifically between residues 307 and 308 according the method described by Zadeh and coworkers in 2008 (Zadeh *et al.*, 2008)], the overlapping PCR technique previously described was used (Higuchi *et al.*, 1988) (Figure 8). The following couples of primers were utilized:

on one hand,

forward (5'- cggctgggctcagcgatgggcccaaggagccggc-3') and

reverse (5'- *ccc***cttgtcatcgtcgtccttgtagtc***ccc*gccagaggcgggggccatgaccccgctgccg -3');

and on the other hand,

forward (5'-*ggg***gactacaaggacgacgatgacaag***ggg*cctacggtggcaccgctcctgcccCGTACG -3') and

reverse (5'- gctcttccttaaggactgccggctcctcgtgatcc -3'),

where the underlined nucleotides indicate the recognition sequences of restriction endonucleases *BlpI* and *AflII,* respectively; the bold ones indicate nucleotides corresponding to the FLAG sequence; the nucleotides in italics represent glycines added to provide flexibility at the front and at the back of the insert; the nucleotides in uppercase correspond with the insertion of a punctual and non-sense mutation which results in a single *BsiWI* restriction site which serve as reporter of the insertion; and the nucleotides in normal type corresponds to the normal sequence of the channel. PCR conditions included an initial denaturation step that were, in the case of the two first PCR: 98ºC (5') followed by 35 cycles of 98ºC for 1 min, 80ºC for 1 min, and a step at 72ºC for 2 min, and a final elongation step at 72ºC for 10 min; and in the case of overlapping PCR: a step at 95ºC for 30 s, followed by 20 cycles of 95ºC for 30 s, 57ºC for 30 s, and 72ºC for 1 min, and a final elongation step at 72ºC for 10 min.

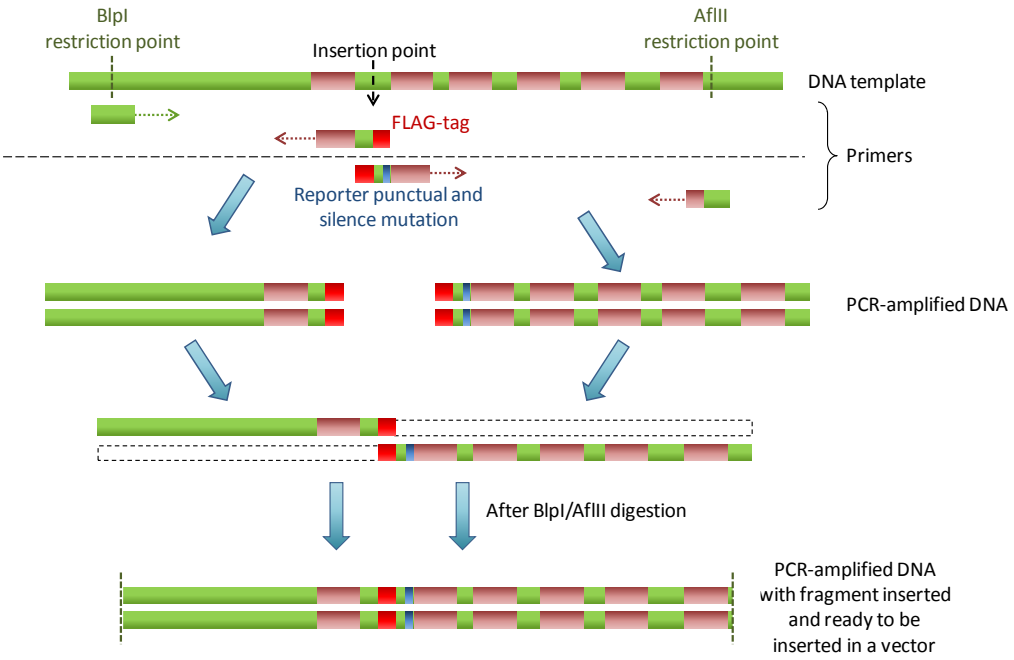

Figure 8: Schematic representation of overlapping PCR technique employed to make pBK-K_vβ1.3-IRES-K_v1.5-FLAG construction. Firstly, it is necessary to find two unique restriction points around the insertion point (between S1 and S2 transmembrane segments), *BlpI* and *AflII* in this case. Then, we ran two 'normal' PCRs, which have the fragment of interest in common, in order to amplify both segments separately. After this step, we put them together taking advantage of the overlapped fragment (FLAG-tag, in red) reconstituting the whole insert that, after the digestion with the restriction enzymes was ready to be inserted in the vector of interest. Note that the introduction of a punctual reporter and silence mutation, which result in the introduction of a novel restriction point (*BsiWI* in our case; in blue), which is highly recommended step in order to can check the different colonies after its bacterial transformation.

3.2.3. Cell transfection

For electrophysiological studies, HEK293 cells were transiently transfected with 0.8 µg of a construction widely characterized (Uebele *et al.*, 1998). Briefly, human K_v1.5 and K_vβ1.3 were cloned into the same pBK vector, with the K_v1.5 subunit placed 3' to the K_vβ1.3 subunit and preceded by an internal ribosome entry sequence (pBK-CMV-K_vβ1.3-IRES-K_v1.5), thus generating a bicistronic messenger RNA as previously described (Kwak *et al.*, 1999b) (kindly provided by Dr. MM Tamkun, Colorado State University, Fort Collins, CO, USA). In all cases, transfection was performed together with 1.6-1.8 µg of the reported plasmid EBO-pcD-Leu2-CD8 (for future selection of the transfected cells). All amounts of cDNA reported were used per 35 mm culture dish.

For the immunocytochemistry assays experiments, 3 µg of different constructions were used:

- pBK-CMV-K_v1.5-HA. Construction with a HA tag introduced into the extracellular K_v1.5 S1-S2 loop was used (kindly provided by Prof. DJ Snyders).

- pCMV-Tag5A-K_vβ1.3. Construction in which the gene encoding K_vβ1.3 was subcloned between the *SacII* and *NotI* restriction sites within the polylinker of the pCMV-Tag5A vector, which generates a recombinant K_vβ1.3-Myc protein.
- pBK-CMV-K_vβ1.3-IRES-K_v1.5-HA. Construction made using the Prof. DJ Snyders´s K_v1.5-HA construct and exchanging the fragments got after *BlpI* and *AflII* enzyme-digestion between this and K_vβ1.3-IRES-K_v1.5 constructions.
- pBK-CMV-K_vβ1.3-IRES-K_v1.5-FLAG: Construction made using the overlapping-PCR technique described below pBK-CMV-K_vβ1.3-IRES-K_v1.5.

For protein expression studies, coimmunoprecipitation, biotinylation and western blot assays, cells were transfected with 8 µg of total amount of cDNA per 100 mm culture dish, of the construction that express K_vβ1.3-IRES-K_v1.5, K_v1.5-HA, K_vβ1.3-myc or K_vβ1.3-IRES-K_v1.5-HA proteins. In the case of FRET and TIRF-FRET experiments, cells were transfected with pECFP-C1-K_v1.5 (kindly supplied by Dr. A Felipe from Universidad de Barcelona), pEYFP-N1-RACK1 cloned between *EcoRI* and *NotI* in the Dr. P de la Peña's laboratory (Universidad de Oviedo) using the pcDNA3.1-RACK1-myc construction kindly provided by Dr. K Ito. In all cases, cells were transfected with 1-2 µg of the total cDNA. For live cell imaging experiments, cells were transfected with 3 µg K_v1.5-HA construction per µ-Dish 35mm, high (from Ibidi®).

In all cases, transient transfections were carried out in HEK293 cells at ~60% confluence following the FuGENE®6-transfection method (Promega) and the experiments were carried out 48 h post-transfection. The ratio µg cDNA:µl Fugene was always 1:3.

3.3. ELECTROPHYSIOLOGICAL RECORDINGS

The patch-clamp technique was first used to resolve currents through single acetylcholine-activated channels in cell-attached patches of membrane of frog skeletal muscle (Neher & Sakmann, 1976). This method is a refinement of the voltage-clamp technique that uses, as an electrode, a glass micropipette pulled to a fine tip of approximately 1-4 µm. The recording electrode or "patch pipette" is filled with a saline solution and sealed (with a high resistance, GΩ) onto a patch on the surface of the cell membrane, allowing the researcher to keep the voltage constant while measuring the current flowing across the membrane of a cell or even form a single channel localized in the membrane patch.

Several configurations of the patch-clamp technique have been developed. The most commonly used, when studying ion currents across the cell, is the whole-cell patch-clamp technique. In this approach, after the seal formation between the electrode and the cell membrane, an additional suction it has to be applied, rupturing the cell membrane in the patch and gaining access to the cytoplasm.

Consequently, the internal pipette solution enters in direct contact with the intracellular space. The membrane of the whole cell is voltage clamped, and the recorded currents are a composite of the currents flowing through all the active channels (Figure 9).

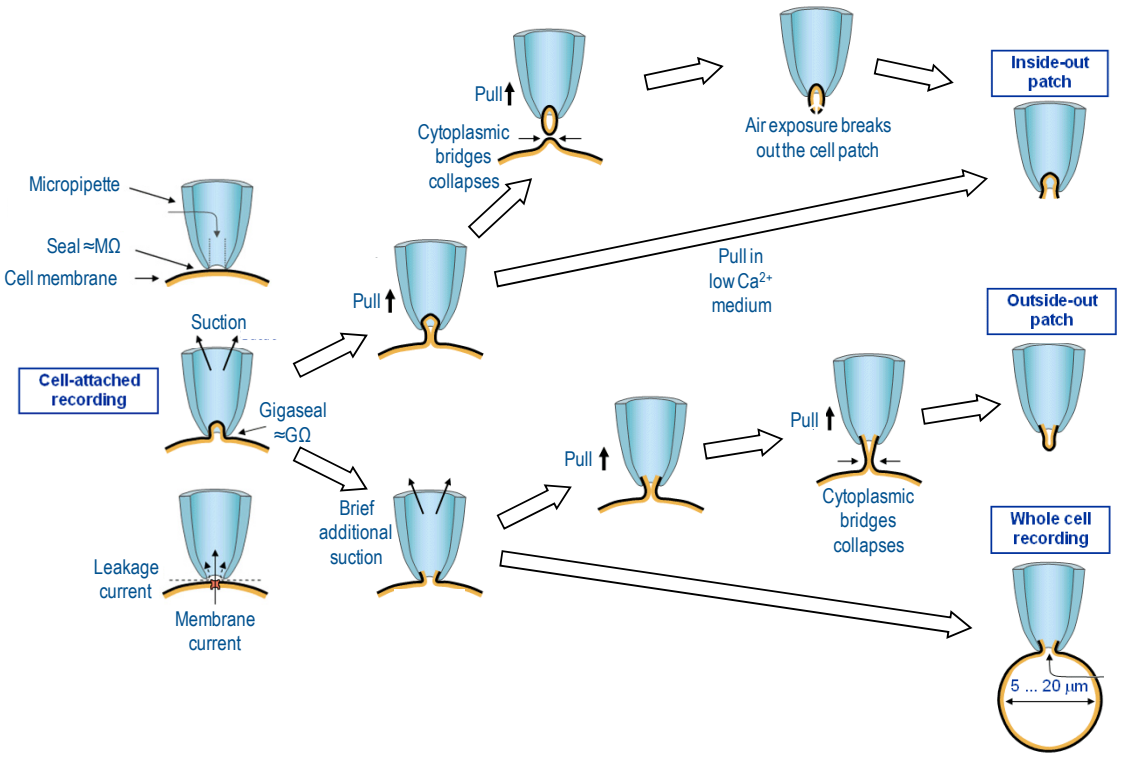

Figure 9: Patch-clamp configurations. *Scheme of the different configurations of the patch-clamp technique.* This Doctoral Thesis has been focused in whole-cell configuration in which there is continuity between the intracellular space and the pipette-filling solution. Dialysis of the cytoplasm is avoided when the perforated patch is used [modified from (Malmivuo & Plonsey, 1995)]

Before experimental use, cells were incubated with polystyrene microbeads precoated with anti-CD8 antibody (Dynabeads®, Invitrogen) (Gonzalez *et al.*, 2002; Arias *et al.*, 2007; David *et al.*, 2012). A suspension of cells was placed on a chamber mounted on the stage of an inverted microscope. Currents were recorded using the whole-cell configuration of the patch-clamp technique by using an Axopatch 200B amplifier (Molecular Devices). Experiments were performed at room temperature (22±2°C). Current recordings were low pass-filtered and sampled at 2 kHz with an analog-to-digital converter DigiData 1440A (Molecular Devices) (data acquisition system). Command voltages and data storage were controlled with pClamp9 software (Molecular Devices). Patch electrodes were pulled from borosilicate glass capillaries (GD-1, Narishige) with a P-87 puller (Sutter Instruments) and were heat polished with a microforge (MF-83, Narishige). After heat-polishing, the resistance of the patch electrodes tip (filled with the internal solution) averaged 2-4 MΩ. The cells were continuously perfused with an external solution containing (in

mM): NaCl 130, KCl 4, $CaCl_2$ 1.8, $MgCl_2$ 1, HEPES 10, and glucose 10 (adjusted to pH 7.4 with NaOH). The electrode solution contained (in mM): K-aspartate 80, KCl 50, phosphocreatine 3, KH_2PO_4 10, MgATP 3, HEPES-K 10, EGTA-K 5 (adjusted to pH 7.25 using KOH), and sterilized with an Acrodisc® Syringe Filters with 0.2 µm pore sizes (Pall, Life Science). Gigaohm seal formation was achieved by suction (≈20 GΩ). Capacitance and series resistance compensation were optimized and, usually, 80% compensation of the effective access resistance was obtained.

The holding potential was set to -80 mV, and the interpulse interval was set to a minimum of 10 seconds. The different voltage protocols used in this Doctoral Thesis were adjusted to adequately determine the biophysical properties of the channels. Time constants of deactivation were determined by fitting the currents recordings with a single or double exponential function:

$$y = A_s \exp(-t/\tau_s) + A_f \exp(-t/\tau_f) + C$$

where τ_f and τ_s are the system time constants, A_s and A_f are the amplitudes of each component of the exponential, and C is the baseline value. The voltage dependence of channel activation was fitted to a Boltzmann equation:

$$y = 1/[1 + \exp(-(E-E_h)/s)]$$

in which s represents the slope factor, E represents the applied voltage, and E_h the voltage at which 50% of the channels are open.

Drug-induced block was measured at the end of 250-ms depolarizing pulses from -80 to +60 mV. The degree of inhibition (f) obtained for each drug concentration ($[D]$) was used to calculate the IC_{50} and Hill coefficient (n_H) values from fitting of these values to Hill equation:

$$f = 1/[1 + (IC_{50}/[D]^{nH}]$$

Concentration-response curve with two components were fitted to a biphasic Hill equation. Microcal Origin 8.5 (Microcal Software) and CLAMPFIT software were used to analyze data and for data presentation.

3.4. DRUGS AND REAGENTS

Racemic bupivacaine and quinidine (B5274 and Q0750 respectively, Sigma-Aldrich) were dissolved in distilled deionized water to yield stock solutions of 10 mM, from which further dilutions were made as previously described (Valenzuela *et al.*, 1995a; Franqueza *et al.*, 1997; Longobardo *et al.*, 2000; Longobardo *et al.*, 2001; Gonzalez *et al.*, 2002; Arias *et al.*, 2007).

Calphostin C (Calbiochem) is a cell permeable, highly specific inhibitor of protein kinase C (IC_{50} = 50 nM) that interacts with the protein regulatory domain by competing at the binding site of diacylglycerol (DAG) and phorbol esters. At higher concentrations calphostin C also inhibits MLCK (IC_{50}>5 μM), PKA (IC_{50}>50 μM), protein kinase G (IC_{50}>25 μM) and $p60^{v\text{-}src}$ tyrosine kinase (IC_{50}>50 μM). However, it does not compete with Ca^{2+} or phospholipids. In the experiments presented in this Doctoral Thesis, calphostin C was previously activated by exposure to fluorescent light for five minutes (following the manufacturer recommendations). Subsequently cells were incubated, with the minimum volume required to cover the dish, for 2 hours with calphostin C at 3 μM and diluted in culture medium at 37 °C under an atmosphere of 5% CO_2.

In those experiments in which the soluble protein in the internal pipette solution was used, the Lgi1 Human Recombinant protein at concentration of 0.5 μg/ml was purchased from Tebu-Bio.

3.5. PROTEIN EXTRACTION

48 hours after transfection, culture cells dishes were washed twice with chilled PBS and centrifuged at 3,000 × g for 10 min. The pellet was incubated for 5 min with an ice-cold lysis buffer (50 mM Tris-HCl, pH 7.4, 150 mM NaCl, 1mM EDTA, 1% Triton X-100), supplemented with Complete Protease Inhibitor Cocktail Tablets (Roche Diagnostics) and then lysed by repeated passing (~10 times) through a 25G (0.45 × 16 mm) needle. Homogenates were further centrifuged at 10,000 × g for 5 min in order to precipitate the cellular organelles. Samples were separated into aliquots and stored at -20°C until their utilization. All steps were carried out at 4ºC and protein concentration was determined using a NanoDrop spectrophotometer (NanoDrop ND-1000 UV-Vis Spectrophotometer).

3.5.1. Western blot assays

In a similar way than immunoprecipitation samples, cell lysates containing equal amounts of protein (30-60 μg per lane) were resuspended in Laemmli Buffer and boiled at 95ºC for 5 min. Protein extracts were loaded and size-separated in 7-10% acrylamide/bis-acrylamide (Bio-Rad) SDS-PAGE gels at 110 mV for 2 h at room temperature. Gels were equilibrated in transfer buffer for 15 min at room temperature previously to transfer them (either, at 375 mA for 2 h or at 90 mA overnight, always at 4°C) to PVDF membranes (GE Healthcare). Membranes were blocked with 5% dry milk in 0.1% v/v PBS-Tween20 for 1 h at room temperature, washed with 0.5% dry milk in 0.1% v/v PBS-Tween20 three times for 10 min at room temperature and processed as recommended by the antibodies suppliers (see Table 2). Specie-specific horseradish peroxidase-conjugated secondary antibodies were used (dilution 1:10,000, Calbiochem).

Immunoblot signals were visualized by chemiluminescence using ECL-plus reagent (Amersham, GE Healthcare). Quantification of band intensity was performed with the Image J software.

Table 2. Primary antibodies used in Western Blot assays.

Antibody	Type and Host	Dilution	Reference and Origin
Anti-β-actin	Polyclonal Goat	1:20,000	Sc-1615, Santa Cruz Biotechnology
Anti-α-tubulin	Monoclonal Mouse	1:40,000	T5168, Sigma-Aldrich
Anti-GAPDH	Monoclonal Mouse	1:1000	MAB374, Merck Millipore
Anti-K_v1.5	Polyclonal Rabbit	1:500-1:1,000	APC-004, Alomone
Anti-$K_v\beta$1.x	Monoclonal Mouse	1:500	[S40-17] (ab99012), Abcam Limited
Anti-PKC α	Monoclonal Mouse	1:200	sc-8393, Santa Cruz Biotechnology
Anti-PKCβI	Polyclonal Rabbit	1:200	sc-209, Santa Cruz Biotechnology
Anti-PKCβII	Polyclonal Rabbit	1:200	sc-210, Santa Cruz Biotechnology
Anti-PKCγ	Polyclonal Rabbit	1:200	sc-211, Santa Cruz Biotechnology
Anti-PKCι	Polyclonal Rabbit	1:200	sc-727, Santa Cruz Biotechnology
Anti-PKCδ	Polyclonal Rabbit	1:200	sc-937, Santa Cruz Biotechnology
Anti-PKCε	Monoclonal Mouse	1:200	sc-1681, Santa Cruz Biotechnology
Anti-PKCζ	Polyclonal Rabbit	1:200	sc-216, Santa Cruz Biotechnology
Anti-PKCθ	Polyclonal Goat	1:200	sc-1875, Santa Cruz Biotechnology
Anti-RACK1	Monoclonal Mouse	1:500	sc-17754, Santa Cruz Biotechnology
Anti-Lgi1	Polyclonal Goat	1:200	sc-9581, Santa Cruz Biotechnology

3.5.2. Membrane protein in cell surface: proteinase K assays

Digestion of surface proteins was carried out as described by Manganas and coworkers in 2001 (Manganas *et al.*, 2001). Briefly, each 35-mm dish was incubated with an enzymatic buffer containing (in mM): HEPES 10, NaCl 150, $CaCl_2$ 2 (pH 7.4) with or without 200 µg/ml Proteinase K at 37°C for 30 min. Then, cells were harvested and centrifuged at 4°C at 1,000 × g in a refrigerated microcentrifuge. Proteinase K digestion was quenched by adding ice-cold PBS containing 25 mM EGTA supplemented with Complete Protease Inhibitor Cocktail Tablets. This treatment was followed by washing three times with ice-cold PBS. Cleared lysates were prepared and analyzed by immunoblotting, as described above.

3.5.3. Co-immunoprecipitation assays

As previously described (David *et al.*, 2012) the protein homogenates obtained were centrifuged at 150,000 x g for 90 min and the pellet was resuspended in HEPES 30 mM (pH 7.4 with NaOH) or in the immunoprecipitation buffer described below. The amount of protein required in the experiments (always >300 µg) of the protein homogenates was dissolved in a final volume of 150 µl of immunoprecipitation buffer or IPB [10 mM HEPES (pH 7.6), 150 mM NaCl, 1% Triton X-100, supplemented with Complete Protease Inhibitor Cocktail Tablets (Roche)], and homogenized by orbital shaking at 4°C for 1 h.

In all cases, samples were pre-washed with 20 µl of immunoprecipitation buffer-prewashed protein A/G-Sepharose beads (Santa Cruz Biotechnology) for 2 h at 4°C in order to eliminate non-specific binding between the reagents used and the proteins. After this time, protein A/G was precipitated (5,000 x g for 45 sec) and discarded. The washed supernatant obtained was incubated with 4 ng of antibody per µg of total protein at 4°C overnight and homogenized by orbital shaker. 24 hours later, 50 µl of protein A/G-Sepharose beads were added to the sample and incubated 2 h at 4°C. Finally, antibody-bound sepharose beads (and therefore, protein-bound antibody) were centrifuged at 5,000 x g for 45 s at room temperature and then washed three times with wash buffer (0.1% Triton X-100, 10 mM HEPES (pH 7.6) and 150 mM NaCl) to remove all the antibody and channel unbound or non-specifically bounded.

In the case of experiments carried out in cardiac tissue, and for detection of the $K_v\beta1.3$ subunit (that has a similar molecular weight that the antibody used in the immunoprecipitation protocol), we covalently bound the anti-$K_v1.5$ antibody to A/G protein with Pierce® Direct IP Kit (Thermo Scientific) and this mixture was added to the protein extract. Using this procedure, the antibody used in the immunoprecipitation will not be present in the western blot and it will be possible to detect the beta subunit if it is present in the protein complex.

All experiments were carried out in parallel together with a negative control in which the primary antibody that detects the protein of interest was not added. This negative control led us to discriminate false positives.

Protein samples, immunoprecipitates and immunoprecipitation-obtained supernatants were resuspended in 20-50 µl of Laemmli SDS Loading Buffer (10% w/v SDS, 10% v/v glycerol, 5% w/v 2-β-mercaptoethanol, 0.002% w/v bromophenol blue, 62.5 mM Tris-HCl, pH 7.4), boiled for 5 min at 95 ºC, and then centrifuged for 3 min at 5,000 x g at room temperature. Protein extracts was separated by SDS-PAGE and analyzed by western blotting.

3.6. IMAGE EXPERIMENTS

3.6.1. Immunocytochemistry

One squared coverslip of 18 mm in each side, and placed into a 35 mm dish (Falcon) per experimental condition, was exposed to UV light for 20 min in order to be sterilized. Then, cells were seeded in them. 48 hours post-transfection cells were washed and fixed with 4% paraformaldehyde for 20 min at 37°C. Then cells were permeabilized with PBS 0.1% v/v Triton X-100 for 20 min at 37°C, blocked (against the non-specific binding of the primary antibody) with goat serum 5% (since none of primary antibodies used were performed in goat) in PBS for 30-60 min at 37°C; and, finally, cells were incubated with the primary antibody that recognizes an extracellular epitope (HA-tag) or the RACK1 protein (Table 3). After that, cells were incubated with the proper secondary antibody, indicated in each Figure or, in the case of the detection of c-myc-tag, with an anti-c-myc-CY3 antibody (a primary antibody tagged directly with a fluorophore). Between each one of the steps described above, cells were washed three times with PBS for 5 min. Finally, and before of mounting the coverslips with Aqua Poly/Mount (Polysciences); cells were incubated with DAPI 1:10,000 (D1306, Molecular Probes) for 20 min at 37°C. Stained cells were visualized using a LSM510 ZEISS (Carl Zeiss) or Leica TCS SP5 (Leica Microsystems) confocal microscopes, and images were analyzed with Zeiss, Leica, and ImageJ software (NIH).

Table 3. Primary antibodies used in immunocytochemistry assays.

Antibody	Type and Host	Dilution	Reference and Origin
Anti-K_v1.5	Polyclonal Rabbit	1:500-1:1,000	APC-004, Alomone
Anti-c-myc-CY3	Monoclonal Mouse	1:250	C6594, Sigma
Anti-HA	Polyclonal Mouse	1:250-1:500	NB600-366, Novus Biologicals
Anti-RACK1	Monoclonal Mouse	1:500	sc-17754, Santa Cruz Biotechnology

For the internalization experiments, four coverslips per experimental condition were exposed to UV light for 20 min to sterilize them. Then, cells were seeded into 35 mm dishes (Falcon). 48 h post-transfection the antibody anti-HA was added to the culture media without serum and antibiotics, for 30 min at 4°C under soft shaking conditions, previous to the incubation indicated in the Figures of this Doctoral Thesis. After 2 h at 37°C, cells were fixed with 4% paraformaldehyde for 20 min, then were blocked with goat serum 5% in PBS and then incubated with the secondary antibody (goat Anti-rabbit Alexa-568 1:500). After that, cells were washed and permeabilized with 0.5% v/v Triton X-100 and Goat Serum 5% in PBS for 30 min at 37°C. Then, cells were incubated with a similar blocking solution and incubated with the internal secondary (goat Anti-rabbit Alexa-488 1:500). All incubations were performed in a wet chamber (see a scheme of the process in Figure 10)

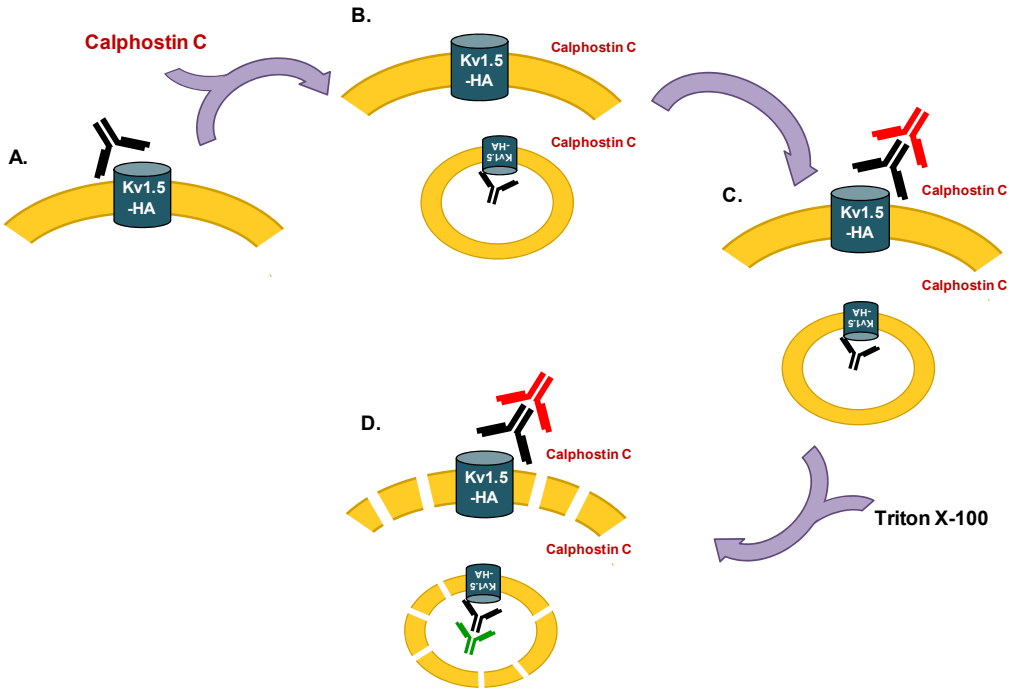

Figure 10: Scheme of the internalization assay of $K_v1.5$ in the presence of calphostin C. *In* these experiments an HA-tagged $K_v1.5$ construction **(A)** was used in order to label the channel present in cell surface. After this, the cells were treated with calphostin C. At this time, channels have been internalized **(B)**. Thus, the amount of the channels which remains in the membrane of the cell was labeled in red **(C)**, and then, the cells were permeabilized and the internalized channel were labeled in green **(D)**. Note that in this way, only will be reachable for the second secondary antibody, those channels that were present previously in the membrane.

In that experiments performed to analyze effects of Lgi on the actin cytoskeleton, cells were transfected with $K_v1.5$-CFP (provided by Dr. A Felipe), Lgi1-GFP (provided by Dr S Adhikari), phalloidin-Alexa546 5:200 (Molecular Probes) for labeling the actin cytoskeleton and To-Pro-3 1:500 (Molecular Probes) for the labeling of the nucleuses.

Finally, and before mounting the coverslips with ProlongGold® antifade reagent (Molecular Probes); cells were incubated with DAPI 1:10,000 (Molecular Probes) for 20 min at 37°C (less in that experiments performed to analyzed the Lgi1 effects) and the coverslips were briefly immersed in distilled water, MilliQ quality, and ethanol 100%. Stained cells were visualized using a Confocal Scanning Microscope LSM 710 (from Zeiss) and a 63x objective. Values of intensity fluorescence and quantification were obtained performed with Image J software (NIH).

3.6.2. Live cell imaging

HEK293 cells were cultured in 35 mm μ-dishes for live cell imaging (Ibidi GmbH), transfected with K_v1.5-HA-K_vβ1.3 construction and labeled as previously described (Zadeh *et al.*, 2008). Briefly, cells were incubated with mouse-anti-HA (1:250, Novus Biologicals) at 4°C for 30 min in culture medium without serum or antibiotics. After this period, cells were washed and labeled with a 1:500 dilution of a goat anti-mouse Alexa-488 (Molecular Probes) for 30 min at 4°C in a similar medium. Then, cells were washed three times with cold medium and live-imaged using a Microscope Cell Observer Z1 system (Carl Zeiss MicroImaging GmbH) equipped with a controlled environment chamber (37°C constant temperature, 5% CO_2 atmosphere) and Camera Cascade 1k. Images were collected every 5 min with a 63x Plan Apochromat objective, from 0 to 3 h. After image stabilization, all images were deconvolved with Huygens Professional software version 4.0 (Scientific Volume Imaging) using a theoretical point spread function for each channel and the Quick Maximum Likelihood Estimation algorithm (QMLE) and the theorist Point Spread Function (PSF). The signal to noise ratios and background intensities were manually determined and taken into account during the deconvolution process. Finally time-lapse movies were formatted using ImageJ software and exported in *.avi format.

3.6.3. Fluorescence resonance energy transference (FRET)

Fluorescent resonance energy transfer (FRET) involves the radiation-less transfer of energy from a "donor" fluorophore to an "acceptor" fluorophore. But to that phenomena take place both fluorophores ("donor" and "acceptor") has to meet: a) both spectra have to overlap, so that the donor emission spectrum coincides, at least in part with the absorption spectrum of the acceptor; and b) both fluorophores has to approximate, not only to a short distance, but also in the adequate orientation (Figure 11). FRET-based assays are able to transduce a near-field interaction into a far-field signal, a unique optical tool to assess biological phenomena well below the resolution of standard optical microscopy (Roy *et al.*, 2008). Due to the light attenuation, FRET can only allow energy transfer to occur when the distance between the donor and the acceptor fluorophores are within 1–10 nanometers (nm) of each other. An excited fluorophore emits an essentially virtual photon, which is then absorbed by a receiving fluorophore (Zadran *et al.*, 2012). And, for all these reasons, FRET is commonly utilized to demonstrate near-field communication or interaction between two molecules (Day *et al.*, 2001). Due to these physical properties, different biological applications of this technique can be carried out. Among them, it is possible to do

possible estimation of interfluorophore distances between amino acyl residues in disordered or partially folded proteins and, the performance of "multiple molecular triangulation" with fluorophores located at various positions, provided a useful initial constraint on the coarse structure of the proteins (Miranda *et al.*, 2008; Miranda *et al.*, 2013).

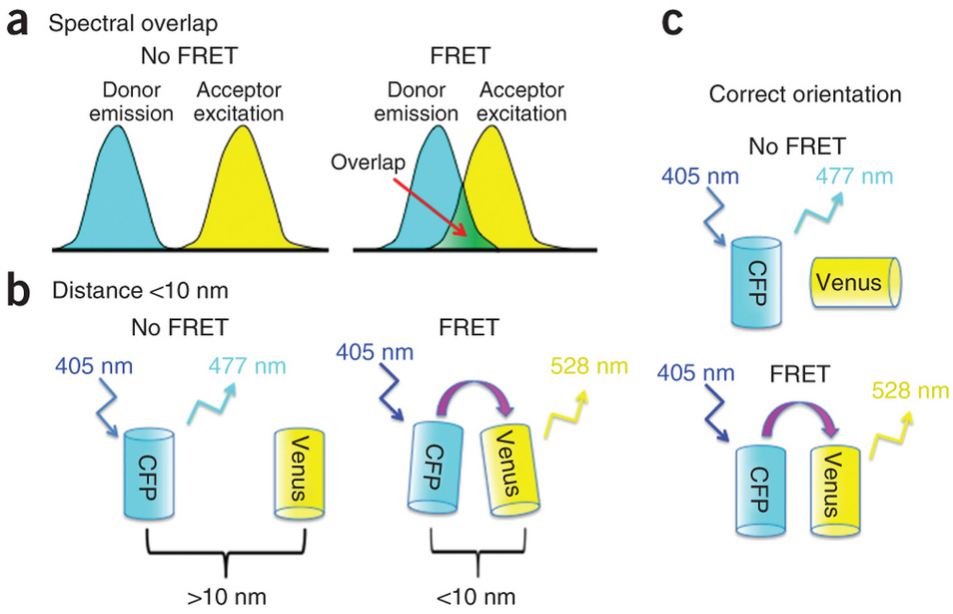

Figure 11: Scheme of FRET technique. **A,** The energy of donor emission must be an energy that the acceptor can absorb. In other words, the emission spectrum from the donor fluorophore must overlap with the excitation spectrum of the acceptor fluorophore. **B,** If the FRET donor and acceptor are more than 10 nm apart, then no FRET occurs and the donor emits fluorescence. If the donor and acceptor are within ≈10 nm of one another, then energy transfer can occur from the donor (CFP) to the acceptor (Venus). **C,** If the donor and acceptor fluorophore dipoles are perpendicular to one another, then the donor molecule will emit fluorescence. However, if the dipoles are parallel to each other, FRET will occur [taken from (Broussard *et al.*, 2013)].

After tagging and transfection of the used proteins, measurements of FRET by acceptor photobleaching as previously described (Miranda *et al.*, 2013). Briefly, FRET measurements were performed in cells bathed in standard extracellular saline following the increase (dequenching) in donor (CFP) fluorescence signal during incremental photobleaching of acceptor (V/YFP). Background fluorescence of both fluorophores was determined from a region of the same field located outside the cell and the averaged pixel intensity of this area was subtracted from the mean intensities measured in the regions of interest corresponding to the individual fluorescent cell areas. A Zeiss Axiovert 100 microscope with a 40x/0.75 Plan-NeoFluar objective (Carl Zeiss) was used. The fluorescence imaging system (Till-Photonics) consisted of a monochromator Polychrome IV, a dual band CFP/YFP filter set and a 12-bit CCD camera (IMAGO) combined with a DUAL-View Micro-Imager (Optical Insights) for dual emission image acquisition. Control of monochromator and camera as well as image recording and processing were

performed with TILLvisION software (Till-Photonics). The standard acceptor bleach protocol consisted of 30 cycles every 2 s with 50–100 ms of exposure of donor and acceptor near their excitation maximum (at 440 and 515 nm, respectively) to detect CFP and V/YFP fluorescence without V/YFP-bleaching, followed by 180–240 additional cycles separated by periods in which the V/YFP remains permanently illuminated at 515 nm to photobleach it. Photoconversion of V/YFP into CFP-like species was negligible under our photobleaching conditions as evidenced by the total absence of fluorescence in the CFP channel when cells expressing exclusively V/YFP-labeled proteins were submitted to the standard acceptor bleaching protocol. Individual cells showing dim fluorescence leading to very low signal-to-noise ratios and those in which the fluorescence of V/YFP did not average at least 13 or 10 fold that of the lower intensity CFP probe, respectively, were discarded to prevent low acceptor-to-donor ratio contributing to uncontrolled and reduced FRET signals. This implies that almost exclusively 2:2 and/or 1:3 CFP:V/YFP-tagged subunit stoichiometries will contribute to FRET. Quantitative FRET levels were expressed as FRET efficiency (E_{FRET}), defined as the proportion of the excited states of the donor that become transferred to the acceptor and calculated as follows:

$$E = (Fd-Fa)/ Fd$$

in which *Fa* and *Fd* are the fluorescence intensities of the donor before and after complete photobleaching of the acceptor.

3.6.3.1. Total internal reflection fluorescence microscopy-FRET (TIRFM-FRET) system

In addition, measurements were performed under total internal reflection microscopy (TIRFM) to selectively measure FRET in the proximity of the plasma membrane Figure 12A, because only fluorescent proteins illuminated by the evanescent wave, at a distance of ≈100 nm above the glass coverslip, where the cells are attached are studied, thus avoiding most of the contamination from cytoplasmic signals (Axelrod, 2003; Fernandez-Trillo *et al.*, 2011). This fact is possible thanks to the refractive indices of the glass slide (1.518) and the aqueous specimen medium (approximately 1.35) which are appropriate to support total internal reflection within the glass slide. With adjustment of the laser excitation incidence angle to a value greater than the critical angle, the illuminating beam is entirely reflected back into the microscope slide upon encountering the interface, and an evanescent field is generated in the specimen medium immediately adjacent to the interface. On the other hand, this technique led us to get images, with a higher contrast, less background and higher sharpness images of the cell and its membrane (Figure 12B), which has a direct effect in the goodness of the data derived from them. This is very important because it could be possible that only a reduced fraction of the total fluorescence, corresponding to properly assembled and fully functional complexes, is detected in the perimeter (i.e. the plasma membrane) of the channel-labeled expressing cells (Miranda *et al.*, 2008).

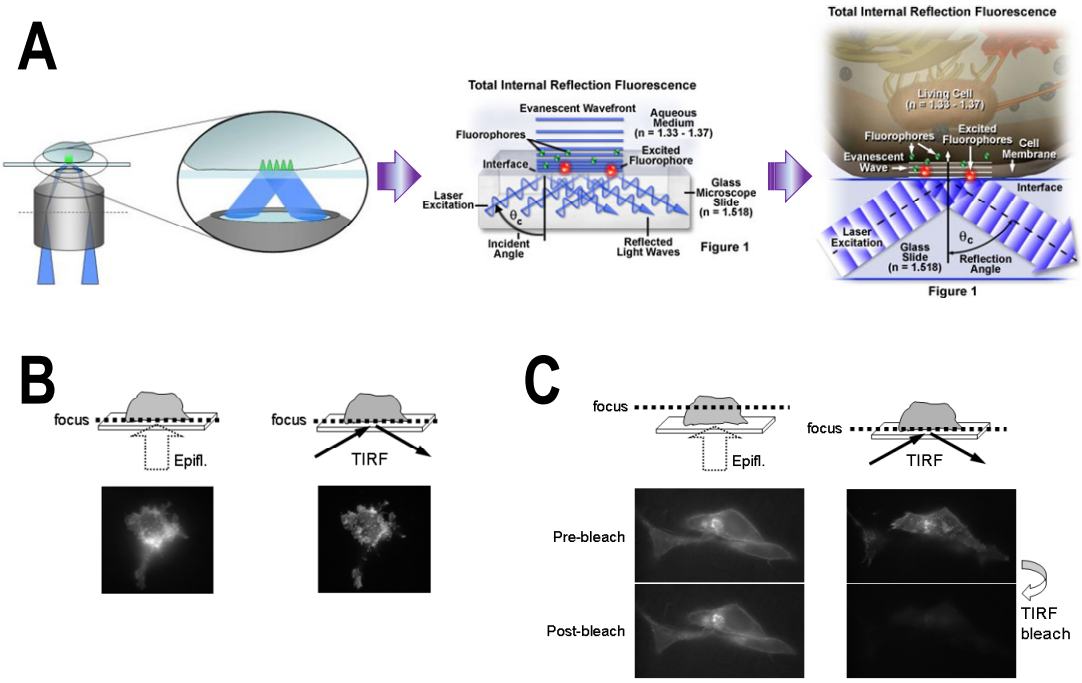

Figure 12: Theoretical and practical representation of TIRFM technique. **A,** Right panel: generation of structured evanescent illumination by interference of two plane waves; middle and right panels: schematic representation showing how the fluorophores in contact with the slide are illuminated [taken from (Axelrod & Davidson, 2012; Ross *et al.*, 2013; Gerrer *et al.*, 2013)]. **B,** Comparison of wide-field epi-fluorescence (left) and TIRF illumination (right) after focusing the objective at the level of the glass coverslip-water interface. Note the notorious reduction of the background and out-of-focus fluorescence under TIRF conditions, associated with a remarkable increase in the sharpness and contrast of the layer corresponding to the cell footprint in contact with the glass, mainly representing the plasma membrane environment. **C,** TIRF-induced preferential photobleaching of labeled proteins in and near the plasma membrane abutting the coverglass. Note the very similar fluorescence levels observed in the cells imaged with epifluorescence microscopy and focused near the cell center, both before and after nearly complete selective photobleaching [B and C, taked from (Fernandez-Trillo *et al.*, 2011)].

Subsequently, a CFP-YFP construction was used as a positive control linked in tandem by a pleckstrin homology domain (CFP-PH-YFP), which can bind phosphatidylinositol lipids within biological membranes. By using this construction, not only we can make sure that we obtain the maximum value of E_{FRET} (since both proteins are closed), but also this construction it can be used as plasma membrane marker in the trafficking of proteins or to delimit the cells in fluorescence assays.

3.6.4. Immunohistochemistry

Sections (4 µm) of paraffin-embedded tissues mounted on slides coated with 3-aminopropyltriethoxy-silane (Sigma Chemical Co.) were deparaffinized and submitted twice to microwave pretreatment for 2.5 min at 800 W in sodium citrate buffer 0.01 M (pH 6). Subsequently, the tissue was blocked with Tris-buffered saline containing 1% BSA. All sections were incubated overnight at 4°C. After incubation with the primary antibody and a biotinylated secondary antibody, an ABC method was used (a complex performed by Avidin DH and biotinylated horseradish peroxidase H, Vector Laboratories). Then,

sections were carefully washed and the supersensitive peroxidase detection system (BioGenex) was used. These reactions were revealed by incubation with DAB (3,3-diaminobenzidine/H_2O_2). Positive controls were treated with anti-collagen or anti-vimentin antibodies. Nucleuses were counterstained with Harris haematoxylin and the sections were mounted in Dpex mounting medium (Panreac) or aqueous mounting medium (ClearMount Solution, Zymed Laboratories).

3.7. TRAFFICKING ASSAYS

3.7.1. Biotinylation of membrane proteins

In these experiments HEK293 cells were transfected with pBK-K_vβ1.3-IRES-K_v1.5-FLAG construction, described above. Cell surface biotinylation was carried out with the Pierce® Cell Surface Protein Isolation Kit (Pierce) following the manufacturer instructions. Briefly, 48 h after transfection, the cells were washed twice with chilled PBS and then all cell surface proteins, including FLAG-tagged K_v1.5, were biotin-labeled using Sulfo-NHS-SS-biotin (sulfosuccinimidyl-2-(biotinamide) ethyl-1,3-dithiopropionate; Pierce) and incubated at 4°C under soft shaking conditions for 30 min. The unreacted biotin was quenched and cells were warmed at 37°C to allow channel endocytosis for different times, as indicated. The remaining cell surface biotin was stripped using MesNa solution (100 mM sodium 2-mercaptoethanesulfonate, 50 mM Tris, 100 mM NaCl, 1 mM EDTA, 0.2% BSA). Then, cells were washed in chilled PBS and lysed with in ice-cold lysis solution (Figure 13). The protected (endocytosed) biotin-tagged channels were subjected to pulldown using 25 µl of NeutrAvidin-agarose that was added to 500 µg of total protein. Proteins were resolved by SDS-PAGE (10% gel) and transferred to PVDF membranes by immunoblot analysis of K_v1.5 channels internalyzed using polyclonal rabbit antibody anti-K_v1.5 (Alomone).

3.1.1. Trafficking disruptors

In these experiments cDNA constructions with single point mutations known to confer a GTP-bound/constitutively active state of Rab GTPase 4 and 11 were used and kindly provided by Dr. JA Esteban (CBMSO, CSIC-UAM). HEK293 cells were transiently co-transfected K_v1.5-K_vβ1.3 and with constitutively active mutants of Rab 4 (Q67L) and 11 (Q70L) using the same transfection protocol previously stated in this Doctoral Thesis. The constructions of these mutants have been widely described previously (Gerges *et al.*, 2004). Briefly, Rab4a and Rab11a coding sequences were cloned by PCR from a commercial rat brain cDNA preparation (catalog no. 7150; Clontech).

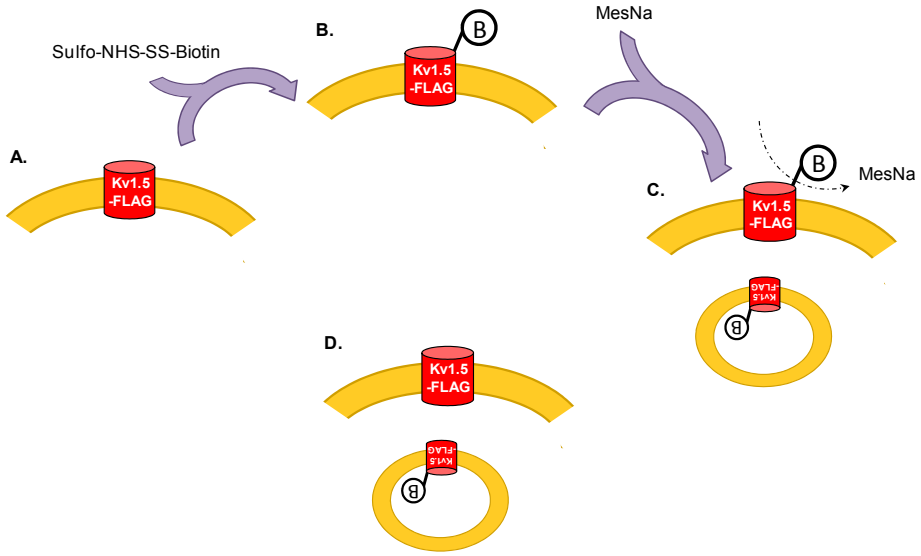

Figure 13: Scheme of the recycling study of K_v1.5 by biotinylation. In these experiments a Flag-tagged K_v1.5 construction (**A**) was used in order to take the free lysines present in the tag (-GDYKDDDKG-) since the Sulfo-NHS-SS-Biotin (**B**) used needs the presence of free amino groups in the external side of the cell to bind them. After that, a reducer solution such as MesNa (sodium 2-mercaptoethanesulfonate) will strip the remained biotin bonded to cell surface proteins (**C**). In this way, biotin only will remain tagged those proteins protected or endocytosed (**D**).

3.2. STATISTICAL ANALYSIS

Results are expressed as mean±SEM. Direct comparisons between mean values in control conditions versus mean values in the presence of drugs for a single variable were performed by a paired Student's *t* test. ANOVA was used to compare more than two groups. Student's *t* test was also used to compare two regression lines. Differences were considered significant when *P*-value was less than 0.05.The curve-fitting procedure used a non-linear least-squares (Gauss-Newton) algorithm; results were displayed in linear format. Goodness of fit was judged by the χ^2 criterion and by inspection for systematic non-random trends in the difference plot.

Table 4. Principal reagents and drugs used in this Doctoral Thesis.

Name	Brief description	Reference and Origin
Penicilin	Antibiotic	10270-106, Gibco
Streptomycin	Antibiotic	15140-122, Gibco
Calphostin C	PKC inhibitor	208725, Calbiochem
Dynabeads®	Microbeads precoated antibodies	11147D, Invitrogen
Lgi1 protein	Human recombinant protein	H00009211-P01-0002, Tebu-Bio
Protease inhibitor	Protease inhibitor cocktail	11836145001, Roche Diagnostics
Pierce® Direct IP Kit	Antibodies covalent binding	26148, Thermo Scientific
ECL-plus reagent	Chemiluminiscent signal for WB	RPN2132, GE Healthcare
ProlongGold®	Mounting medium	P36930, Molecular Probes
DAPI	Nucleus marker	D1306, Molecular Probes
3-aminopropyltriethoxy-silane	Coating glass reagent	440140, Sigma Chemical Co
Sulfo-NHS-SS-biotin	Membrane proteins marker	21331, Pierce
Racemic bupivacaine	Local anesthetic	B5274, Sigma-Aldrich
Racemic quinidine	Antiarrhythmic drug	Q0750, Sigma-Aldrich

4. RESULTS

4.1 PROTEIN KINASE C ACTIVITY REGULATES FUNCTIONAL EFFECTS OF $K_v\beta1.3$ SUBUNIT ON $K_v1.5$ CHANNELS: IDENTIFICATION OF A CARDIAC *CHANNELOSOME*.

4.1.1 Effects of PIP_2 and OAG on $K_v\beta1.3$-induced fast inactivation

It has been proposed that PIP_2 associates with the amino terminus of the $K_v\beta1.3$ subunit, and when the β subunit dissociates from PIP_2, it assumes a hairpin structure that can enter the central cavity of an open $K_v1.5$ channel, triggering $K_v\beta1.3$-induced N-type inactivation. Therefore, it is assumed that $K_v\beta1.3$-induced fast inactivation is mediated by equilibrium binding of the amino terminus of $K_v\beta1.3$, which switches between binding to phosphoinositides (PIPs) and the inner pore region of $K_v1.5$ channels (Decher *et al.*, 2008). Stimulation of α1-receptors activates PLCγ is capable of cleaving PIP_2 into IP_3 and DAG, thus activating classical and novel PKCs.

The effects of PIP_2 and OAG (a non-degradable DAG analog) were analyzed by adding these compounds to the internal solution (Figure 14). Cells dialyzed with PIP_2 exhibited a lower degree of fast inactivation just after patch rupture in comparison with control cells (55 ± 4% versus 68 ± 6%, n = 4, $p<0.05$) (Figure 14A). However, after 8 min of dialysis with PIP_2, the degree of N-type inactivation increased significantly (from 55 ± 4% to 70 ± 4%, n = 4, $p<0.05$) (Figure 14A). These effects could be because of a decrease of the PIP_2 concentration due to its cleavage into IP_3 and DAG. In fact, the degradation of PIP_2 would increase the ability of the N terminus of $K_v\beta1.3$ to inactivate $K_v1.5$ (Decher *et al.*, 2008). In contrast, cells dialyzed with OAG exhibited a similar degree of N-type inactivation than control cells, both after patch rupture and after 8 min of dialysis with OAG (65 ± 3% to 67 ± 2%, n = 5, $p>0.05$) (Figure 14B). These results are in agreement with the involvement of classical and novel PKC isoforms in the effects of calphostin C and PKC siRNA on the fast $K_v\beta1.3$-induced inactivation. To test whether the PIP_2 effects at different times (t=0 or 8 min) were due to the cleavage of PIP_2 into DAG and IP_3, a series of experiments in which cells previously incubated with a PLC inhibitor (U73122, 10 μM) and dialyzed with PIP_2 was performed (Figure 14C). Under these experimental conditions, the degree of fast inactivation was reduced (from 69 ± 2% to 62 ± 2%, n = 9, $p<0.01$. Figure 14Ca) and, more importantly, the $K_v\beta1.3$-induced fast inactivation was abolished, in such a way that the time constant of the fast inactivation was increased (Figure 14Cb) and the contribution of the fast component of inactivation decreased (Figure 14Cc).

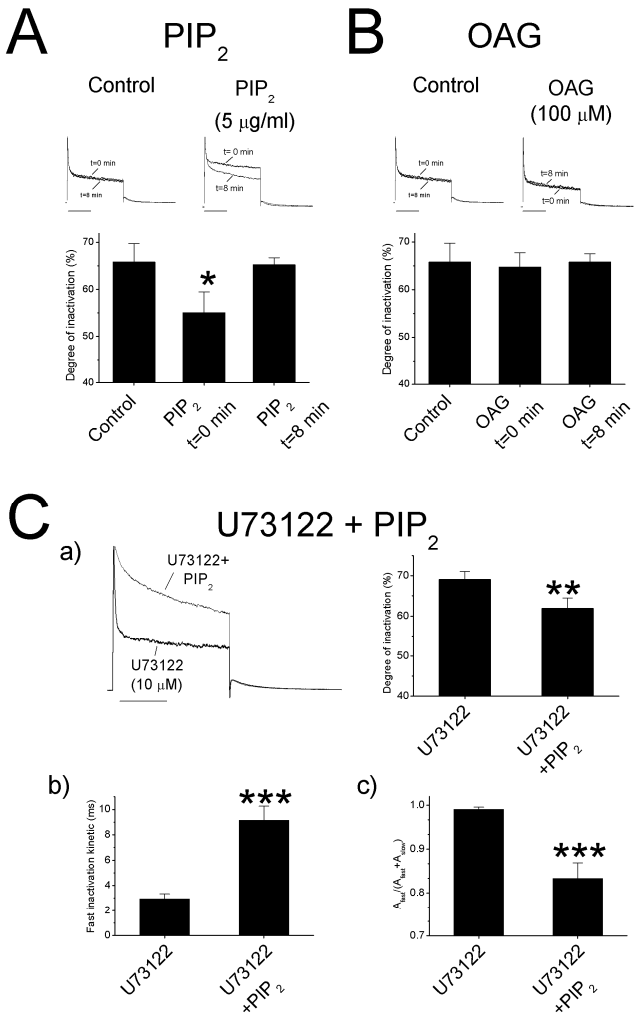

Figure 14: Effects of PIP_2, OAG, and PLC on $K_v\beta1.3$-induced fast inactivation. A, Representative current traces obtained after depolarization from a holding potential of −80 mV to +60 mV, just after patch rupture (t = 0 min) and after 8 min (t = 8 min), in control conditions and during PIP_2 dialysis. The graph shows the degree of inactivation in control cells and in cells dialyzed with PIP_2 at t = 0 min and t = 8 min. Note that at t = 0, the degree of fast inactivation was significantly lower than that after 8 min of dialysis in PIP_2 and control dialyzed cells. **B,** Representative current traces obtained at +60 mV at t = 0 and t = 8 min in control conditions and during OAG dialysis. The graph shows the degree of fast inactivation in control cells and in cells dialyzed with OAG at t = 0 min and t = 8 min. The degree of fast inactivation was similar in all experimental conditions. **C,** Representative current traces obtained at +60 mV at t = 0 (U73122, 10 μm) and t = 8 min (U73122 + PIP_2) after inhibition of PLC with U73122 and after PIP_2 dialysis. The upper right (**Ca**), bottom left (**Cb**), and bottom right (**Cc**) of the panel show graphs of the degree of fast inactivation, the fast inactivation kinetics, and the contribution of the fast component of inactivation to the total process ($A_{fast}/(A_{fast} + A_{slow})$) under both experimental conditions, respectively. *, p<0.05; **, p<0.01; ***, p<0.001.

4.1.2 PKC inhibition results in a shift of the inactivation curve.

Assembly of the $K_v\beta1.3$ subunit causes fast inactivation of the $K_v1.5$ outward current (Hoshi *et al.*, 1990; England *et al.*, 1995a; England *et al.*, 1995b; Leicher *et al.*, 1996). Therefore, it was surprising to observe that even when these subunits remained assembled, $K_v\beta1.3$-induced fast inactivation was abolished either by inhibition of PKC with calphostin C or by silencing PKC. $K_v1.5$-$K_v\beta1.3$ current is activated at −30 mV and inactivates at potentials positive to 0 mV, exhibiting a degree of inactivation of 70 ± 2% (n = 23) when measured at +60 mV (David *et al.*, 2012). After PKC inhibition with calphostin C- or siRNA-mediated PKC silencing, $K_v1.5$-$K_v\beta1.3$ currents showed a degree of slow inactivation that ranged between 20 and 30%, whereas pulse steps to potentials positive to +60 mV revealed the presence of the typical $K_v\beta1.3$-induced fast inactivation (Figure 15A). Figure 15A also shows the mean values of the inactivation degrees obtained at +100 mV recorded in at least four experiments. These results further suggest that $K_v1.5$ and $K_v\beta1.3$ remain assembled after PKC inhibition. This outcome suggests that after PKC inhibition, the inactivation curve of $K_v1.5$-$K_v\beta1.3$ current is shifted toward more positive membrane potentials. To test this hypothesis, a series of experiments was performed in which a double-pulse protocol was applied (Figure 15B).

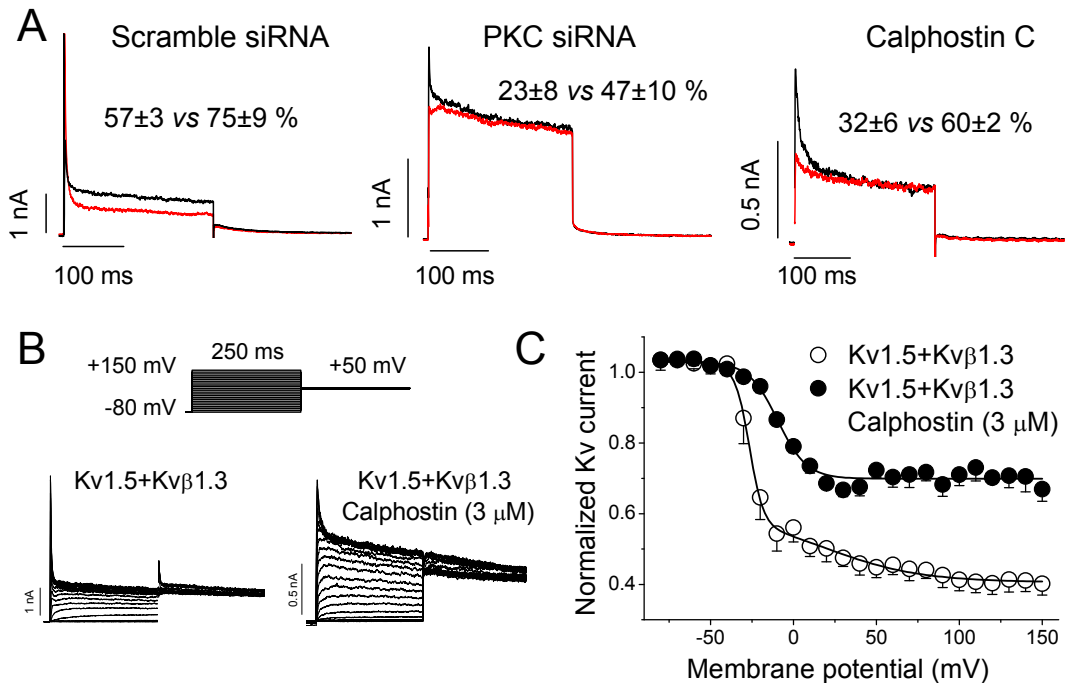

Figure 15: Voltage dependence of inactivation of $K_v1.5$ and $K_v1.5$-$K_v\beta1.3$. **A,** Current traces obtained after depolarization from a holding potential of −80 mV to +60 (red) and +100 mV (black) in HEK293 cells transfected with $K_v1.5$-$K_v\beta1.3$ and with scrambled siRNA (50 nM) (left), with PKC siRNA-transfected cells (middle) and in calphostin C-treated cells (right). **B,** Original current records obtained in control and calphostin C-treated cells. **C,** Voltage dependence of inactivation under control and after calphostin C treatment. Note that calphostin C shifts the inactivation curve to more positive potentials.

These results show that the inactivation curve in calphostin C-treated cells was shifted toward more positive potentials (V_h = −26.5 ± 0.6 versus −8.5 ± 1.9 mV in the presence and in the absence of calphostin C, respectively; n = 10; see Figure 15C and Table 5). Moreover, the degree of inactivation in calphostin C-treated cells decreased from 47.3 ± 5.7% (n = 5) to 34.6 ± 2.2% (n = 7) ($p<0.05$)

.

TABLE 5. Voltage-dependent inactivation parameters. V_h: half voltage of inactivation. *s*: slope of the Boltzmann equation. Data represent the mean ± S.E.M. (n = 7 experiments). Statistically significant differences are indicated by asterisks.

	V_{h1} (mV)	V_{h2} (mV)	s_1 (mV)	s_2 (mV)
K_v1.5-K_vβ1.3	-26.5±0.6	19.0±0.6	4.2±0.6	28.7±7.8
K_v1.5-K_vβ1.3 (Calphostin C)	-8.5±1.9*		9.8±.9*	

4.1.3 The K_v1.5 macromolecular complex in HEK293 cells contains K_v1.5, K_vβ1.3, RACK1, PKCβI, PKCβII, and PKCθ.

Several ion channels have been reported to be modulated by PKC via RACK1 (Ron *et al.*, 1994). We hypothesized that K_v1.5, K_vβ1.3, and PKC form a functional complex in which PKC activity is an essential requirement for the induction of fast and incomplete channel inactivation by K_vβ1.3. To assess this hypothesis, immunocytochemistry experiments were performed (Figure 16). Figure 16A shows confocal images of cells transfected with K_v1.5-HA and K_vβ1.3, in which we stained for K_v1.5 and RACK1. Figure 16B shows confocal images of cells transfected with K_v1.5 and K_vβ1.3-Myc, in which we stained for K_vβ1.3 and RACK1. As shown, under both experimental conditions, colocalization was consistent between K_v1.5 and RACK1, as well as between K_vβ1.3 and RACK1. Given the widespread immunolocalization patterns, we confirmed subunit association using immunoprecipitation experiments. We immunoprecipitated K_v1.5 channel and blotted for PKCβII to confirm the presence of this enzyme in the protein complex. Western blots against RACK1 confirmed the interaction of K_v1.5 with this adaptor protein. Collectively, these results demonstrate the presence of a functional complex or *channelosome* that includes K_v1.5, K_vβ1.3, RACK1, and PKCβII. This interaction was demonstrated in controls and was found to be absent in PKC-silenced cells (David *et al.*, 2012).

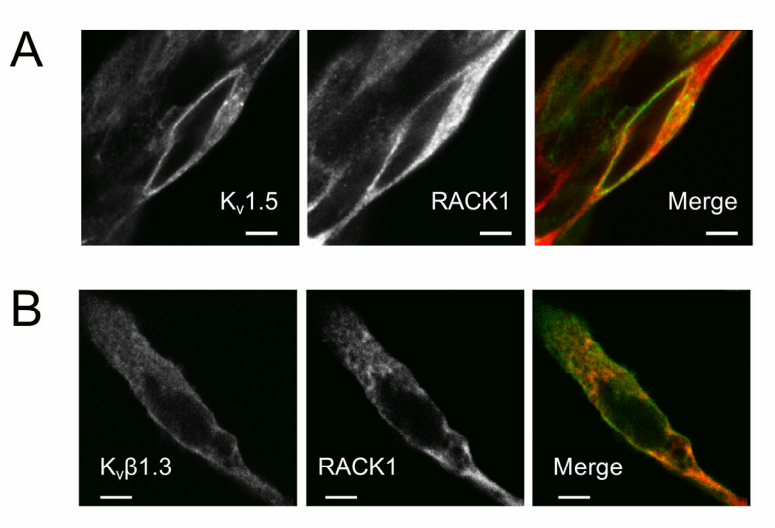

Fidure 16: Immunocytochemical staining of K_v1.5-HA or K_vβ1.3-Myc and RACK1 proteins. **A,** Cells stained with anti- K_v1.5-HA, anti-K_vβ1.3-Myc, or anti-RACK1. Colocalization appears as yellow fluorescence due to the merge of the green (K_v1.5-HA) and red (RACK1) channels after detection with secondary fluorescent antibodies. Cells were cotransfected with K_v1.5-HA+K_vβ1.3-Myc. RACK1 is an endogenous protein. **B,** Cells stained with anti-Myc (green) and anti-RACK1 (red). Cells were transfected with K_vβ1.3-Myc alone. In all pictures, the bar represents 5 µm.

Along to that experiments, we performed other immunocytochemistry experiments, similar to that show in Figure 16, in which we only transfected K_v1.5 and stained for K_v1.5 and RACK1 (data not shown) detecting a lower colocalization degree in these cells than in cells transfected with K_v1.5-K_vβ1.3+RACK1. All these data, led us to hypothesize a 'linker' role of K_vβ1.3 in the K_v1.5-RACK1 interaction. In order to test this hypothesis, after checking the availability of the system with our positive control (CFP-PH-YFP tandem construction with an E_{FRET} = 38.22 ± 0.84, n=14; Figure S1) we performed TIRF-FRET experiments between K_v1.5-CFP and RACK1-YFP constructions in the absence (Figure 17A), and in the presence of K_vβ1.3 subunits (Figure 17B). In Figure 17 it can be observed that while we obtained a negative FRET (E_{FRET} = -2.08 ± 0.51 %, n=50) in the absence of K_vβ1.3 subunit, a positive FRET (E_{FRET} = 6.67 ± 1.18, n=3) was obtained in 3 from 16 cells analyzed in the presence of K_vβ1.3 (≈ 20 % of cells studied).

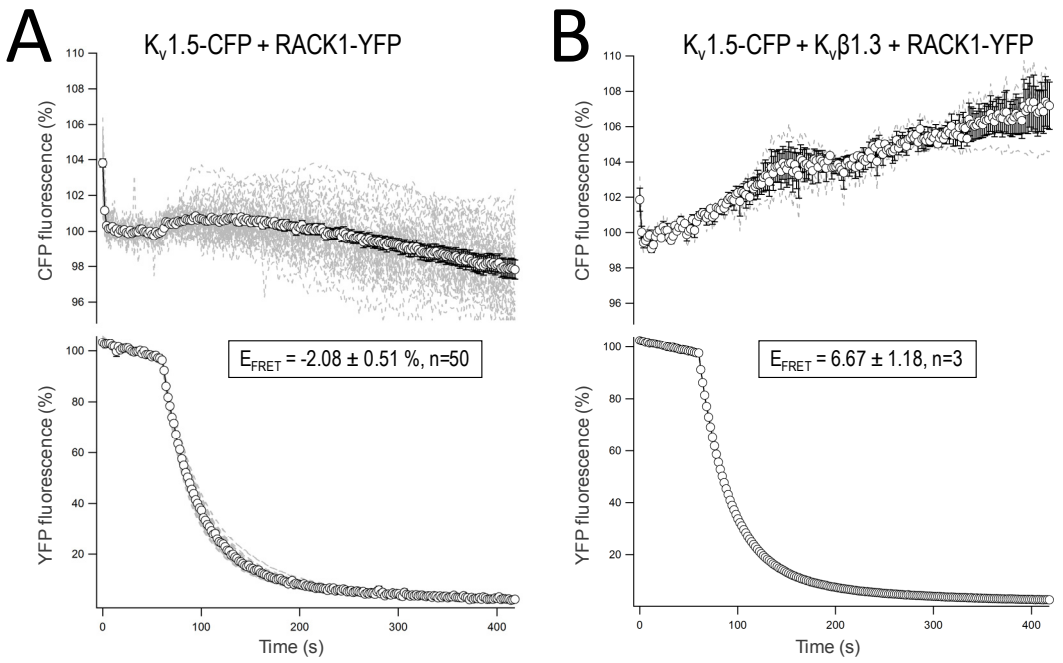

Figure 17: Determination of donor fluorescence recovery during disruption of energy transfer by selective acceptor photobleaching. Transiently transfected HEK293 cells were imaged for co-expressed K_v1.5 amino terminally fused to CFP and RACK1 carboxy terminally fused to YFP in the absence (**A**) an in the presence of K_vβ1.3 subunit (**B**). Shown are the relative increases in CFP intensities (in percentages) over initial levels and the remaining fluorescence intensity of YFP. The symbols represent the calculated mean ± SEM, whereas the thin dotted lines correspond to single cell traces.

4.1.4 Characterization of the K_v1.5 *channelosome*

To determine which PKC isoforms are present in this macromolecular complex, a series of coimmunoprecipitation experiments were performed in which we immunoprecipitated K_v1.5 channels and blotted for all PKC isoforms present in HEK293 cells (Figure 18). We observed that only PKCβI, PKCβII, and PKCθ were present in the K_v1.5 *channelosome*.

4.1.5 The K_v1.5 *channelosome* is present in rat ventricular but not in atrial myocytes

In order to determine the physiological relevance of our results, we performed experiments in rat cardiac tissue (Figure 19). We performed coimmunoprecipitation experiments in which we immunoprecipitated K_v1.5 channels and blotted for PKCβI, PKCβII, PKCθ, RACK1, and K_vβ1.x. Samples from ventricular homogenates presented a K_v1.5 *channelosome* composed of K_v1.5, K_vβ1, RACK1, PKCβI, and PKCβII (Figure 19A). Importantly, atrial tissue did not display this K_v1.5 protein complex (Figure 19B) since none of the proteins studied, which are forming the K_v1.5 *channelosome* in ventricle, coimmunoprecipitated with K_v1.5 in atrial tissue.

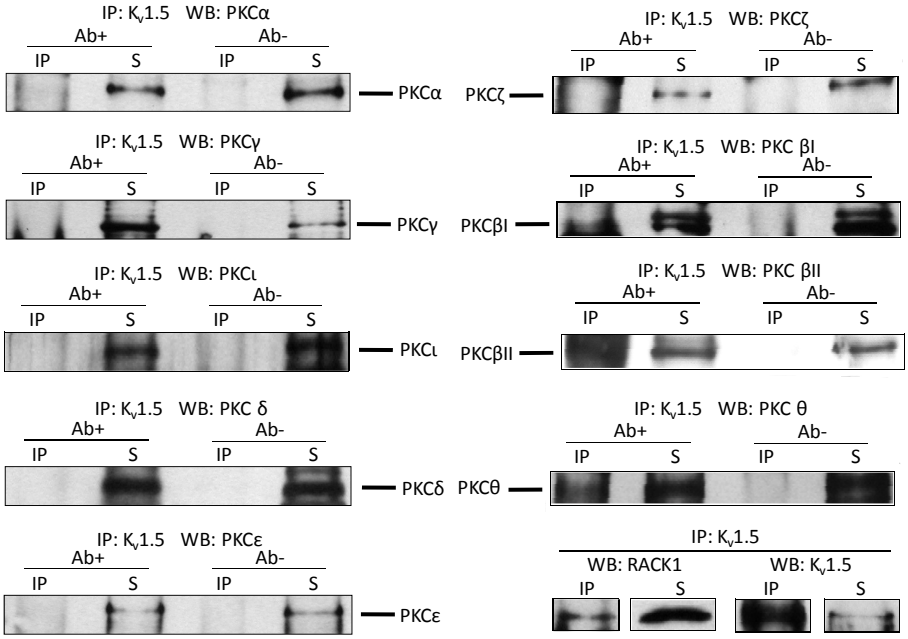

Figure 18: **Immunoprecipitation of $K_v1.5$-$K_v\beta1.3$ channel *with PKCs*.** Negative (Ab−) and positive (Ab+) immunoprecipitations (IP) blotted against the different PKCs isoforms present in HEK293 cells. Note that only PKCβI, PKCβII, and PKCθ coimmunoprecipitated with $K_v1.5$-$K_v\beta1.3$ channels (n = 3). WB, Western blot; S, supernatants.

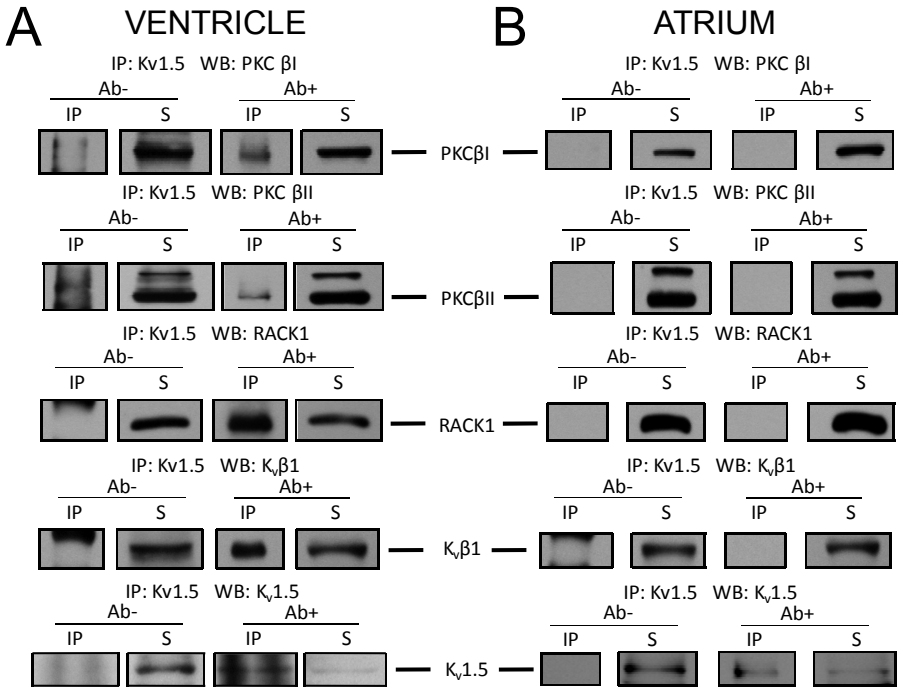

Figure 19: Immunoprecipitation of $K_v1.5$ channel in cardiac tissue. Negative (Ab−) and positive (Ab+) immunoprecipitations (IP) blotted against the different PKC isoforms present in HEK293 *channelosome* (Figure 18). Note that a very similar *channelosome* has been found in ventricular (A), but not in atrial (B), tissue (n = 3). WB, Western blot; S, supernatants.

4.2 PHARMACOLOGICAL CONSEQUENCES OF PROTEIN KINASE C INHIBITION ON K_v1.5-K_vβ1.3 CHANNELS.

4.2.1 K_vβ1.3-induced fast inactivation is abolished by PKC inhibition.

Figure 20 shows the effects of the K_vβ1.3 subunit on the K_v1.5 channel, which induces a fast and partial inactivation, a greater degree of slow inactivation, a slower deactivation process and a shift of the activation curve towards more negative potentials (Figure 20A and B, and Table 6). PKC inhibition with calphostin C prevents K_vβ1.3-induced fast inactivation of K_v1.5 channels (Murray *et al.*, 1994; Kwak *et al.*, 1999a; Kwak *et al.*, 1999b) as a consequence of a shift in the inactivation midpoint towards more positive potentials (David *et al.*, 2012). K_v1.5-K_vβ1.3 channels expressed in cells treated with calphostin C (K_v1.5-K_vβ1.3-calphostin C channels) exhibited an activation curve intermediate between that observed for the K_v1.5 and K_v1.5-K_vβ1.3 channels (Table 6), and similar deactivation kinetics to K_v1.5-K_vβ1.3 channels (Figures 20B and C). To analyze the electrophysiological characteristics of the inactivation process of K_v1.5-K_vβ1.3-calphostin C channels, we applied the double-pulse protocol shown at the top of Figure 21. Figure 21A shows the inactivation curves of K_v1.5, K_v1.5-K_vβ1.3 and K_v1.5-K_vβ1.3-calphostin C channels. PKC inhibition shifted the inactivation curve towards more positive potentials, which was similar to the V_h observed in K_v1.5 channels (Table 7). Although the degree of inactivation of K_v1.5-K_vβ1.3-calphostin C was decreased in comparison to K_v1.5-K_vβ1.3 channels, it was not fully reverted back to that observed in K_v1.5 channels (Figures 20 and 21, and Table 7).

TABLE 6. Voltage-dependent activation parameters of K_v1.5, K_v1.5-K_vβ1.3 and K_v1.5-K_vβ1.3-calphostin C channels. *V_h:* Half-inactivation voltage. *s:* Slope of the Boltzmann equation. Data represent the mean ± SEM of n>7 experiments.

	V_h (mV)	*s* (mV)
K_v1.5	0.2 ± 3.1	9.0 ± 0.8
K_v1.5+ K_vβ1.3 Control	-23.6 ± 2.4	3.9 ± 0.2
K_v1.5+ K_vβ1.3 calphostin C	-15.3 ± 1.2	6.0 ± 0.6

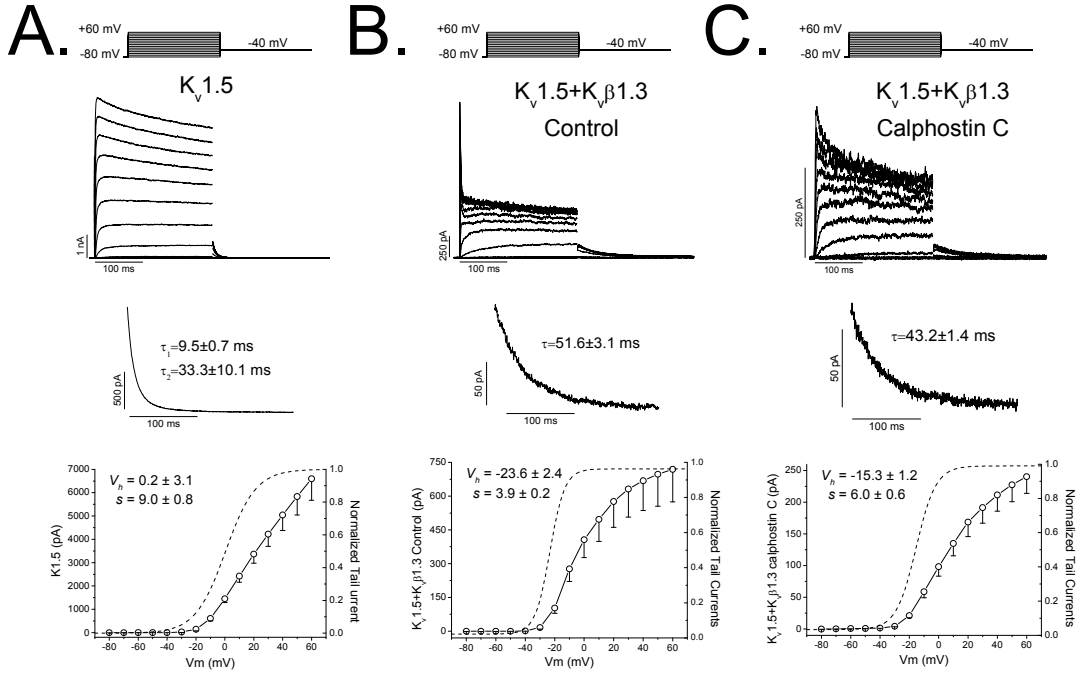

Figure 20: Original recordings obtained upon depolarization from a holding potential of −80 mV to +60 mV in 10 mV steps and upon repolarization to −40 mV. **A,** Current recordings obtained from the activation of K_v1.5 channels. **B,** Current recordings of K_v1.5 channels in the presence of the K_vβ1.3 subunit. **C,** Current recordings of K_v1.5 channels in the presence of a K_vβ1.3 subunit in cells that had been previously treated with calphostin C (3 μM) for 2 h. In all cases, the current (top), the deactivation process recorded at -40 mV after a prepulse to +60 mV (middle), as well as the IV relations and activation curves (dashed line) obtained (bottom) are shown. Note that the deactivation process is faster when the K_v1.5 channel is expressed alone. When PKC is inhibited, the linearity of the IV is recovered, and the activation process is shifted toward more negative potential when the K_vβ1.3 subunit is present.

The degree of inactivation of K_v1.5-K_vβ1.3 channels continued to increase as membrane potential was more positive, indicating that K_vβ1.3-mediated fast inactivation is voltage-dependent, as previously reported (Uebele *et al.*, 1998). However, the inactivation of K_v1.5-K_vβ1.3-calphostin C channels did not increase, similar to that observed in K_v1.5 channels (Figure 21A).

To isolate the fast component of the inactivation induced by the K_vβ1.3 subunit, a double-pulse protocol using a 10 ms prepulse from -80 mV to +150 mV in 10 mV steps was applied (Uebele et al., 1998). Figure 21B shows the inactivation curve obtained after applying this double-pulse protocol. After applying this short prepulse, K_v1.5 channels do not inactivate, because they exhibit a slow inactivation with a time constant of ≈200 ms. K_v1.5-K_vβ1.3 channels, which exhibit a fast inactivation with a time constant of ≈3 ms, display an inactivation curve with a V_h = -5.2 ± 2.5 mV and s = 5.3 ± 0.9 mV (n=4). This inactivation curve only represents the voltage-dependence of K_vβ1.3-fast inactivation induced, since when cells were treated with calphostin C this process is abolished. Figure 21B also shows that when this pulse protocol is applied, the fractional inactivation of K_v1.5-K_vβ1.3 channels did not increase with membrane potential, exhibiting similar behavior to that observed when a 250 ms in duration prepulse was applied in calphostin C-treated cells (Figure 21B and Table 7). However, when PKC was

inhibited, the inactivation process was completely abolished, exhibiting the same phenotype as $K_v1.5$ channels alone.

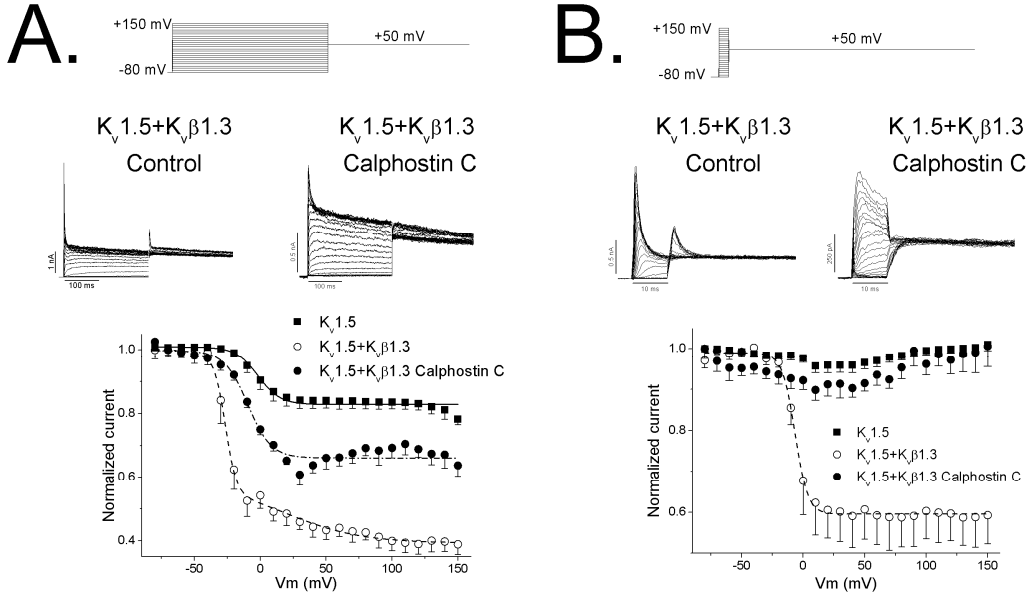

Figure 21: Voltage dependence of $K_v1.5$-$K_v\beta1.3$ channel inactivation treated or non-treated with calphostin C. **A,** Voltage dependence of inactivation following a 250 ms in duration prepulse. **B,** Voltage dependence of the inactivation following a 10 ms in duration prepulse.

TABLE 7. Voltage-dependent inactivation parameters of $K_v1.5$, $K_v1.5$-$K_v\beta1.3$ and $K_v1.5$-$K_v\beta1.3$-calphostin C channels obtained after applying a 250 ms prepulse. V_h: Half-inactivation voltage. *s*: Slope of the Boltzmann equation. Data represent the mean ± SEM of n>7 experiments *: Statistically significant difference between calphostin C and control conditions. #: Statistically significant difference between calphostin C and $K_v1.5$ channel alone.

	V_h (mV)	*s* (mV)	Degree of inactivation (%)
$K_v1.5$	-1.3 ± 3.4	9.79 ± 1.6	18.0 ± 3.4
$K_v1.5$-$K_v\beta1.3$ Control	-26.5	4.2	48.0 ± 3.0
$K_v1.5$-$K_v\beta1.3$ calphostin C	-6.5 ± 1.8*	10.1 ± 1.1*	33.8 ± 2.2*#

4.2.2 The pharmacological properties of $K_v1.5$-$K_v\beta1.3$ channels after calphostin C treatment mimic those of $K_v1.5$ channels in the absence of the $K_v\beta1.3$ subunit.

In previous studies, we have demonstrated that mutations of the $K_v1.5$ channel or its assembly with the $K_v\beta1.3$ subunit modify the pharmacological properties of the channel (Franqueza *et al.*, 1997; Gonzalez *et al.*, 2002; Arias *et al.*, 2007). Therefore, we studied the bupivacaine- and quinidine-induced blockade of $K_v1.5$-$K_v\beta1.3$ channels after PKC inhibition. Figure 22 shows current recordings through $K_v1.5$-$K_v\beta1.3$-calphostin C channels obtained in the absence and presence of bupivacaine (50 µM) or quinidine (30 µM). The current-voltage (I-V) relationships obtained after plotting the current amplitude measured at the end of 250-ms depolarizing pulses at different membrane potentials between −80 and +60 mV, in the absence and presence of either drug, are shown in the right panels of Figure 22. Both compounds decreased the magnitude of the current at all membrane potentials tested. This blockade was not voltage-dependent, exhibiting a similar degree of blockade when measured at +60 to that at 0 mV (72.3 ± 3.1 *vs.* 67.9 ± 2.3%, n = 6, p>0.05 for bupivacaine, and 50.7 ± 3.7 *vs.* 50.4 ± 5.3%, n = 5, p>0.05 for quinidine) (Figure 22).

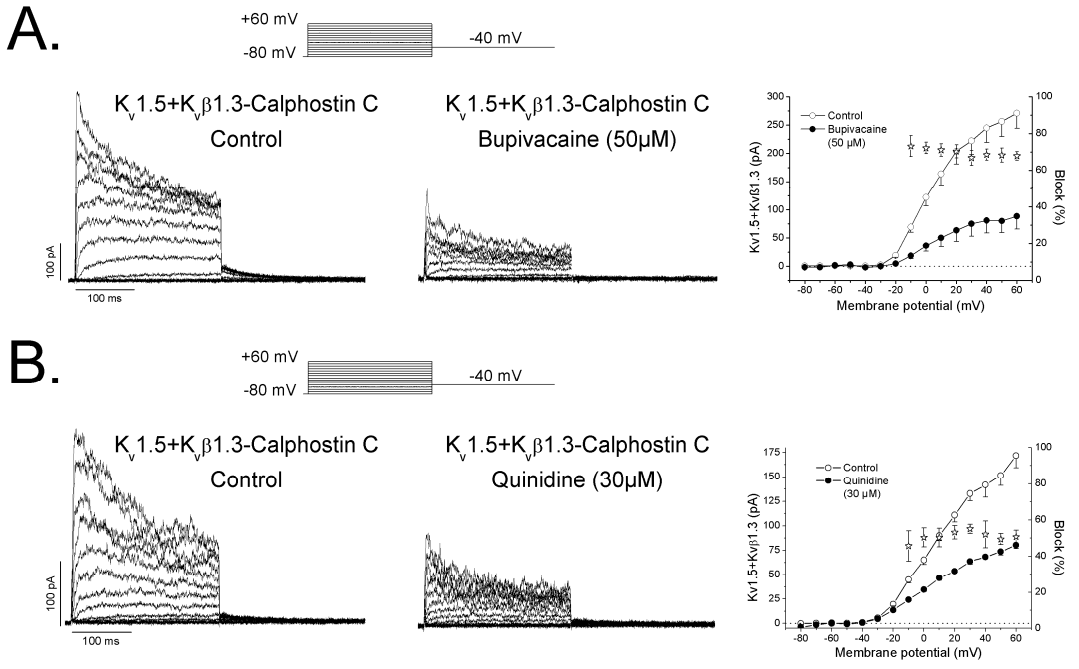

Figure 22: Effects of bupivacaine (50 µM) and quinidine (30 µM) on $K_v1.5$-$K_v\beta1.3$ channels in cells that have been treated with calphostin C (3 µM) for 2 h. **A,** Current recordings, voltage dependence of the blockade (☆) and IV relationships obtained in the absence (○) and presence of bupivacaine (●). **B,** Current recordings, voltage dependence of the blockade (☆) and IV relationships obtained in the absence (○) and presence of quinidine (●). The blockade induced by both drugs was measured at the end of the pulse at +60 mV. Each point represents the mean ± S.E.M. of six and five experiments, respectively.

4.2.3 Bupivacaine and quinidine exhibit lower potency for blocking $K_v1.5$-$K_v\beta1.3$ channels after PKC inhibition.

The concentration-response curves obtained for bupivacaine- and quinidine-produced blockade of $K_v1.5$, $K_v1.5$-$K_v\beta1.3$ and $K_v1.5$-$K_v\beta1.3$-calphostin C channels are shown in Figure 23. The suppression of the current at the end of 250 ms depolarizing pulses at +60 mV was used as an index of blockade. In contrast to the blockade previously reported for $K_v1.5$-$K_v\beta1.3$ channels (Gonzalez *et al.*, 2002), bupivacaine-induced blockade of $K_v1.5$-$K_v\beta1.3$-calphostin C channels showed a biphasic curve, with an $IC_{50(1)}$ of 0.2 ± 0.1 nM and an $IC_{50(2)}$ of 21.4 ± 4.1 µM (n = 41). Note that the $IC_{50(2)}$ was similar to that of $K_v1.5$ channels (Gonzalez *et al.*, 2002). PKC inhibition did not modify the n_H value (0.74 ± 0.06 *vs.* 0.71 ± 0.08 for bupivacaine-produced blockade of $K_v1.5$-$K_v\beta1.3$ and $K_v1.5$-$K_v\beta1.3$-calphostin C channels, respectively) (Gonzalez *et al.*, 2002) (Figure R23A). Similarly, quinidine-induced blockade of $K_v1.5$-$K_v\beta1.3$ channels was modified by calphostin C treatment (Figure 23B). Indeed, the concentration-response curve was also a biphasic concentration-response curve, with $IC_{50(1)}$ and $IC_{50(2)}$ values of 3.4 ± 5.4 µM and 70.4 ± 15.4 µM (n=50), respectively. Interestingly, the $IC_{50(1)}$ value was similar to that reported for quinidine-produced blockade of $K_v1.5$ channels (Yeola *et al.*, 1996), whereas the $IC_{50(2)}$ value was similar to the value reported for blockade of $K_v1.5$-$K_v\beta1.3$ channels (Gonzalez *et al.*, 2002). The $n_{H(1)}$ and $n_{H(2)}$ values for this concentration-response curve were 0.34 ± 0.07 and 1.36 ± 0.46, respectively. The $n_{H(2)}$ value was similar to that observed in the concentration-response curve of quinidine-induced blockade of $K_v1.5$-$K_v\beta1.3$ channels (Gonzalez *et al.*, 2002).

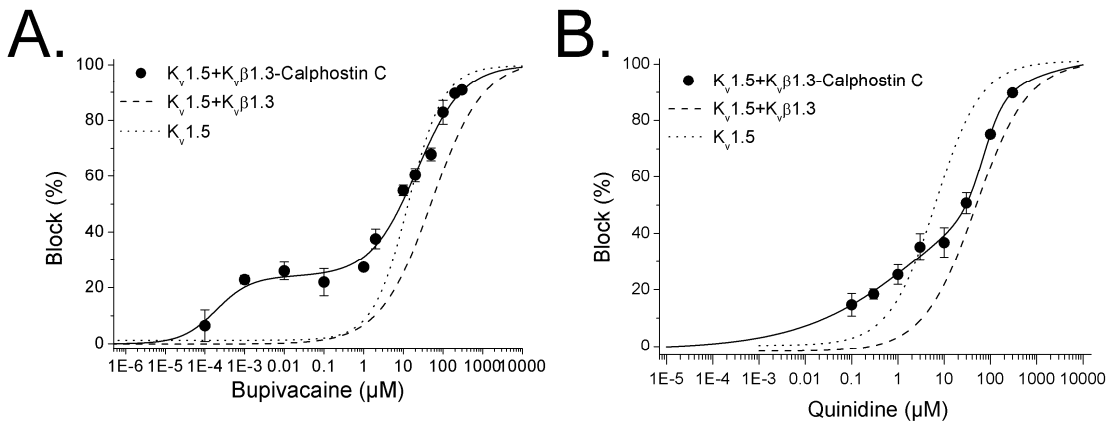

Figure 23: Concentration dependence of bupivacaine-induced A. and quinine-induced B. blockade of calphostin C-treated $K_v1.5$-$K_v\beta1.3$ channels. The dotted and dashed lines represent the dose-response curves obtained for the bupivacaine- and quinidine-produced blockade of $K_v1.5$ channels alone and $K_v1.5$-$K_v\beta1.3$ channels, respectively (taken from Gonzalez et al., 2002). Reduction in the current (relative to the control) at the end of depolarizing steps from −80 to +60 mV was used as an index of blockade. Each point represents the mean ± S.E.M. of three to eight experiments. The continuous line represents the fit of the experimental data to a biphasic Hill equation.

4.2.4 Time-dependency of block of $K_v1.5$-$K_v\beta1.3$ channels produced by bupivacaine and quinidine after PKC inhibition

Bupivacaine- and quinidine-produced blockade of $K_v1.5$-$K_v\beta1.3$-calphostin C channels was time-dependent, as indicated by the normalized current in the insets of the left panels of Figure 24. To analyze the kinetics of blockade induced by both drugs, we plotted the ratio of the drug-sensitive current and the current under control conditions $[(I_{Control}-I_{Drug})/I_{Control}]$ during the first 40 ms in the presence of 20, 50 and 100 μM bupivacaine and 10, 30, and 100 μM quinidine (right panel of Figures 24A and B, inset). Blockade exponentially increased during depolarization, and the time constant of this process was faster at higher drug concentrations. Thus, this time constant was considered to be a good index of the development of blockade (τ_{Block}). Based on the τ_{Block} values obtained at different bupivacaine concentrations, the association (*k*) and dissociation (*l*) rate constants were derived, averaging 5.9 ± 0.5 $\mu M^{-1}s^{-1}$ and 252.3 ± 33.0 s^{-1} versus 3.8 ± 0.3 $\mu M^{-1}s^{-1}$ and 108.3 ± 14.3 s^{-1} (n=14) in $K_v1.5$-$K_v\beta1.3$ and $K_v1.5$-$K_v\beta1.3$-calphostin C channels, respectively (Figure 24A) (Gonzalez *et al.*, 2002). The IC_{50} value calculated from these values (28.5 μM = *l*/*k*) was very similar to that obtained from the concentration-response curve (21.4 μM). In the case of quinidine, the *k* and *l* values for $K_v1.5$-$K_v\beta1.3$ channels were 5.1 ± 0.51 $\mu M^{-1}s^{-1}$ and 454.7 ± 38.05 s^{-1}, while the *k* and *l* values for $K_v1.5$-$K_v\beta1.3$-calphostin C channels were 5.0 ± 0.02 $\mu M^{-1}s^{-1}$ and 196.4 ± 1.1 s^{-1} (n=11) (Figure 24B). However, in this case, the IC_{50} value calculated from these values (39.6 μM = *l*/*k*) was not similar to that obtained from the concentration-response curve (70.4 μM). Although the blockade induced by both drugs exhibited time dependence, as observed during depolarization pulses from -80 to +60 mV, this time dependence was not evident in the tail currents recorded at -40 mV (Figure 25).

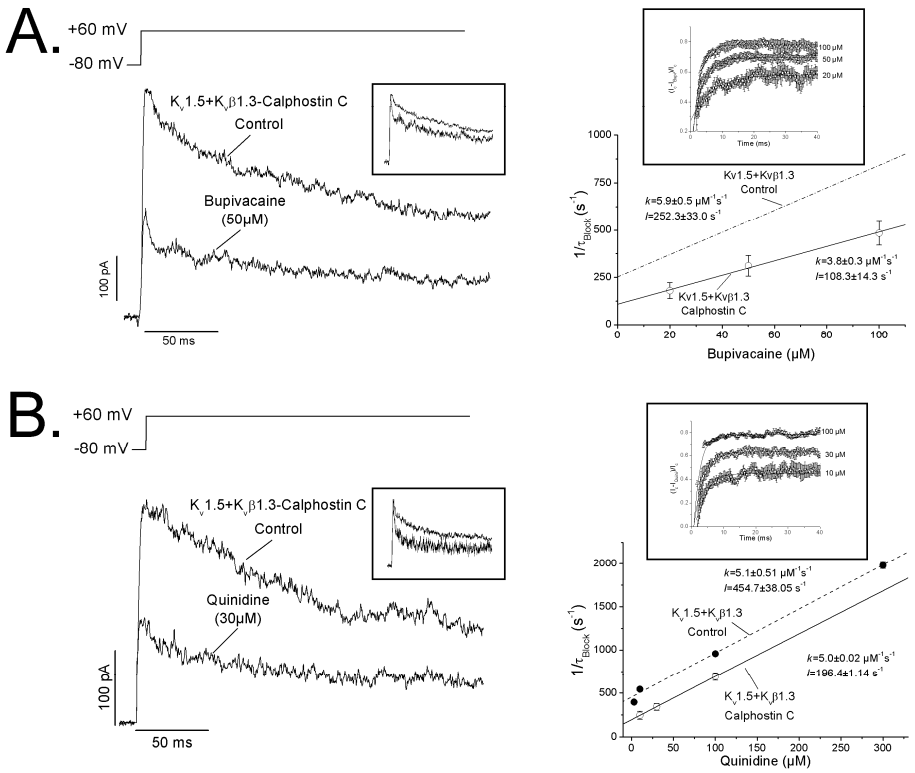

Figure 24: Time dependence of bupivacaine- A. and quinidine-induced B. blockade of calphostin C-treated $K_v1.5$-$K_v\beta1.3$ channels. *Left:* Superimposed traces for the steps from -80 to +60 mV and those normalized to the control values (inset). *Right:* Relationship between $1/\tau_B$ values at different concentrations of bupivacaine (20, 50 and 100 μM) and quinidine (10, 30 and 100 μM). Each point represents the mean ± SEM of three to six experiments. For a first-order blocking scheme, a relationship is expected: $1/\tau_B = k \times [\text{Drug}] + l$. The lines represent the fit from which the apparent binding (k) and unbinding (l) rate constants were obtained in the control (dashed) and PKC-inhibited (solid) conditions. The relationship between the sensitive current and depolarizing time $[(I_{Control} - I_{Drug})/I_{Control}]$ at three different drug concentrations is plotted in the inset of each panel.

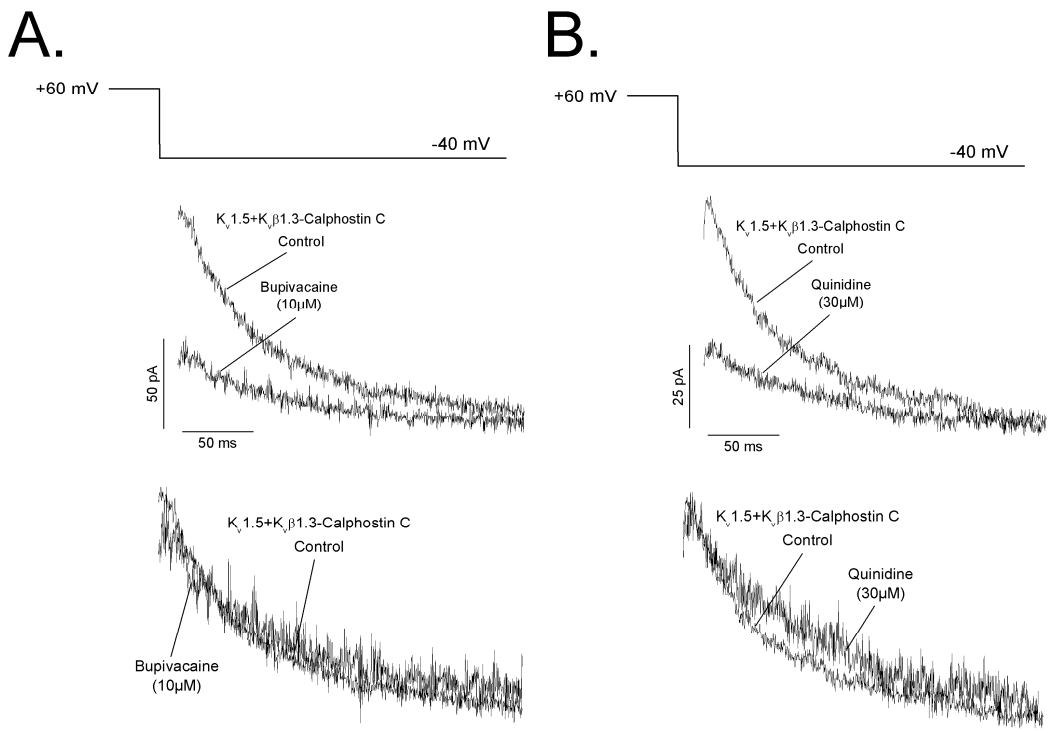

Figure 25: Bupivacaine- A. and quinidine-induced B. effects on the deactivation kinetics of calphostin C-treated $K_v1.5$-$K_v\beta1.3$ channels. The currents were obtained after applying the protocol outlined at the top of the figure. The tails were superimposed (*top*) and normalized (*bottom*) to show the similar deactivation kinetics in the absence and presence of both drugs.

4.3 PKC REGULATES THE K_v1.5 CHANNEL TRAFFICKING

4.3.1 PKC inhibition reduces the amount of K_v1.5 channel in the cell surface

Figure 20 shows that PKC inhibition not only modifies the characteristics of the current; abolishing the $K_v\beta$1.3-induced fast inactivation and voltage dependence of K_v1.5-$K_v\beta$1.3 channels, as previously described (David *et al.*, 2012); but also produces a lower magnitude of the current (from 719.2 ± 145.2 pA under control conditions, n=14, to 240.4 ± 26.5 pA after PKC inhibition with calphostin C, n=41, $p<0.05$). It was also observed that the magnitude of the currents became smaller with the time (data not shown). A possible explanation for this result could be that PKC inhibition results in a decrease level of K_v1.5 at the plasma membrane. To assess this hypothesis, we performed an extracellular enzymatic digestion of K_v1.5-$K_v\beta$1.3 channels with proteinase K, followed by a western blot analysis (Figure 26). This kind of test represents a very sensitive assay for analyzing cell surface protein expression, since cytoplasmic proteins are unaffected when this enzyme is applied in living cells (Figure 6A) (Manganas *et al.*, 2001; Choi *et al.*, 2005). Densitometric analysis shown in Figure 26B demonstrates that cell treatment for two hours with calphostin C results in a significant decrease of the channel amount (32.6 ± 7.1%, n=5, $p<0.05$), without changes in the total channel amount (3.8 ± 4.1 *vs.*, n=5, $p>0.05$).

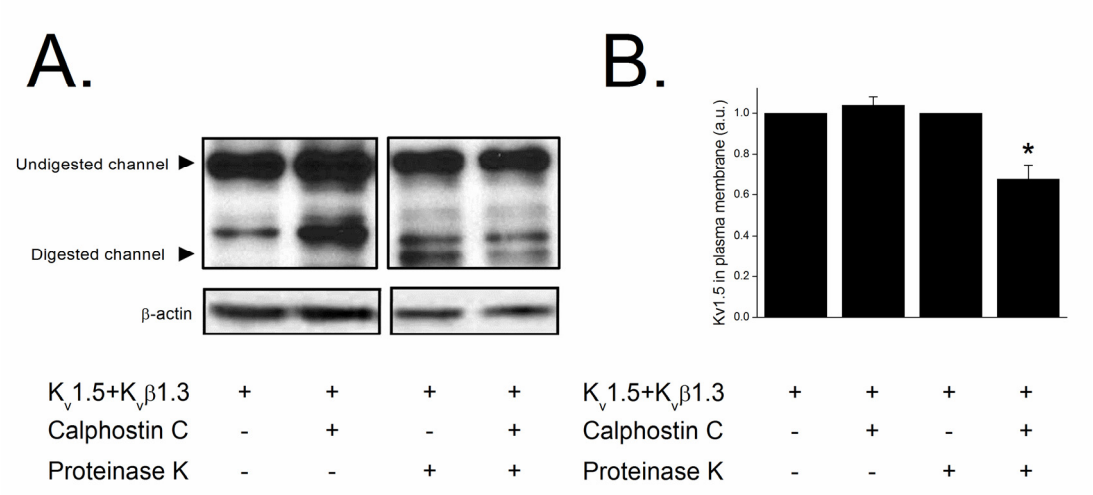

Figure 26: PKC inhibition significantly decreases K_v1.5 surface expression. HEK293 cells expressing K_v1.5-$K_v\beta$1.3 channels and treated or untreated with calphostin C 3 µM for 2h and treated with Proteinase K externally applied (lanes 3 and 4) or buffer alone (lanes 1 and 2). **A,** Representative experiment in which the arrows indicate the molecular weight at which surface K_v1.5 (digested form) and intracellular K_v1.5 (undigested form) appear. The immunoblot of β-actin at the bottom indicates that equal amounts of protein were loaded in each line. **B,** Densitometric analysis of 5 experiments like that shown in panel A. Each data represents the mean ± SEM of five experiments, *, $p<0.05$.

4.3.2 Inhibition of PKC with Calphostin C reduces the channel present in the cell membrane, increasing its amount into the cytoplasm

The reduction of the $K_v1.5$ protein amount at the cell surface after PKC inhibition suggests that the trafficking of the $K_v1.5$ *channelosome* can be modified either by: 1) an increase of the internalization of $K_v1.5$ channels, or 2) a decrease in the recycling of this protein from endosomes to plasma membrane. In order to discriminate between these possibilities, a series of biotinylation experiments were performed in which a FLAG-tagged $K_v1.5$-$K_v\beta1.3$ construction was used in order to increase the likelihood of biotinylation (see a representative experiment in Figure 27A). To determine whether the functional characteristics of the channels encoded by this construction were affected by the presence of the FLAG epitope at the S1-S2 extracellular loop, electrophysiological experiments were performed (Figure S2). As it is observed, in Figure S2, the electrophysiological characteristics of the $K_v1.5$-$K_v\beta1.3$ channels were not changed in comparison with $K_v1.5$-$K_v\beta1.3$ observed in those channels without the extracellular FLAG epitope. The results obtained in the biotinylation assays are shown in Figure 27B and suggest that the protected $K_v1.5$-$K_v\beta1.3$ channel behavior after PKC inhibition is similar to that observed under control conditions at shorter times than 60 min from the beginning of the treatment with calphostin C. However calphostin C-treated cells show a significant increase in the amount of intracellular channel after two hours of treatment (13.6±1.6 % in control condition *vs.* 20.7±1.9 % in calphostin C treated cells, n=3, $p<0.05$), suggesting that PKC is involved in the recycle of the channel.

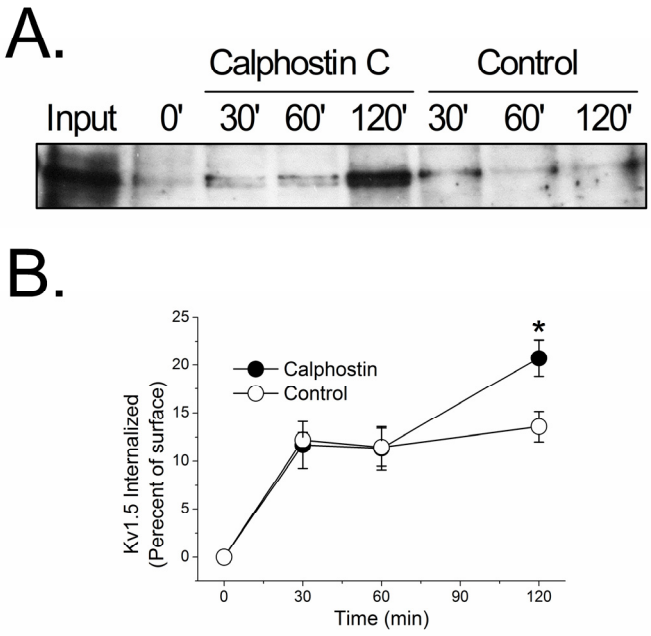

Figure 27: PKC inhibition significantly modify the $K_v1.5$ recycling. Recycling rates were measured using a biotinylation assay (see "Experimental Procedures"). **A,** Representative Western blot of biotinylated channels (internalized) at different times (30, 60 and 120 min). **B,** Densitometric analysis of experiments like that showed in panel A. Each data represents the mean ± SEM of three experiments. *, $p<0.05$.

In order to analyze this process by using another experimental approach, we performed immunocytochemical experiments that permitted us to discriminate the internalization of the channel after calphostin C treatment. To this end, a K_v1.5-HA+K_vβ1.3 construction was used (with similar electrophysiological characteristics than the K_v1.5-FLAG+K_vβ1.3 construction, Figure S3). As it is shown in Figure S3, the electrophysiological characteristics of the K_v1.5-K_vβ1.3 channels were unchanged in comparison with those observed in those channels without the extracellular HA epitope. These experiments were performed in two steps (for more details see the 3.7.2 section of Materials and Methods): 1) first we labeled the channel present in the cell membrane with anti-HA before the beginning of the treatment with calphostin C. Then, 2) cells were fixed and stained with the secondary antibodies. Figure 28 shows representative confocal images of cells transfected with K_v1.5-HA+K_vβ1.3 under control conditions and after PKC inhibition with calphostin C. Under control conditions, most cells exhibited K_v1.5-HA+K_vβ1.3 channels mainly in the cell membrane (red color) (*top*); whereas after PKC inhibition, all stained cells exhibited most K_v1.5-HA+K_vβ1.3 channels in the cytoplasm (green color) and less amount of the channels at the cell membrane (*bottom*).

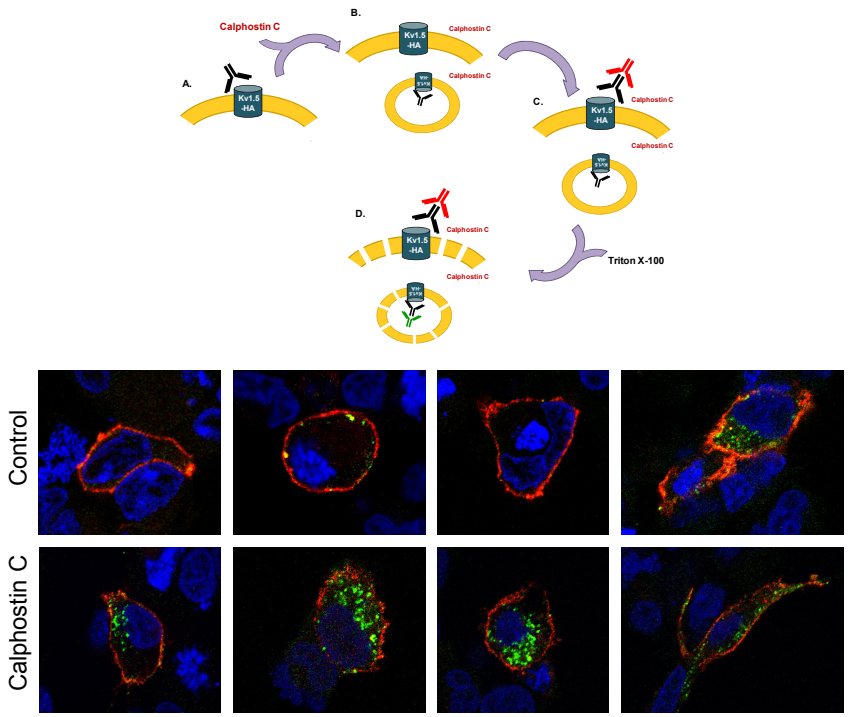

Figure 28: PKC inhibition increases the amount of internalized channel. Representative images of cells in control conditions (*upper panels*) and after PKC inhibition after calphostin C treatment (*bottom panels*). Note that while in control conditions, cells show mainly, although not only, a high red signal (channel present in plasma membrane); calphostin C-treated cells exhibit a weaker red signal and significant higher green signal (channel internalized and non-recycled towards the cell membrane). In the top part of the figure it has been represent a scheme of the process carried out in these assays.

Moreover, in calphostin C treated cells the amount of channels inside the cells is much greater than in control cells. Also it can be seen these results in the Figure S4 where the orthogonal projection of these cells have shown where it can be observe a 'whole' representation of the staining of each cell.

4.3.3 Channel dynamics is also disrupted

In order to analyze whether the effects of PKC inhibition was modified, not only the channel location at the end of the treatment, but also to be able to discriminate the cellular traffic of the channels in live cells; we performed live cell imaging assays in a Cell Observer equipment using fluorescence. As it shown in Figure 29 and in Videos 1A-C in control conditions, and 2A-C after PKC inhibition (Videos 1D-F and 2D-F show the same experiments but in the maximal projection instead of one representative section as showed in 1A-C and in 2A-C), we observed a dramatic decrease or abolishment of the channel dynamic.

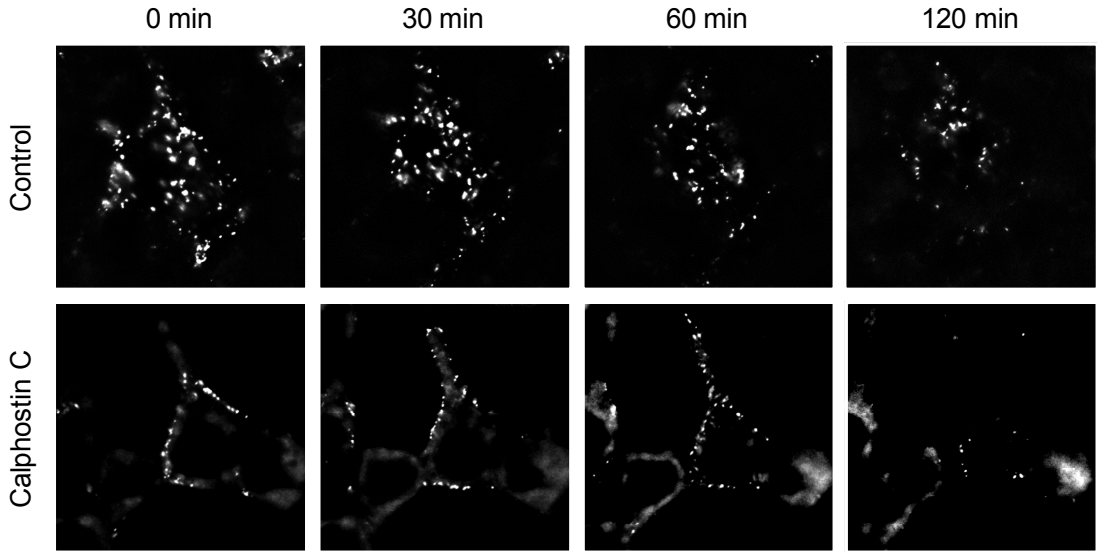

Figure 29: Influence of PKC inhibition on $K_v\beta1.3$-IRES-$K_v1.5$-HA mobility in HEK293. K_v1.5-HA labelled by fluorescence staining of live cell under control conditions (*upper panels*) and after PKC inhibition by calphostin C treatment (*bottom panels*) and visualized at different times. Frames extracted from Videos 1B for control and Video 2B for calphostin C.

4.3.4 PKC is involved in the slow recycling of the channel

Rab-GTPases regulate the trafficking of vesicles between plasma membrane and intracellular compartments by regulating sorting, tethering and docking of trafficking vesicles. Rab4, associated with the early endosome (EE), mediates the fast recycling process while Rab11, linked to the recycling endosome (RE), is involved in slow recycling of proteins back to the cell surface (Balse *et al.*, 2009). Because we have observed that PKC inhibition strongly decreases the K_v1.5 trafficking, we hypothesized that PKC activity is necessary to some of these processes. In order to know which one (fast or slow recycling) is involved, immunocytochemistry experiments were carried out. Figure 30

shows representative confocal images of cells transfected with K_v1.5-HA+K_vβ1.3 and, either, Rab4 or Rab11 constitutively actives (CA). The results shown in this Figure suggest that only in the presence of Rab11CA, the amount of channel internalized (green color) (*bottom*) after calphostin C treatment is decreased in comparison with that observed in cells cotransfected with K_v1.5-HA+K_vβ1.3+Rab4CA (*top*) or those cotransfected with K_v1.5-HA+K_vβ1.3 channels (at *bottom of Figure 28*) and treated with calphostin C. Also, it can be seen these results in the Figure S5 where the orthogonal projection of these cells have shown where it can be observe a 'whole' representation of the staining of each cell.

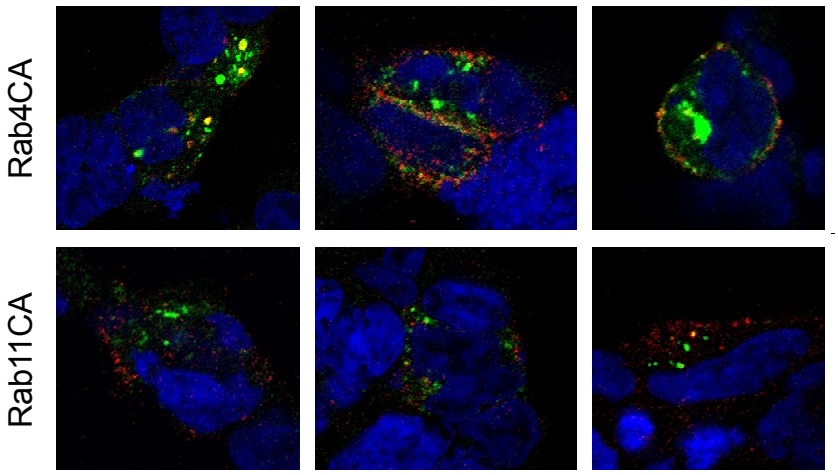

Figure 30: The cotransfection of K_v1.5-K_vβ1.3 with Rab11CA abolishes the increase of the internalization PKC inhibition-mediated. Representative images of cells after cotransfection of K_v1.5-K_vβ1.3 channels with Rab4CA (*upper panels*) and with Rab11CA (*bottom panels*), after calphostin C treatment. Note that only in the presence of Rab11CA, the amount of channel internalized (green color) (*bottom*) after calphostin C treatment is decreased in comparison with that cell cotransfected with K_v1.5-HA+K_vβ1.3+Rab4CA (*top*) or those cotransfected with K_v1.5-HA+K_vβ1.3 channels (at *bottom of Figure 28*). The amount of channel present in plasma membrane is shown in red color.

In order to confirm this hypothesis, electrophysiological experiments were performed in which Rab4CA or Rab11CA were cotransfected with K_v1.5-K_vβ1.3. Figure 31 shows representative records obtained of outward potassium current after cell cotransfection with K_v1.5-K_vβ1.3 and Rab4CA, and treated with calphostin C after 48h post-transfection. As it can be observed, currents obtained exhibited similar properties and magnitude than those recorded from cells transfected with K_v1.5-K_vβ1.3 and treated with calphostin C (240.4±26.5 pA in K_v1.5-K_vβ1.3 calphostin-treated channels *vs.* 273.4±58.1 pA in K_v1.5-K_vβ1.3+Rab4CA, n=5-8, $p>0.05$, Figure R31A). However, currents recorded from cells cotransfected with K_v1.5-K_vβ1.3 and Rab11CA exhibited a greater magnitude at potentials positive to -10 mV (240.4±26.5 pA in K_v1.5-K_vβ1.3 calphostin-treated channels *vs.* 511.6±94.2 pA in K_v1.5-K_vβ1.3+Rab22CA, n=5-8, $p<0.05$, Figure 31B).

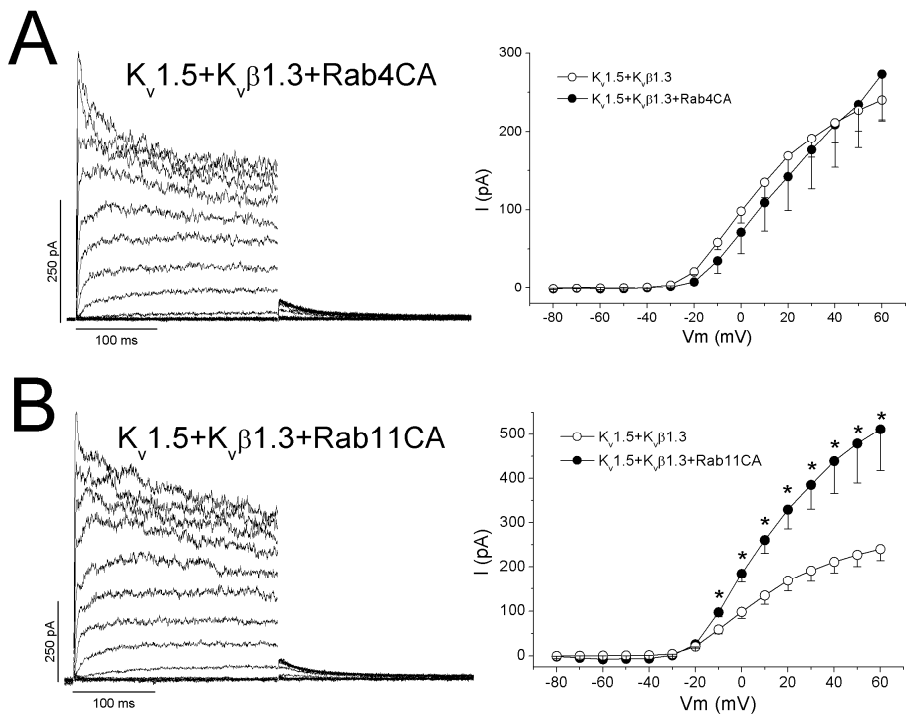

Figure 31: PKC activity is involved in K_v1.5-K_vβ1.3 recycling Rab11-meadiated. Representative recordings (left panels) and IV relationships (right panels) obtained after calphostin C treatment when Rab4CA (**A**) or Rab11CA (**B**) is co-transfected with K_v1.5-K_vβ1.3 channels. In both cases, IV relationships are compared with K_v1.5+ K_vβ1.3 channels. Note that only when Rab11CA is co-transfected we obtain significant differences and these are observed at potentials positive than -10 mV.

4.4 Lgi1 effects on K_v1.5-K_vβ1.3 channel complex. Possible role on human ventricle

4.4.1 Lgi1 is present in rat ventricle but not in atria

Lgi1 interferes with K_vβ1-conferred inactivation of K_v1 channels, suggesting that Lgi1 can modulate the gating of K_v1 channels. However, the molecular basis of the Lgi1 effect on K_v1 channel inactivation is presently unknown (Schulte *et al.*, 2006). It is known that, even when K_vβ1.3 and K_v1.5 subunits are expressed in human myocardium, a current with the K_v1.5-K_vβ1.3 phenotype has not been registered in any territory of the human heart (atrium or ventricle). One possible explanation could be that a given protein present in this tissue effect modifies the activity of the K_vβ1.3 subunit. To address this hypothesis, we first wanted to confirm the presence of this protein in cardiac tissue. To that end, we performed western blots of proteins from rat cardiac tissue (atria and ventricle). Figure 32 shows the results of these experiments that demonstrate the presence of Lgi1 protein in rat ventricle but not in atria. At least, if there is Lgi1 in rat atria, the level of expression is much lower than in ventricle, as it can be observed in Figure 32, comparing them with HEK293 cells transfected with Lgi1.

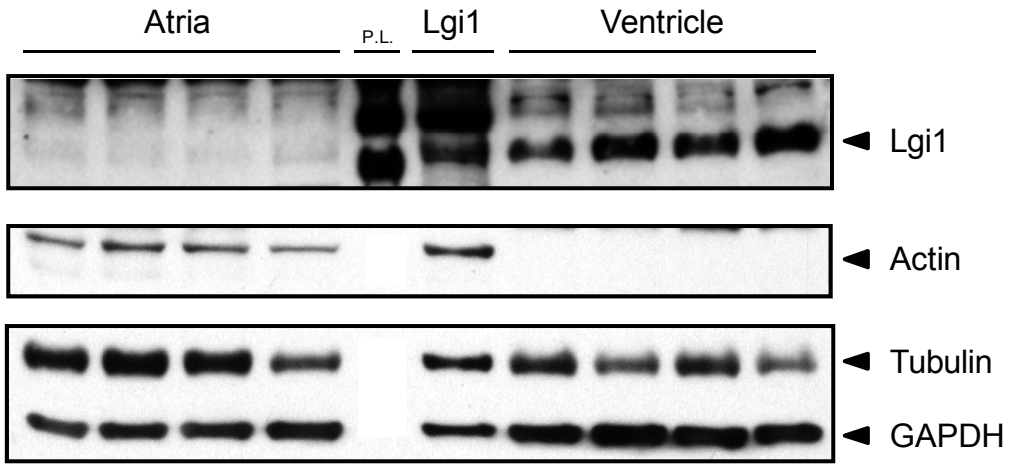

Figure 32: Lgi1 protein is expressed mainly in ventricle. Figure shows an immunoblotting against Lgi1 protein in four rat atria and four rat ventricles. HEK293 cells transfected with Lgi1 were used as a positive control (Lgi1 in the Figure). Also, this Figure shows a Protein Ladder (P.L.), which is showing two bands with 75 and 100 kDa of molecular weight. Note that, to get a weak signal in the case of atria, the film had to be highly exposed.

Next, we analyzed whether Lgi1 is another protein of the K_v1.5 *channelosome*. In order to assess this hypothesis, we performed immunoprecipitation assays in which we immunoprecipitated K_v1.5 and immunobloted for Lgi1, and *vice versa.* Figure 33 shows the results from these experiments. When we immunoprecipiteted K_v1.5 channels and we blotted for Lgi1, a band for Lgi1 was observed in the positive IP. Unfortunately, when the coIP was performed immunoprecipitating Lgi1 and blotting for K_v1.5, we observed a positive band both in the Ab- and in the Ab+ immunoprecipitations, because we

only got a positive immunoprecipitation when the samples were not pre-washed with A/G-protein previously to the immunoprecipitation process (Figure 33).

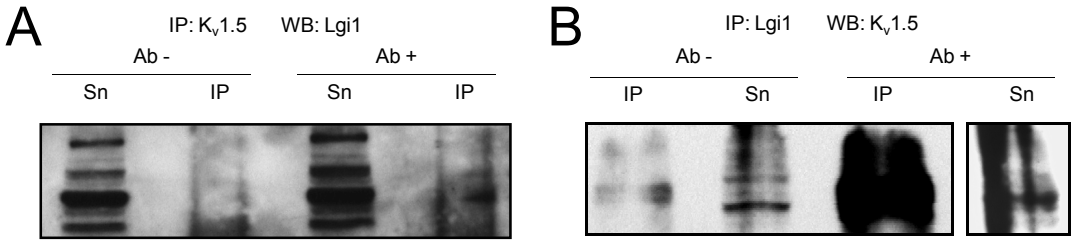

Figure 33: Immunoprecipitation of K_v1.5-Lgi1 complex in rat ventricular cardiac tissue. **A,** Immunoprecipitation of K_v1.5 channel and blotted against Lgi1 protein. **B,** Immunoprecipitation of Lgi1 protein and blotted against K_v1.5 channel. In both cases, negative (Ab−) and positive (Ab+) immunoprecipitations (IP) were performed. Note that when Lgi1 is immunoprecipitated, a residual and unspecific fraction of protein is apparent even in the negative IP (n = 3). WB, Western Blot; Sn, Supernatant.

4.4.2 Electrophysiological effects of Lgi1 are beta subunit-dependent

Given the overlap in the expression pattern between K_vβ1.3 and Lgi1 proteins in cardiac tissue, mainly in ventricular tissue, we wonder if Lgi1 subunits produced a functional relevance on K_v channels when cotransfected in heterologous system, like HEK293 cells. In these experiments (Figure 34A), we observed that cells cotransfected with K_v1.5-K_vβ1.3 and Lgi1 exhibited an outward current without K_vβ1.3-induced fast inactivation, a small magnitude of the current, a shift in the activation curve towards more positive potentials, as well as an increase in the slope of the activation curve (from V_h = -23.6± 2.4 mV and s = 3.9 ± 0.2 mV, n=14 , for K_v1.5-K_vβ1.3 channels and V_h = -13.2 ± 1.3 mV and s = 6.4 ± 0.9 mV for K_v1.5-K_vβ1.3+Lgi1, n=12 , $p<0.05$ in both cases). Beside this, K_v1.5-K_vβ1.3+Lgi1 channels showed an electrophysiological behavior more similar to that exhibited by K_v1.5 channel when they are transfected alone (Figure 34B). However, when Lgi1 protein is cotransfected with K_v1.5, without K_vβ1.3, we obtained a current of a smaller magnitude, but similar electrophysiological properties (V_h = 0.2 ± 3.1 mV and s = 9.0 ± 0.8 mV, n=9, for K_v1.5 channels, and V_h = 0.6 ± 4.3 mV and s = 9.4 ± 2.1 mV for K_v1.5+Lgi1, n=3, $p>0.05$; Figure 34B).

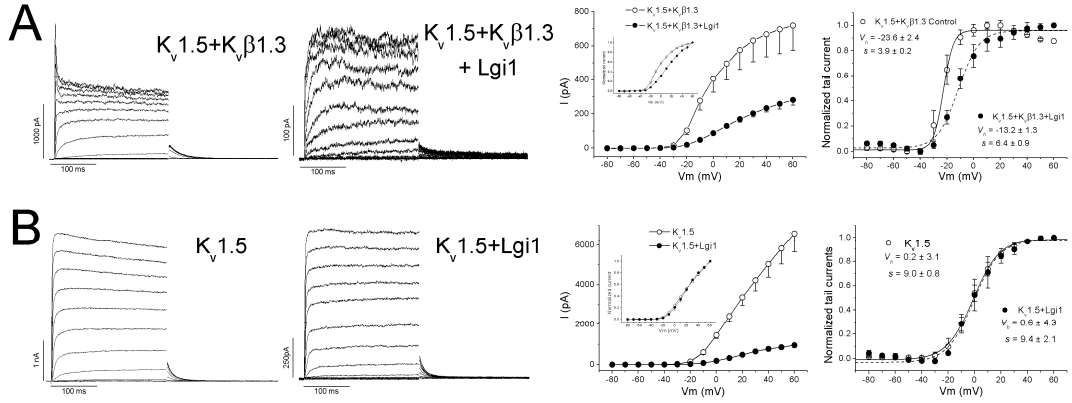

Figure 34: Effects of Lgi1 protein on the K_v1.5 current with and without the presence of K_vβ1.3 subunit. **A,** Effects of Lgi1 on K_v1.5-K_vβ1.3 channels: *Left panels,* Recordings obtained in the absence and in the presence of Lgi1, respectively; *Middle panel*, IV relationships before and after normalization by +60 mV value (*inset*); *Right panel*, Activation curves of both conditions. **B,** *Left panels,* Effect of Lgi1 protein on K_v1.5 channels expressed alone and in the presence of Lgi1; *Middle panel*, IV relationships before and after normalization by +60 mV value (*inset*); *Right panel*, Activation curves of both conditions.

4.4.3 Lgi1 reduces the amount of channel in the cell surface. The effects on the actin cytoskeleton are channel-dependent

Similarly to that observed with the calphostin C treatment on K_v1.5-K_vβ1.3 channels, the K_vβ1.3-induced fast inactivation abolishment appeared in parallel with a reduction of the magnitude of the current. In order to analyze if the amount of the channel protein in the cell surface decreased, experiments with proteinase K were performed. As Figure 35 shows, the co-transfection of K_v1.5-K_vβ1.3 with Lgi1 protein results in a significant decrease in the amount of the channel (32.1 ± 1.9%, n=5, $p<0.05$). It has been widely described, and also showed in the present Doctoral Thesis, that after treatment with proteinase K the amount of actin decreased even when the same amount of protein was analyzed (Manganas *et al.*, 2001; Choi *et al.*, 2005) (Figure 26). However, the dramatic effect observed in this case on the actin cytoskeleton, was only observed when the protein was co-transfected with the K_v1.5 channel (Figure 36), being therefore a channel-dependent effect. Moreover, this effect was also observed when tubulin was used as a loading control Figure 36B, but not when using GAPDH (Figures 35A and 36).

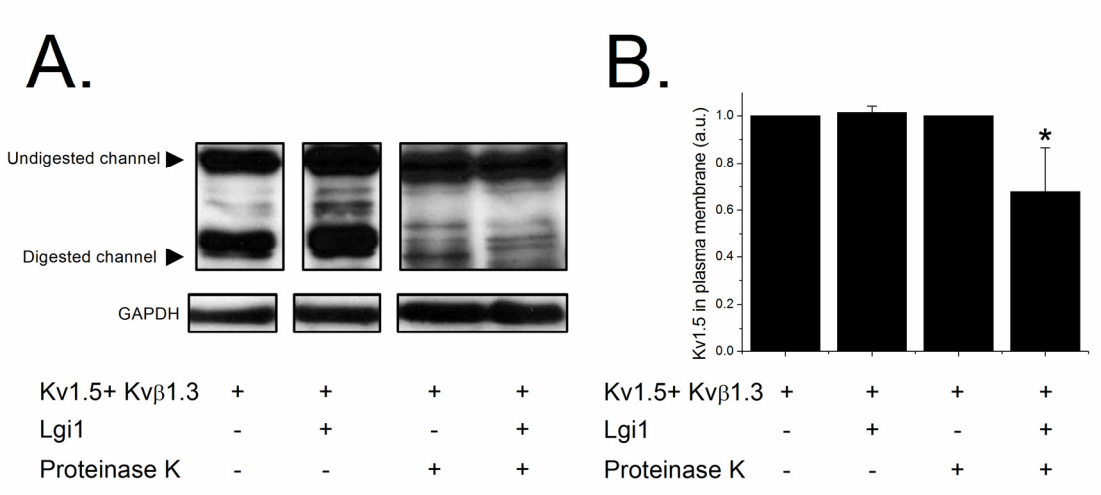

Figure 35: Lgi1 promotes a significant decrease in K_v1.5 surface expression. HEK293 cells expressing K_v1.5-K_vβ1.3 channels in the presence and in the absence of Lgi1 and with the external application of Proteinase K (lanes 3 and 4) or buffer alone (lanes 1 and 2). **A,** Representative experiment in which the arrows points out the surface K_v1.5 (digested form) and the intracellular K_v1.5 (undigested form) channel. The immunoblot of GAPDH at the bottom indicates that equal amounts of protein were loaded in each line. **B,** Densitometric analysis of similar experiments to that showed in panel A. Each data represents the mean ± S.E.M. of five experiments; *, p<0.05.

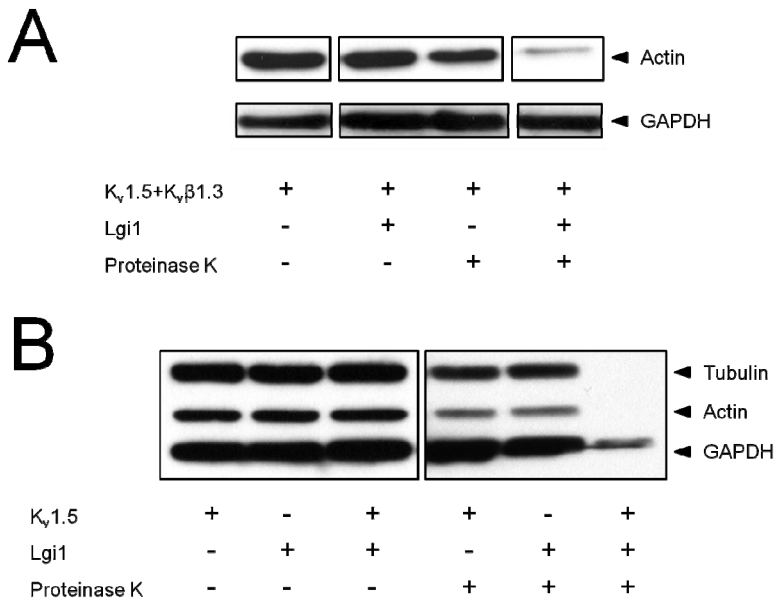

Figure 36: The effects of the Lgi1 on the actin cytoskeleton are channel-dependent. **A,** The effects of Lgi1 on actin cytoskeleton only appear when this protein is co-transfected with K_v1.5-K_vβ1.3 channels. **B,** The effects of Lgi1 on the actin cytoskeleton also appears when this protein is co-transfected with K_v1.5 alone. Note that this effect is not observed when any of the proteins (K_v1.5 or Lgi1) are transfected separately.

4.4.4 Lgi1 effects are, at least in part, due to extracellular signaling

In order to study the mechanism of action by which Lgi1 abolishes the $K_v\beta1.3$-induced fast inactivation in "real time" we used two different experimental approaches. In the first one, we tried to inhibit the inhibitory effects of Lgi1 on the beta subunit using an anti-Lgi1 antibody in the internal solution of the patch pipette. But, in these experiments the phenotype of the current elicited was similar to that obtained after activate $K_v1.5$ channels alone, suggesting that after the binding of the anti-Lgi1 antibody to its epitope, the activity of $K_v\beta1.3$ subunit is compromised (Figure 37).

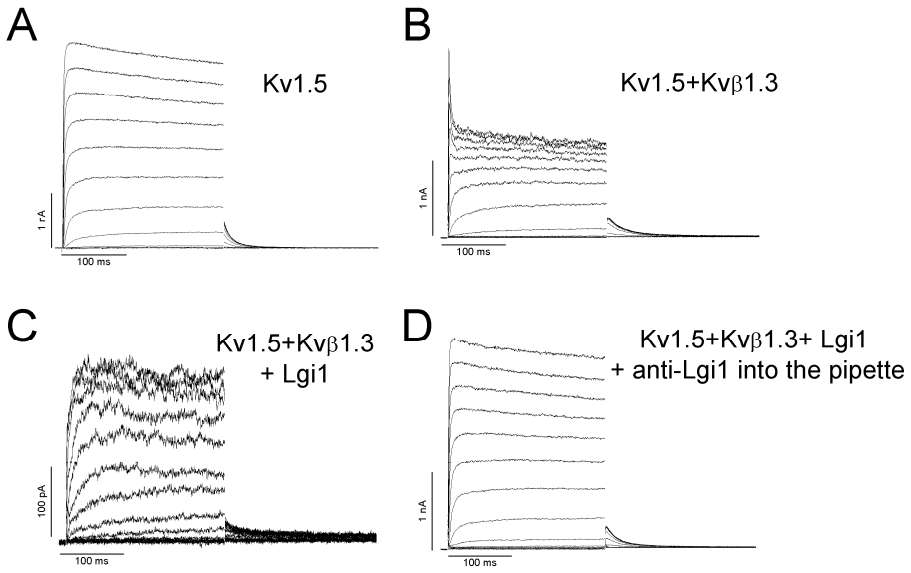

Figure 37: Effects of anti-Lgi1 present into the solution of the patch pipette. **A,** Current records of $K_v1.5$. **B,** Current records obtained from the activation of $K_v1.5$-$K_v\beta1.3$ channels. **C,** Current records obtained in cells cotransfected with $K_v1.5$-$K_v\beta1.3$ and Lgi1. **D,** Current records obtained from cells transfected with $K_v1.5$-$K_v\beta1.3$+Lgi1 and with anti-Lgi1 in the internal solution of the patch pipette. Note that the current elicited by $K_v1.5$-$K_v\beta1.3$ channels in the presence of Lgi1 into the pipette results in a similar abolishment of that showed by them after the cotransfection and closer to $K_v1.5$ current.

Secondly, we carried out experiments in cells transfected with the $K_v1.5$-$K_v\beta1.3$ construction and, filling the internal solution of the pipette with the Lgi1 purified protein (0.5 µg/ml). In these experiments, if we broke the seal just after we got it, Lgi1 was not able to abolish the $K_v\beta1.3$-induced fast inactivation (Figure 38A). In fact, only when we waited at least 2 min after seal formation, the $K_v\beta1.3$-induced fast inactivation was abolished (Figure 38B).

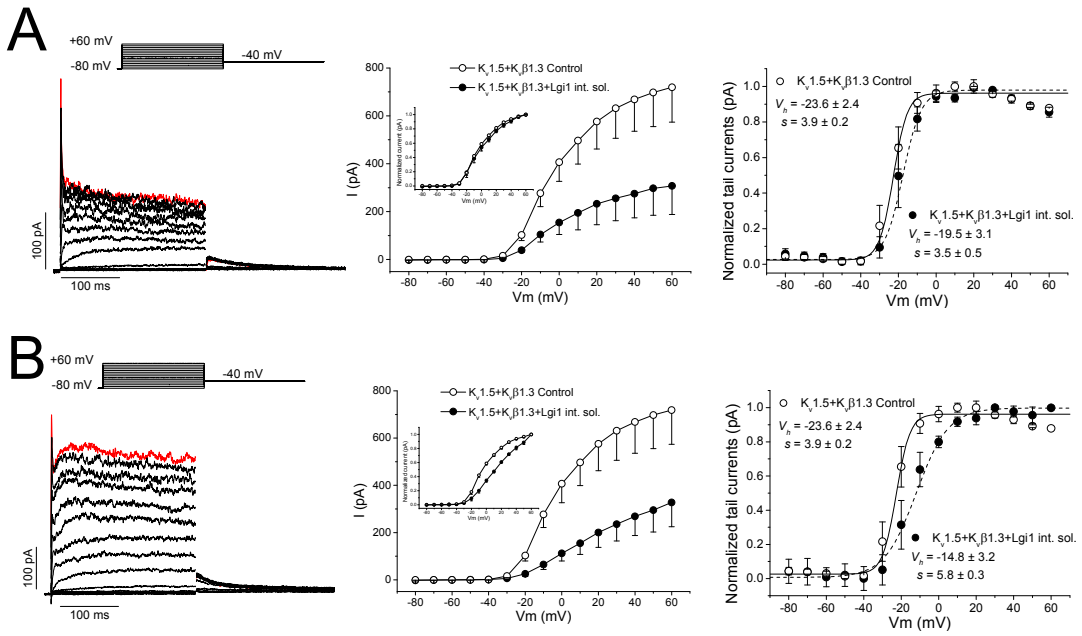

Figure 38: Lgi1 present into the patch pipette produces its effects on K_v1.5-K_vβ1.3 channels through the external side of the cell. **A,** Representative recordings, IV relationships non- and normalized by +60 mV value (inset) and activation curves comparing them with K_v1.5-K_vβ1.3 (from left to right side, respectively) obtained just after the rupture of the seal. **B,** Representative recordings, IV relationship non- and normalized by +60 mV value (inset) and action curves comparing them with K_v1.5-K_vβ1.3 (from left to right side, respectively) obtained after 2 min. after seal formation.

4.4.5. Cellular and tissular location of Lgi1

Although part of our results seems that the intracellular actions of Lgi1 protein are carried out after the binding of this protein from outside beginning a signaling cascade (Figure 38); the fact that the same protein has also effects on the actin cytoskeleton makes us wonder which is the cellular location of Lgi1 to be able to perform both roles in the cell at the same time. To solve this question we performed immunocytochemistry experiments in HEK293 cells cotransfecting Lgi1-GFP and Phalloidin-AF546 in the absence and in the presence of K_v1.5-CFP. As it is shown in Figure 39, the presence of Lgi1 is not enough to produce those cytoskeleton disorders observed in the western blot assays (Figure 36). However, after cotransfection with K_v1.5, the labeling of the actin cytoskeleton is highly decreased not only in those cells that express the protein, but also in those that are around (Figure 39).

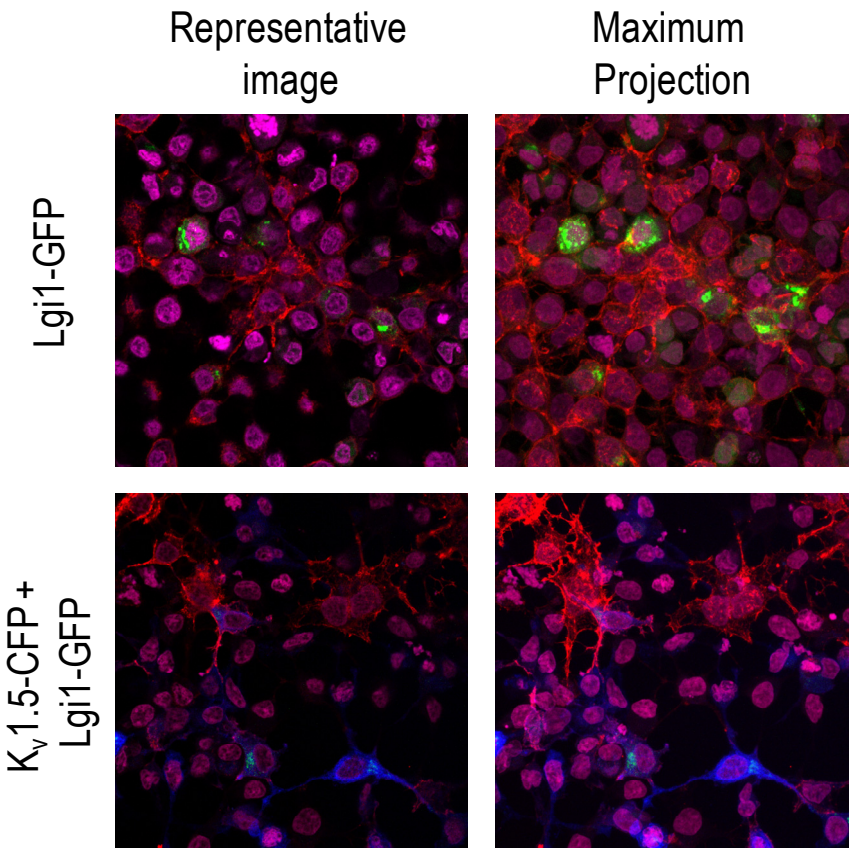

Figure 39: Lgi1 needs the presence of the channel to disrupt the cytoskeleton structure in both auto- and paracrine way. The Figure shows representative images of the effect exerted by Lgi1 on the actin cytoskeleton. Note that cells, and their neighbors, that only express Lgi1 protein *(in green)* present a cytoskeleton labeling *(in red)* well defined. However, those cells that express Lgi1 and K_v1.5 channel *(in blue)*, as well as their neighbors, does not. Nucleuses are shown in magenta.

The presence of Lgi1 in human heart it has been previously described (Gu *et al.*, 2002). However, we wanted to know the specific location into the cardiac human tissue and compare it with that shown by K_v1.5 channel in the same tissue. To this end, we carried out immunohystochemistry assays using ventricular human slices to elucidate not only the location of Lgi1 but also whether if its expression pattern overlaps with that showed by K_v1.5 (Figure 40). Figure 40A shows the expression pattern shown by K_v1.5 in human ventricle. This channels has a membrane expression pattern (arrowheads) and is specifically present at the intercalated disks (arrows), as it was previously described (Mays *et al.*, 1995). Figure 40B shows the expression pattern obtained for Lgi1 and, very surprisingly, this protein also expresses in the membrane with an expression pattern very similar to that showed by K_v1.5 channel.

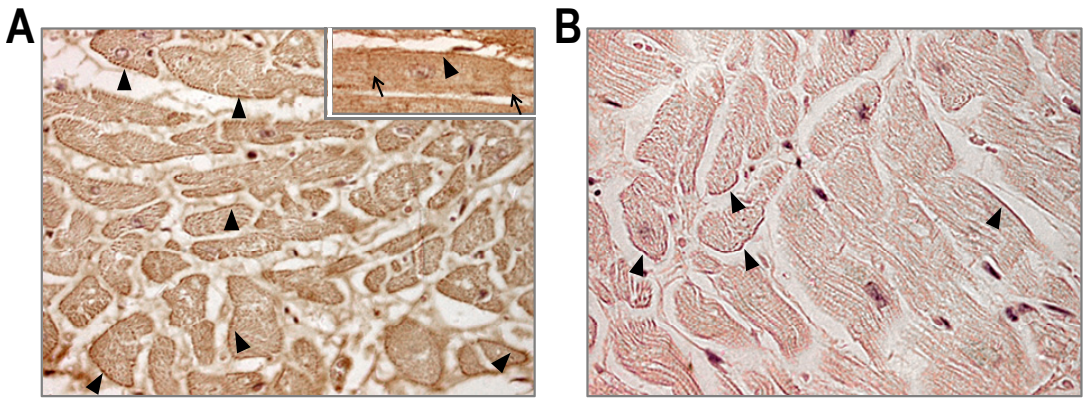

Figure 40: K_v1.5 channel and Lgi1 protein show a similar expression pattern in human ventricle. Figure show representative images of: **A,** Immunodetection of the K_v1.5 channel protein in human myocardium. 5 µm sections were prepared from adult ventricle and stained as described in Methods. **B,** Staining of Lgi1 protein in human ventricle following the same procedure than in A. *Arrowheads,* point out K_v1.5 in the cell membrane. *Arrows,* mark the presence of the channel in the intercalated disks.

5. DISCUSSION

5.1 PROTEIN KINASE C ACTIVITY REGULATES FUNCTIONAL EFFECTS OF $K_v\beta1.3$ SUBUNIT ON $K_v1.5$ CHANNELS: IDENTIFICATION OF A CARDIAC *CHANNELOSOME*.

In the present Doctoral Thesis, we have analyzed the mechanisms by which PKC inhibition calphostin C-mediated abolishes $K_v\beta1.3$-induced fast inactivation of the $K_v1.5$ channel. We have demonstrated that the inhibition of, at least, classical and novel PKC isoforms is required to abolish $K_v\beta1.3$-induced fast inactivation (Kwak *et al.*, 1999a; Kwak *et al.*, 1999b). Furthermore, this effect was not due to $K_v1.5$-$K_v\beta1.3$ dissociation but to a positive shift of the inactivation curve driven by PKC inhibition, because both subunits remained assembled as shown by immunocytochemistry, immunoprecipitation and electrophysiological experiments. We have also showed that, at least, $K_v\beta1.3$, RACK1, PKCβI, PKCβII and PKCθ are associated with $K_v1.5$ in HEK293 cells, forming a *channelosome*. Finally, for the first time, we provide evidence pointing to the existence of a native ventricular cardiac $K_v1.5$ *channelosome*, whose composition is similar to that found in HEK293 cells (with the exception of PKCθ, absent in this tissue according to our western blot analyses, data not shown).

The stimulation of α1-receptors leads to activation of PLCγ. This enzyme cleaves PIP_2, generating IP_3 and DAG, which activates most PKC isoforms either alone or with Ca^{2+}, with the exception of atypical PKCs. The N-terminus of the $K_v\beta1.3$ subunit associates with membrane-bound PIP_2 and when it dissociates from PIP_2, it assumes a hairpin structure that enters the central cavity of an open $K_v1.5$ channel, inducing fast inactivation. Thus, $K_v\beta1.3$-induced fast inactivation is mediated by a competitive binding between phosphoinositides (PIPs) and the inner pore region of $K_v1.5$ channels for the N-terminus of $K_v\beta1.3$ (Decher *et al.*, 2008). The present results obtained for PIP_2 and OAG are in agreement with previous reports and indicate a fine-tuned regulation of $K_v\beta1.3$-induced fast inactivation by PKC and PIP_2. Moreover, the effects of PIP_2 in cells in which the PLC was inhibited produced a marked decrease of the $K_v\beta1.3$-induced fast inactivation. In the absence of PIP_2 into the internal solution, the effects observed were qualitatively similar (data not shown), suggesting a role of PLC on the fast inactivation induced by this β subunit.

Most PKC isoforms redistribute into different subcellular compartments upon activation, depending on the PKC isoform and the cell type (Dorn & Mochly-Rosen, 2002). A surprising finding of the present study was that all of the PKC inhibitors tested (Gö6976, Gö6983, hispidin, and PKCζ-PI), with the exception of calphostin C, failed to abolish $K_v\beta1.3$-induced fast inactivation. This result is likely due to the different mechanisms of action of the PKC inhibitors used. Indeed, calphostin C inhibits PKC by binding to its C1 domain (DAG and phorbol ester binding site) and then irreversibly inactivates the enzyme. Gö6983 and Gö6976 are competitive inhibitors of ATP binding to the catalytic domain of PKC, whereas hispidin affects both PKCβI and PKCβII translocation (Kobayashi *et al.*, 1989; Qatsha *et al.*, 1993; Sossin, 1997; Wadsworth & Goldfine, 2002; Young *et al.*, 2005). Our results suggest that inhibition of classical and novel, but not atypical, PKC isoforms counteracts $K_v\beta1.3$-induced fast

inactivation and shifts the V_h of the activation curve to values closer to those of $K_v1.5$ observed in the absence of $K_v\beta1.3$, as has been previously described (Kwak *et al.*, 1999b). The potential dissociation of α-β caused by PKC inhibition was also analyzed in the present study. Colocalization, immunoprecipitation and electrophysiological experiments revealed that these subunits remained assembled in the plasma membrane despite PKC inhibition by calphostin C. These results are in agreement with the notion that $K_v1.5$ and $K_v\beta1.3$ subunits assemble in the endoplasmic reticulum during the early stages of their biosynthesis (Nagaya & Papazian, 1997), and 2 h incubation with calphostin C is sufficient to eliminate the typical fast inactivation induced by $K_v\beta1.3$ (Kwak *et al.*, 1999b). Moreover, previous results reported by Kwak and coworkers showed that a tandem construction of $K_v1.5$ and $K_v\beta1.3$, which generates a unique protein, showed similar responses to calphostin C (a shift in V_h to more positive potentials and a loss of fast inactivation) (Kwak *et al.*, 1999b). These results indicate that mechanisms other than subunit dissociation must be involved in the abolishment of $K_v\beta1.3$-induced fast inactivation produced by calphostin C.

Although we were able to rule out a role for atypical PKCs, the involvement of a specific PKC isoform in this process has not yet been demonstrated. In addition, experiments in which the membrane potential was depolarized to +100 mV indicated that despite PKC inhibition (calphostin C or PKC siRNA), $K_v\beta1.3$ was still capable of conferring fast inactivation and thus remained associated with $K_v1.5$. Furthermore, the co-immunoprecipitation experiments showed that $K_v\beta1.3$ remained associated with $K_v1.5$ despite PKC inhibition by calphostin C or by PKC silencing by siRNA. These data suggest that $K_v1.5$ and $K_v\beta1.3$ subunits form a stable complex following their biosynthesis in the endoplasmic reticulum and that PKC inhibition and/or activation modulates the inactivating effect of $K_v\beta1.3$. It has been demonstrated that residues R5 and T6 of the $K_v\beta1.3$ subunit are involved in PIP_2 binding and mutations (alanine or cysteine) at these residues dramatically increase the degree of $K_v\beta1.3$-induced fast inactivation (Decher *et al.*, 2008). It has been described that calphostin C does not modify the gating of the $K_v1.5$ in the absence of β subunits (Kwak *et al.*, 1999b). Therefore, it is likely that the effects shown in the present study involve the phosphorylation of some residues present in the $K_v\beta1.3$ subunit. One candidate could be threonine at position 6 (T6) of $K_v\beta1.3$. Thus, we may hypothesize that PKC phosphorylation of this threonine or another threonine/serine at the N-terminus of the $K_v\beta1.3$ subunit can lead to a diminished capability to bind PIP_2, thus avoiding the abrogation of fast inactivation caused by PIP_2. These findings provide an explanation for the effects of PKC inhibition on the $K_v\beta1.3$-induced inactivation, assuming that phosphorylated $K_v\beta1.3$ cannot bind PIP_2. Non-phosphorylated $K_v\beta1.3$ would be able to bind PIP_2 and this binding would abolish N-type inactivation (Decher *et al.*, 2008). However, further experiments are necessary to elucidate the residue/s involved in this effect.

In the past decade, myriads of protein-protein interactions involved in intracellular signaling have been described (Hubbard & Cohen, 1993; Mochly-Rosen, 1995; Burack & Shaw, 2000; Wang *et al.*, 2002). Determination of the subcellular localization of signal transduction proteins, enzymes, substrates and mediators has revealed the rapid and efficient transmission of signals from either the extracellular medium or from intracellular sites as an essential feature of optimal signaling (Pawson & Nash, 2003). Despite the high degree of

homology between PKC isoforms at both sequence and structural levels, especially within the catalytic domain, each PKC isoform mediates unique subcellular functions (Dempsey *et al.*, 2000; Jaken & Parker, 2000) that are dependent on the target substrate (Carpenter *et al.*, 1987; Parker *et al.*, 1989). These location mechanisms are especially common in plasma membrane proteins because incoming stimuli must be integrated and transmitted with a high degree of efficiency. In the present study, we have demonstrated that $K_v1.5$ and $K_v\beta1.3$ form a highly stable protein complex, which is tightly regulated by classical and novel, but not atypical, PKC isoforms. Furthermore, our results show that PKCβI, PKCβII and RACK1 coassemble with $K_v1.5$ and $K_v\beta1.3$. Therefore, the $K_v1.5$ functional *channelosome* contains, at least, $K_v1.5$, $K_v\beta1.3$, RACK1, PKCβI, PKCβII, and PKCθ. Besides, a similar *channelosome* has been found in ventricular, but not in atrial tissue, showing a parallel distribution to that of $K_v\beta1.3$ (England *et al.*, 1995a), which suggests an important role of this beta subunit in the constitution of the macromolecular complex.

The presence of RACK1 in other ion channel complexes has been previously reported. Indeed, RACK1 binds to the C-terminus of KCa1.1 channels (Isacson *et al.*, 2007). Moreover, the overexpression of RACK1 with KCa1.1 channels in *Xenopus* oocytes shifts the activation curve towards more positive potentials in the absence, but not in the presence, of ectopically expressed β channel subunits (Isacson *et al.*, 2007). Furthermore, PKCβII, which is recruited by RACK1, down-regulates $Ca_v1.2$ activity following activation (Dorn & Mochly-Rosen, 2002). Besides, the functional $K_{ir}3.1$ complex contains PKA, PP1, PP2A/C and RACK1. Within this complex, RACK1 binds directly to Gβγ (Dell *et al.*, 2002) and PKC (Ron *et al.*, 1994). Recently, it has been described that TRPC3 regulates IP_3 receptor (IP_3R) function by mediating interaction between IP_3R and the scaffolding protein RACK1, as well as the importance of the Orai1-STIM1-TRPC3-RACK1-IP_3R complexes in the fine modulation of intracellular Ca^{2+} stimulated by agonists of these receptors (Woodard *et al.*, 2010). Thus, RACK1 is emerging as an important adaptor protein that may play very important roles in the modulation of different ion channels and in the interaction between ion pores and ancillary subunits. The variety of signaling proteins linked to RACK1 (Schechtman & Mochly-Rosen, 2001), which include PKCβII (Ron *et al.*, 1994; Csukai *et al.*, 1997), PLCγ (Disatnik *et al.*, 1994), Src (Chang *et al.*, 1998) and dynamin-1 (Rodriguez *et al.*, 1999), among others, could explain the diverse effects of PKA and PKC on the $K_v1.5$-$K_v\beta1.3$ current (Murray *et al.*, 1994; Li *et al.*, 1996; Kwak *et al.*, 1999a; Kwak *et al.*, 1999b) and the requirement for simultaneous inhibition of numerous PKC isoforms to abolish fast inactivation.

In conclusion, we have analyzed the mechanisms by which calphostin C abolishes $K_v\beta1.3$-induced fast inactivation. Our experiments demonstrate that this effect is not due to the dissociation of $K_v1.5$ and $K_v\beta1.3$ subunits and that these subunits remain assembled following PKC inhibition. Our experiments also demonstrate that PLC is also involved in the regulation of the $K_v\beta1.3$-induced fast inactivation. In addition, we have characterized a $K_v1.5$ *channelosome* in which $K_v1.5$, $K_v\beta1.3$, RACK1, PKCβI, PKCβII and PKCθ physically and functionally interact. Importantly, we have identified a very similar macromolecular complex in rat ventricular tissue. The description and functional characterization of this *channelosome* opens up a variety of possible mechanisms to explain the differences between I_{Kur} recorded in ventricle and atrium in different animal species.

Differential composition of this $K_v1.5$ complex could constitute a primary mechanism of capital importance for the modulation of cardiac excitability.

5.2 PHARMACOLOGICAL CONSEQUENCES OF PROTEIN KINASE C INHIBITION ON $K_v1.5$-$K_v\beta1.3$ CHANNELS.

In the second part of this Doctoral Thesis, we analyzed the electrophysiological and pharmacological consequences of PKC inhibition induced by calphostin C in $K_v1.5$-$K_v\beta1.3$ channels. We demonstrated that the voltage-dependence of $K_v1.5$-$K_v\beta1.3$ channel inactivation after PKC inhibition resembles that observed in $K_v1.5$ channels alone. Inhibition of PKC using calphostin C partially reverted the changes in the pharmacologic properties induced by the assembly of the $K_v\beta1.3$ subunit with $K_v1.5$ channels (Gonzalez *et al.*, 2002; Decher *et al.*, 2005) in such a way that the pharmacology of these channels in cells pre-treated with calphostin C resembled that exhibited by $K_v1.5$ channels in the absence of the $K_v\beta1.3$ subunit (Snyders *et al.*, 1992; Valenzuela *et al.*, 1995a).

PKC inhibition induced by calphostin C results in the abolishment of $K_v\beta1.3$-induced fast inactivation due to a shift in the inactivation midpoint of the $K_v1.5$-$K_v\beta1.3$ channels (David *et al.*, 2012). Surprisingly, the voltage dependence of inactivation of $K_v1.5$-$K_v\beta1.3$-calphostin C and that of $K_v1.5$ channels were similar. These results suggest not only that the voltage-dependent inactivation induced by this beta subunit is abolished but also that the complex behaves as if the $K_v\beta1.3$ subunit does not assemble with $K_v1.5$ channels. The $K_v\beta1.3$-mediated fast inactivation is voltage dependence, in contrast to the N-type inactivation of *Shaker* channels and the fast inactivation produced by $K_v\beta1.2$ on $K_v1.5$ channels, both of which are insensitive to membrane potential (Zagotta *et al.*, 1989; De Biasi *et al.*, 1997; Uebele *et al.*, 1998). The voltage-dependence of $K_v\beta1.3$-mediated inactivation may be due to the charge within the blocking particle sensing the transmembrane potential, as well as to some voltage-dependent changes in the $K_v1.5$ channel that are involved in the interaction with the $K_v\beta1.3$ subunit. To discriminate between these possibilities, experiments using a pulse protocol with 10 ms depolarizing pre-pulses were performed. These experiments led us to isolate the fast inactivation induced by the $K_v\beta1.3$ subunit from the slow inactivation characteristic of $K_v1.5$ channels. Indeed, inactivation curves obtained from $K_v1.5$-$K_v\beta1.3$ and $K_v1.5$-$K_v\beta1.3$-calphostin C channels were similar after applying 10 ms and 250 ms pre-pulse protocols, respectively. Taken together, these data suggest that the voltage dependence of $K_v\beta1.3$-mediated inactivation is independent of the electrophysiological properties of the $K_v1.5$ channel.

Bupivacaine- and quinidine-induced blockade of $K_v1.5$ channels result from their binding to an external and an internal receptor sites (Yeola *et al.*, 1996; Franqueza *et al.*, 1997; Longobardo *et al.*, 2000; Longobardo *et al.*, 2001). Although the molecular determinants of the external binding site remain unknown, both drugs share a common internal receptor site, which is located at the S6 segment and that involves a polar interaction with T507 and two hydrophobic interactions with L510 and V514 (Yeola *et al.*, 1996; Franqueza *et al.*, 1997; Arias *et al.*, 2007). Moreover, the bupivacaine binding site on $K_v1.5$ channels overlaps with the binding site of the $K_v\beta1.3$ subunit in such a way that bupivacaine blocks to a lesser extent $K_v1.5$-$K_v\beta1.3$ channel than $K_v1.5$ channels alone

(Arias *et al.*, 2007). The pharmacology of the $K_v1.5$-$K_v\beta1.3$ channels was modified after PKC inhibition for bupivacaine and quinidine, decreasing the IC_{50} for both drugs. In fact, both compounds lost the characteristic voltage-dependent blockade that was previously described for the $K_v1.5$ and $K_v1.5$-$K_v\beta1.3$ channels (Snyders *et al.*, 1992; Valenzuela *et al.*, 1995a; Gonzalez *et al.*, 2002). These results can be explained by the decrease in the dissociation rate values obtained in $K_v1.5$-$K_v\beta1.3$-calphostin C channels with bupivacaine and quinidine, which indicates that the drug-channel complex becomes more stable than in $K_v1.5$-$K_v\beta1.3$ channels, but less stable than that observed in $K_v1.5$ channels. However, the association rate constants remained nearly unchanged in comparison to those reported for $K_v1.5$ and $K_v1.5$-$K_v\beta1.3$ channels (Gonzalez *et al.*, 2002; Arias *et al.*, 2007). This fact also corroborates the finding that the phenotype of $K_v1.5$-$K_v\beta1.3$-calphostin C channels is closer to that of $K_v1.5$ channels alone (Arias *et al.*, 2007). This gain of potency is a very important result if we keep in mind that the expression levels of α- and β-adrenergic receptors, as well as the release of catecholamines, can be modified in several cardiac pathologies (Schlaich *et al.*, 2003; Schlaich *et al.*, 2005), and may have important consequences in cardiac pharmacology (Longobardo *et al.*, 1998; Gonzalez *et al.*, 2002; Gonzalez *et al.*, 2010; Ravens & Wettwer, 2011).

In summary, we have characterized the functional contribution of PKC to the modulation of the $K_v1.5$ *channelosome* from an electrophysiological and pharmacological perspective. Importantly, PKC inhibition changes the electrophysiological and pharmacological characteristics of $K_v1.5$-$K_v\beta1.3$ channels, causing them to be more similar to those observed in the absence of the $K_v\beta1.3$ subunit. This functional characterization of the $K_v1.5$ *channelosome* opens up a variety of possible mechanisms that may underlying the development of cardiac hypertrophy or other cardiovascular diseases involving modifications in PKC activity.

5.3 K_v1.5-K_vβ1.3 CHANNELS TRAFFICKING IS PKC-DEPENDENT

Membrane proteins are removed from the cell surface by endocytosis and are then either recycled back to the membrane or subjected to degradation. These sorting mechanisms provide the cell with the ability to adjust the density of a given protein at the plasma membrane. In the present Doctoral Thesis, we have analyzed the mechanisms underlying the decrease in the K_v1.5-K_vβ1.3 current magnitude observed after inhibition of PKC with calphostin C. This study demonstrated that the inhibition of PKC results in a reduction in the number of channels present in the cell membrane along to a dramatic accumulation of channels into the cytoplasm. In addition, we have demonstrated that this accumulation is not due to an increase in the internalization of the channel, whereas it is the consequence of a decrease in the recycle rate. In fact, the results obtained suggest that PKC is involved in the proper function of the K_v1.5 slow-recycling Rab11-mediated previously described (Balse *et al.*, 2009).

We have shown that the current magnitude generated after activation of K_v1.5-K_vβ1.3 channels in cells whose PKC has been inhibited is smaller than that recorded under control conditions and this effect seems to be due to a decrease of ≈30% in the channel surface density. These data, are in contrast with the role attributed to PKC in other ion channels like KCNK3, NMDAR, Ca_v2 or K_{ATP} channels (Lin *et al.*, 2006; Zhang *et al.*, 2008; Manna *et al.*, 2010; Gabriel *et al.*, 2012), which are inhibited or even down-regulated after PKC activation. But, although PKC activation has not been analyzed in the present Doctoral Thesis, it has been reported that the effects of PMA (10 nM for 30 min) does not produce electrophysiological changes on the current generated upon their activation (Kwak *et al.*, 1999b; Williams *et al.*, 2002). Our results indicate that PKC is involved in the regulation of the channel density in the cell membrane because its inhibition results in a dramatic reduction of the number of channels without modifying the total amount of the protein channel. This decrease can be due, at least in part, to an increase in the internalization rate or to a decrease in the recycling or going back to the membrane. The biotinylation assays suggest that while at the beginning of the calphostin C treatment the behavior is very similar to that observed in K_v1.5-K_vβ1.3 channels under control conditions, the amount of internalized channels significantly increased at times longer than 1 h. Moreover, live cell imaging experiments showed an abolishment of the recycling to the membrane of K_v1.5-K_vβ1.3 channels in cells in which PKC was inhibited. In these cells, we observed how the channels were endocytosed but their recycling to the cell membrane was avoided.

Finally, in this part of the present Doctoral Thesis we demonstrated that PKC is involved in the trafficking of K_v1.5-K_vβ1.3 via slow-recycling Rab11-mediated. In fact, cotransfection of K_v1.5-K_vβ1.3 channels with Rab11CA in HEK293 cells, elicited potassium currents with similar electrophysiological properties obtained after calphostin C treatment but with a greater magnitude. Rab11 is found in pericentriolar recycling endosomes, a population of endosomes through which most membrane proteins recycle (Ullrich *et al.*, 1996), and it is also found in the *trans*-Golgi network and post-Golgi vesicles, where it is involved in the trafficking of newly synthesized proteins from that organelle to the cell surface (Grosshans *et al.*, 2006). One explanation could be that K_v1.5 channels are marked for transport to Rab11-positive vesicles only after multiple Rab4-dependent

recycling events, or targeted for degradation (Zadeh *et al.*, 2008). In fact, it has been recently described that both processes (recycling and degradation) are PKC-dependent (Manna *et al.*, 2010; Pavarotti *et al.*, 2012) and, more interestingly, that PKCα and PKCβII colocalize with Rab11, this last isoform present in the K_v1.5 *channelosome*.

The evidence that classical PKCs regulate trafficking through the endocytic and exocytic pathways is increasing. Indeed, these kinases have been suggested to control the levels of epidermal growth factor receptor (EGFR) and transferrin (Idkowiak-Baldys *et al.*, 2009; Pavarotti *et al.*, 2012). Likewise, serotonin receptor stimulation that activates classical PKCβII produces the retention of serotonin receptors at the endocytic recycling compartment (ERC) (Idkowiak-Baldys *et al.*, 2009). Additional reports show that PMA-induced PKC activation diverts internalized EGFR and PAR-1 from a degradative to a recycling pathway controlled by Rab11 (Bao *et al.*, 2000).

Another explanation for the specific role of PKC in the K_v1.5-K_vβ1.3 traffic regulation would be the following. In the same manner that PKC activity can be modulated, not only directly, but also regulating the levels or the activity of other proteins that act as scaffold or its receptor, RACK1; the function of Rab proteins is also controlled by several families of interacting proteins or FIP_s. Indeed, FIP2 directly interacts with the actin-based myosin Vb motor protein and this interaction appears to be critical for several aspects of FIP2 function, including regulation of plasma membrane recycling (Hales *et al.*, 2002; Horgan & McCaffrey, 2009). It is also important to highlight that the activities of Rip11 and FIP2 are regulated by phosphorylation and phospholipids-mediated (Horgan & McCaffrey, 2009).

All these results may have an important therapeutic relevance in future studies concerning the basis of K_v1.5 trafficking. Moreover, they can stand the molecular basis of the K_v1.5 channels trafficking, together with previous reports (McEwen *et al.*, 2007; Zadeh *et al.*, 2008; Balse *et al.*, 2009; Schumacher & Martens, 2010; Burg *et al.*, 2010; Svoboda *et al.*, 2012; Mia *et al.*, 2012; Boycott *et al.*, 2013). The effects of quinidine on these potassium channels have been partially attributed to its capability to internalize K_v1.5 (Schumacher *et al.*, 2009). Therefore, the results obtained in this work show an additional way to reduce the channel amount in plasma membrane: through PKC inhibition. Thus, the levels and/or the degree of PKC activity have to be taken into account in the antiarrhythmic drug treatment of patients (Gonzalez *et al.*, 2010).

In summary, we have characterized the contribution of the PKC inhibition to the modulation of K_v1.5 *channelosome*. Importantly, PKC inhibition modifies the electrophysiological characteristics of K_v1.5-K_vβ1.3 controlling the slow-recycling Rab11-mediated and, therefore, the amount of the channels in the cell surface. This characterization of the K_v1.5 functional complex or *channelosome* opens up a variety of possible mechanisms that can help to understand the variations that can underlay the development of cardiovascular diseases involving modifications in PKC activity.

5.4 LGI1 EFFECTS ON K_V1.5-K_Vβ1.3 CHANNEL COMPLEX. POSSIBLE ROLE ON HUMAN VENTRICLE

In the last part of the present Doctoral Thesis, we have analyzed the electrophysiological and cellular effects of Lgi1 on K_v1.5-K_vβ1.3 channels, as well as its presence in cardiac tissue, including human myocardium. Lgi1 is a protein that has been related with certain types of epilepsy (Nobile *et al.*, 2009; Striano *et al.*, 2011; Kusuzawa *et al.*, 2012; Baulac *et al.*, 2012; Manna *et al.*, 2013; Irani *et al.*, 2013). However, its role in the human heart is currently unknown. It has been reported that Lgi1 protein interferes with K_vβ1-conferred fast inactivation of K_v1 channels, suggesting that it can modulate the gating of K_v1 channels although the molecular basis by which Lgi1 produces this effect on K_v1 channel inactivation is presently unknown (Schulte *et al.*, 2006). On the other hand, it has been demonstrated that its differential expression in mice results in a model of cardiac hypertrophy (Mohamed *et al.*, 2012). In this Doctoral Thesis we have demonstrated that Lgi1 is expressed in rat heart with a similar pattern of expression to that reported for K_vβ1.3, with a higher extent of expression in ventricle than in atria, becoming a possible member of the K_v1.5 *channelosome*. Lgi1 produces a dramatic decrease in the channel amount present in the cell membrane as well as in the inactivation of the K_v1.5-K_vβ1.3, which is apparent after cotransfection of K_v1.5-K_vβ1.3 and Lgi1, or after adding the Lgi1 soluble protein into the patch pipette. Also, a very dramatic effect on the actin cytoskeleton was observed when Lgi1 was present. Finally, and very importantly, we demonstrated that Lgi1 is expressed in human ventricle with a pattern of expression very similar to that observed for K_v1.5 channels.

Lgi1 decreases the amount of K_v1.5 in the cell membrane and also modifies the conformation of the actin cytoskeleton of the cell. It is likely that both actions are related since it has been described that the microtubule cytoskeleton is involved in the internal trafficking of K_v1.5 in both heterologous and native cells (cardiac) (Choi *et al.*, 2005). On the other hand, ADAM 22/23 (one of the proteins described as Lgi1 receptor) appear to be involved in cell adhesion (Liu et al., 2009), which is consistent with the suggestion that Lgi1 influences cell movement and invasion through reorganization of the actin cytoskeleton (Kunapuli *et al.*, 2010b). Lgi1 is a secreted protein (Senechal *et al.*, 2005; Head *et al.*, 2007) and it has been described that, in glioma cells, exerts its effects from the external side of the cell membrane, increasing the stress fiber formation in the cytoskeleton (Kunapuli *et al.*, 2010b). This report is in agreement with the results obtained in this Doctoral Thesis, in which we need, at least, two minutes to observe the electrophysiological effects induced by Lgi1 when Lgi1 was added to the internal solution of the patch pipette as a soluble protein. Although we do not have enough data to state a complete affirmative conclusion, we can hypothesize that Lgi1 needs to bind to some membrane protein that acts like a receptor and whose binding leads to the activation or repression of a cascade of second messengers responsible of the modulation of K_v1.5-K_vβ1.3 channel activity. In addition, the stress in the fiber formation

can produce a deficiency of the anterograde transport of the proteins to the plasma membrane, as well as a re-distribution of the cytoskeleton with modifications in the location of K_v1.5 *channelosome* as it can be observed in the cytoskeleton blots (in both heterologous and native cells) in which the integrity of actin is clearly compromised.

The effects of Lgi1 on the $K_v\beta$ subunit have been described on neural tissue, where the electrophysiological effects induced by Lgi1 on K_v1-$K_v\beta$1 were related to the Lgi1 capability to abolish the fast inactivation $K_v\beta$1-induced. Mutations in the *LGI1* gene have been widely related with epilepsy, as well as with some neurodegenerative diseases (Borrie *et al.*, 2012); although the molecular basis of the Lgi1 effects on K_v1 channels inactivation are presently unknown. However, the effects on cardiac diseases have been only reported by Ottman and coworkes. They proposed that Lgi1 mutations have been related to certain types of epilepsy, some of them associated to autonomic symptoms (visceral/epigastric and cardiac palpitations) that occurred in 45% of patients (Ottman *et al.*, 1995), thus suggesting the existence of a link between epilepsy and some cardiac pathologies, that may be represented by Lgi1. As it has been shown in the present Doctoral Thesis, Lgi1 is expressed in rat cardiac ventricle with a pattern of expression closer to that described for the $K_v\beta$1.3 subunits and induces its actions not only decreasing the amount of K_v1.5 channel in the cell membrane, but also abolishing the fast inactivation $K_v\beta$1.3-dependent. There are two possible explanations for these results: 1) Lgi1 locates in between the α-β either; or 2) Lgi1 binds to the $K_v\beta$1.3 subunit and therefore, its activity is directly compromised. The results obtained with K_v1.5-$K_v\beta$1.3+Lgi1 *vs.* K_v1.5+Lgi1, as well as those obtained using the anti-Lgi1 antibody in the patch pipette, suggest the second possibility as the most likely to occur. Lgi1 effects were observed when this protein was cotransfected with K_v1.5-$K_v\beta$1.3 complex and they were absent when K_v1.5 channels were expressed alone. Besides that, in these experiments the electrophysiological phenotype was close to K_v1.5. In addition, the results obtained using the anti-Lgi1 in which the electrophysiological phenotype of the current was similar to that elicited by the activation of K_v1.5 channels alone instead of K_v1.5-$K_v\beta$1.3, led us to hypothesize the possibility that this antibody is forming a complex with Lgi1-$K_v\beta$1.3 that avoids the binding within the inner pore of K_v1.5 resulting in a K_v1.5 phenotype. All these data suggest that Lgi1 acts not only like a 'new modulatory subunit' but also as a regulatory subunit of modulatory subunits.

In summary, the coexpression of Lgi1 with K_v1.5-$K_v\beta$1.3 in HEK293 cells results in non-inactivating currents with a much smaller magnitude, and it has a dual effect: a), Lgi1 seems to produce an intracellular effect mostly K_v1.5-related, which affect the traffic of the channel dramatically reducing the channel in the cell surface; and b) an extracellular time-dependent effect in which, its effects seems to be more $K_v\beta$ subunit dependent. Finally, and very importantly, we demonstrated that Lgi1 is expressed in human ventricle with a pattern of expression very similar to that observed for K_v1.5 channels.

6. CONCLUSIONS

1. Calphostin C abolishes $K_v\beta1.3$-induced fast inactivation in $K_v1.5$ channels, due to a shift of the inactivation curve towards more positive potentials. Also, PLC activity and PIP_2 levels regulate $K_v\beta1.3$-induced fast inactivation. We propose that $K_v\beta1.3$ subunit acts as the 'linker' between $K_v1.5$ and the PKC receptor, RACK1, and the proteins linked to this channel complex.

2. We have characterized a $K_v1.5$ *channelosome* in which $K_v1.5$, $K_v\beta1.3$, RACK1, PKCβI, PKCβII, and PKCθ physically and functionally interact. This macromolecular complex has been also identified in rat ventricular myocardium. The description and functional characterization of this *channelosome* opens up a variety of possible mechanisms that can explain the differences between I_{Kur} recorded in ventricle and atrium in different animal species. Differential composition of this $K_v1.5$ complex could constitute a primary mechanism of crucial importance for the modulation of cardiac excitability.

3. PKC inhibition modifies the electrophysiological and pharmacological characteristics of $K_v1.5$-$K_v\beta1.3$ channels, leading to a similar pharmacological phenotype to that observed in $K_v1.5$ channels in the absence of $K_v\beta$ subunits. The pharmacological characterization of $K_v1.5$ *channelosome* opens up new pharmacological maneuvers useful in the treatment of cardiac pathologies that involve modifications in the PKC activity.

4. PKC activity is essential in the maintenance of the channels in the membrane and therefore, for the regulation of their current magnitude. Indeed, PKC activity is crucial for the slow recycling Rab11-mediated and its inhibition by calphostin C results in an increase of the channel in the cytoplasm of the cell.

5. Lgi1 is a protein present in the cardiac tissue that regulates the activity of $K_v1.5$ channels. This modulation can be summarizes as follows, it: 1) decreases the $K_v1.5$ current magnitude due to a reduction in the number of the channels in the cell membrane; 2) abolishes the fast inactivation $K_v\beta1.3$-induced likely due to an interaction between both proteins; 3) is capable to produce its effects from the external side of the cell, after it is secreted from the cell, likely activating or repressing a second messenger pathway, producing its effects on $K_v1.5$ channels and also on the cytoskeleton structure. Finally, the pattern of expression of this protein is very similar to that shown by $K_v1.5$ channels in the human ventricle. All these data led us to propose Lgi1 as a new and very important modulatory subunit on the $K_v1.5$-$K_v\beta1.3$ channels, as well as a novel molecular target useful in several cardiac diseases.

1. La calfostina C elimina la inactivación rápida inducida por la subunidad $K_v\beta1.3$ en los canales $K_v1.5$, debido a un desplazamiento de la curva de inactivación hacia potenciales más positivos. Asimismo, la actividad de la PLC, así como los niveles de PIP_2, regulan la inactivación rápida inducida por la subunidad $K_v\beta1.3$. Proponemos que la subunidad $K_v\beta1.3$ actúa como molécula 'conectora' de la unión entre el canal $K_v1.5$ y el receptor de PKC, RACK1, así como el resto de las proteínas asociadas al complejo de señalización del canal $K_v1.5$.

2. Hemos caracterizado un *canalosoma* de $K_v1.5$ en el que $K_v1.5$, $K_v\beta1.3$, RACK1, PKCβI, PKCβII y PKCθ interactúan física y funcionalmente. Este complejo macromolecular ha podido ser identificado también en ventrículo de rata. La descripción y caracterización funcional de este *canalosoma* abre un gran número de mecanismos capaces de explicar las diferencias entre las I_{Kur} registradas en miocardio ventricular y auricular en diferentes especies animales. La diferente composición de este complejo de $K_v1.5$ podría constituir un mecanismo de vital importancia para la modulación de la excitabilidad cardíaca.

3. La inhibición de PKC modifica las características electrofisiológicas y farmacológicas de los canales $K_v1.5$-$K_v\beta1.3$, produciendo un fenotipo farmacológico similar al que presentan los canales $K_v1.5$ en ausencia de subunidades $K_v\beta$. La caracterización farmacológica del *canalosoma* de $K_v1.5$ abre una gran variedad de posibles maniobras farmacológicas útiles en el tratamiento de patologías cardíacas asociadas a modificaciones en la actividad de PKC.

4. La actividad PKC es esencial en el mantenimiento de los canales en la membrana y, por lo tanto, para la regulación de la magnitud de la corriente. De hecho, la actividad PKC es crucial para el reciclaje lento mediado por Rab11, y su inhibición por calfostina C genera un aumento del canal internalizado en el citoplasma de la célula.

5. Lgi1 es una proteína presente en tejido cardíaco capaz de regular la actividad del *canalosoma* de $K_v1.5$. Esta modulación se caracteriza porque: 1) disminuye la magnitud de la corriente $K_v1.5$ debido a una reducción en el número de los canales presentes en la membrana plasmática; 2) suprime la inactivación rápida inducida por la subunidad $K_v\beta1.3$; probablemente, debido a una interacción entre ambas proteínas; 3) tras su secreción, Lgi1 produce sus efectos electrofisiológicos desde la cara externa de la membrana, posiblemente activando o reprimiendo una ruta de segundos mensajeros, induciendo así sus efectos sobre los canales $K_v1.5$ y sobre el citoesqueleto. Por último, el patrón de expresión de esta proteína es muy similar al que muestran los canales $K_v1.5$ en el ventrículo humano. Así pues, proponemos que Lgi1 puede representar una nueva e importante subunidad moduladora de los canales $K_v1.5$-$K_v\beta1.3$, así como, una nueva diana terapéutica útil en determinadas patologías cardíacas.

7. REFERENCES

Abbott GW, Xu X, & Roepke TK (2007). Impact of ancillary subunits on ventricular repolarization. *J Electrocardiol* **40**, S42-S46.

Accili EA, Kiehn J, Yang Q, Wang Z, Brown AM, & Wible BA (1997). Separable Kvb subunit domains alter expression and gating of potassium channels. *J Biol Chem* **272**, 25824-25831.

Aiyar J, Rizzi JP, Gutman GA, & Chandy KG (1996). The signature sequence of voltage-gated potassium channels projects into the external vestibule. *J Biol Chem* **271**, 31013-31016.

Al-Reefy S, Osman H, Jiang W, & Mokbel K (2010). Evidence for a pro-apoptotic function of RACK1 in human breast cancer. *Oncogene* **29**, 5651.

Amos GJ, Wettwer E, Metzger F, Li Q, Himmel HM, & Ravens U (1996). Differences between outward currents of human atrial and subepicardial ventricular myocytes. *J Physiol* **491 (Pt 1)**, 31-50.

Aquila LA, McCarthy PM, Smedira NG, Young JB, & Moravec CS (2004). Cytoskeletal structure and recovery in single human cardiac myocytes. *J Heart Lung Transplant* **23**, 954-963.

Archer SL, Souil E, Dinh Xuan AT, Schremmer B, Mercier JC, El Yaagoubi A, Nguyen Huu L, Reeve HL, & Hampl V (1998). Molecular identification of the role of voltage-gated K+ channels, Kv1.5 and Kv2.1, in hypoxic pulmonary vasoconstriction and control of resting membrane potential in rat pulmonary artery myocytes. *J Clin Invest* **101**, 2319-2330.

Arias C, Guizy M, David M, Marzian S, Gonzalez T, Decher N, & Valenzuela C (2007). Kvb1.3 reduces the degree of stereoselective bupivacaine block of Kv1.5 channels. *Anesthesiol* **107**, 641-651.

Axelrod D (2003). Total internal reflection fluorescence microscopy in cell biology. *Methods Enzymol* **361**, 1-33.

Axelrod D & Davidson M. Total internal reflection fluorescence: Introduction and Theoretical Aspects. 2012.
Ref Type: Online Source

Babila T, Moscucci A, Wang H, Weaver FE, & Koren G (1994). Assembly of mammalian voltage-gated potassium channels: evidence for an important role of the first transmembrane segment [published erratum appears in Neuron 1996 May;16(5):following 1060]. *Neuron* **12**, 615-626.

Bahring R, Milligan CJ, Vardanyan V, Engeland B, Young BA, Dannenberg J, Waldschutz R, Edwards JP, Wray D, & Pongs O (2001). Coupling of voltage-dependent potassium channel inactivation and oxidoreductase active site of Kvbeta subunits. *J Biol Chem* **276**, 22923-22929.

Balse E, El-Haou S, Dillanian G, Dauphin A, Eldstrom J, Fedida D, Coulombe A, & Hatem SN (2009). Cholesterol modulates the recruitment of Kv1.5 channels from Rab11-associated recycling endosome in native atrial myocytes. *Proc Natl Acad Sci U S A* **106**, 14681-14686.

Bao J, Alroy I, Waterman H, Schejter ED, Brodie C, Gruenberg J, & Yarden Y (2000). Threonine phosphorylation diverts internalized epidermal growth factor receptors from a degradative pathway to the recycling endosome. *J Biol Chem* **275**, 26178-26186.

Barros F, Dominguez P, & de la Pena P (2012). Cytoplasmic domains and voltage-dependent potassium channel gating. *Front Pharmacol* **3**, 49.

Baulac S, Ishida S, Mashimo T, Boillot M, Fumoto N, Kuwamura M, Ohno Y, Takizawa A, Aoto T, Ueda M, Ikeda A, LeGuern E, Takahashi R, & Serikawa T (2012). A rat model for LGI1-related epilepsies. *Hum Mol Genet* **21**, 3546-3557.

Benavides-Haro DE, Navarro-Polanco RA, & Sanchez-Chapula JA (2003). The cholinomimetic agent bethanechol activates IK(ACh) in feline atrial myocytes. *Naunyn Schmiedebergs Arch Pharmacol* **368**, 309-315.

Benson MD, Li QJ, Kieckhafer K, Dudek D, Whorton MR, Sunahara RK, Iniguez-Lluhi JA, & Martens JR (2007). SUMO modification regulates inactivation of the voltage-gated potassium channel Kv1.5. *Proc Natl Acad Sci U S A* **104**, 1805-1810.

Bezanilla F (2000). The voltage sensor in voltage-dependent ion channels. *Physiol Rev* **80**, 555-592.

Bezanilla F & Stefani E (1998). Gating currents. *Methods Enzymol* **293**, 331-352.

Borjesson SI & Elinder F (2008). Structure, function, and modification of the voltage sensor in voltage-gated ion channels. *Cell Biochem Biophys* **52**, 149-174.

Borrie SC, Baeumer BE, & Bandtlow CE (2012). The Nogo-66 receptor family in the intact and diseased CNS. *Cell Tissue Res* **349**, 105-117.

Boycott HE, Barbier CS, Eichel CA, Costa KD, Martins RP, Louault F, Dilanian G, Coulombe A, Hatem SN, & Balse E (2013). Shear stress triggers insertion of voltage-gated potassium channels from intracellular compartments in atrial myocytes. *Proc Natl Acad Sci U S A* **110**, E3955-E3964.

Braz JC, Bueno OF, De Windt LJ, & Molkentin JD (2002). PKC alpha regulates the hypertrophic growth of cardiomyocytes through extracellular signal-regulated kinase1/2 (ERK1/2). *J Cell Biol* **156**, 905-919.

Brendel J & Peukert S (2003). Blockers of the Kv1.5 channel for the treatment of atrial arrhythmias. *Curr Med Chem Cardiovasc Hematol Agents* **1**, 273-287.

Broussard JA, Rappaz B, Webb DJ, & Brown CM (2013). Fluorescence resonance energy transfer microscopy as demonstrated by measuring the activation of the serine/threonine kinase Akt. *Nat Protoc* **8**, 265-281.

Burack WR & Shaw AS (2000). Signal transduction: hanging on a scaffold. *Curr Opin Cell Biol* **12**, 211-216.

Burg ED, Platoshyn O, Tsigelny IF, Lozano-Ruiz B, Rana BK, & Yuan JX (2010). Tetramerization domain mutations in KCNA5 affect channel kinetics and cause abnormal trafficking patterns. *Am J Physiol Cell Physiol* **298**, C496-C509.

Caballero R, Delpon E, Valenzuela C, Longobardo M, Gonzalez T, & Tamargo J (2001). Direct effects of candesartan and eprosartan on human cloned potassium channels involved in cardiac repolarization. *Mol Pharmacol* **59**, 825-836.

Caballero R, Delpon E, Valenzuela C, Longobardo M, & Tamargo J (2000). Losartan and its metabolite E3174 modify cardiac delayed rectifier K^+ currents. *Circulation* **101**, 1199-1205.

Caballero R, Moreno I, Gonzalez T, Valenzuela C, Tamargo J, & Delpon E (2002). Putative binding sites for benzocaine on a human cardiac cloned channel (Kv1.5). *Cardiovasc Res* **56**, 104-117.

Carpenter D, Jackson T, & Hanley MR (1987). Protein kinase Cs. Coping with a growing family. *Nature* **325**, 107-108.

Catterall WA (1988). Structure and function of voltage-sensitive ion channels. *Science* **242**, 50-61.

Catterall WA (2010). Ion channel voltage sensors: structure, function, and pathophysiology. *Neuron* **67**, 915-928.

Chanda B & Bezanilla F (2008). A common pathway for charge transport through voltage-sensing domains. *Neuron* **57**, 345-351.

Chang BY, Conroy KB, Machleder EM, & Cartwright CA (1998). RACK1, a receptor for activated C kinase and a homolog of the beta subunit of G proteins, inhibits activity of src tyrosine kinases and growth of NIH 3T3 cells. *Mol Cell Biol* **18**, 3245-3256.

Chernova OB, Somerville RP, & Cowell JK (1998). A novel gene, LGI1, from 10q24 is rearranged and downregulated in malignant brain tumors. *Oncogene* **17**, 2873-2881.

Choe S (2002). Potassium channel structures. *Nat Rev Neurosci* **3**, 115-121.

Choi WS, Khurana A, Mathur R, Viswanathan V, Steele DF, & Fedida D (2005). Kv1.5 surface expression is modulated by retrograde trafficking of newly endocytosed channels by the dynein motor. *Circ Res* **97**, 363-371.

Christophersen IE, Olesen MS, Liang B, Andersen MN, Larsen AP, Nielsen JB, Haunso S, Olesen SP, Tveit A, Svendsen JH, & Schmitt N (2013). Genetic variation in KCNA5: impact on the atrial-specific potassium current IKur in patients with lone atrial fibrillation. *Eur Heart J* **34**, 1517-1525.

Coetzee WA, Amarillo Y, Chiu J, Chow A, Lau D, McCormack T, Moreno H, Nadal MS, Ozaita A, Pountney D, Saganich M, Vega Saenz de Miera E, & Rudy B (1999). Molecular diversity of K+ channels. *Ann N Y Acad Sci* **868**, 233-285.

Cogolludo A, Moreno L, Bosca L, Tamargo J, & Perez-Vizcaino F (2003). Thromboxane A2-induced inhibition of voltage-gated K+ channels and pulmonary vasoconstriction: role of protein kinase Czeta. *Circ Res* **93**, 656-663.

Cogolludo A, Moreno L, Frazziano G, Moral-Sanz J, Menendez C, Castaneda J, Gonzalez C, Villamor E, & Perez-Vizcaino F (2009). Activation of neutral sphingomyelinase is involved in acute hypoxic pulmonary vasoconstriction. *Cardiovasc Res* **82**, 296-302.

Cogolludo A, Moreno L, Lodi F, Frazziano G, Cobeno L, Tamargo J, & Perez-Vizcaino F (2006). Serotonin inhibits voltage-gated K+ currents in pulmonary artery smooth muscle cells: role of 5-HT2A receptors, caveolin-1, and KV1.5 channel internalization. *Circ Res* **98**, 931-938.

Corsini E, Viviani B, Lucchi L, Marinovich M, Racchi M, & Galli CL (2001). Ontogenesis of protein kinase C betaII and its anchoring protein RACK1 in the maturation of alveolar macrophage functional responses. *Immunol Lett* **76**, 89-93.

Csukai M, Chen CH, De Matteis MA, & Mochly-Rosen D (1997). The coatomer protein beta'-COP, a selective binding protein (RACK) for protein kinase Cepsilon. *J Biol Chem* **272**, 29200-29206.

David M. Regulación de los canales Na(v)1.5 y K(v)1.5. Papel de las quinasas y de las subunidades beta. 2009. Universidad Complutense de Madrid.
Ref Type: Thesis/Dissertation

David M, Macias A, Moreno C, Prieto A, Martinez-Marmol R, Vicente R, Felipe A, Gonzalez T, Tamkun MM, & Valenzuela C (2012). PKC activity regulates functional effects of K_Vb1.3 on K_V1.5 channels. Identification of a cardiac Kv1.5 channelosome. *J Biol Chem* **287**, 21416-21428.

Day RN, Periasamy A, & Schaufele F (2001). Fluorescence resonance energy transfer microscopy of localized protein interactions in the living cell nucleus. *Methods* **25**, 4-18.

De Biasi M, Wang Z, Accili E, Wible B, & Fedida D (1997). Open channel block of human heart hKv1.5 by the beta-subunit hKv beta 1.2. *Am J Physiol* **272**, H2932-41.

Deal KK, England SK, & Tamkun MM (1996). Molecular physiology of cardiac potassium channels. *Physiol Rev* **76**, 49-76.

Decher N, Gonzalez T, Streit AK, Sachse FB, Renigunta V, Soom M, Heinemann SH, Daut J, & Sanguinetti MC (2008). Structural determinants of Kvbeta1.3-induced channel inactivation: a hairpin modulated by PIP2. *EMBO J* **27**, 3164-3174.

Decher N, Kumar P, Gonzalez T, Renigunta V, & Sanguinetti MC (2005). Structural basis for competition between drug binding and Kvbeta1.3 accessory subunit-induced N-type inactivation of Kv1.5 channels. *Mol Pharmacol* **68**, 995-1005.

Decher N, Pirard B, Bundis F, Peukert S, Baringhaus KH, Busch AE, Steinmeyer K, & Sanguinetti MC (2004). Molecular basis for Kv1.5 channel block: conservation of drug binding sites among voltage-gated K^+ channels. *J Biol Chem* **279**, 394-400.

del Camino D, Holmgren M, Liu Y, & Yellen G (2000). Blocker protection in the pore of a voltage-gated K+ channel and its structural implications. *Nature* **403**, 321-325.

del Camino D & Yellen G (2001). Tight steric closure at the intracellular activation gate of a voltage-gated K(+) channel. *Neuron* **32**, 649-656.

Dell EJ, Connor J, Chen S, Stebbins EG, Skiba NP, Mochly-Rosen D, & Hamm HE (2002). The bg subunit of heterotrimeric G proteins interacts with RACK1 and two other WD repeat proteins. *J Biol Chem* **277**, 49888-49895.

Delpon E, Caballero R, Valenzuela C, Longobardo M, Snyders DJ, & Tamargo J (1999). Benzocaine enhances and inhibits the K^+ current through a human cardiac cloned channel (Kv1.5). *Cardiovasc Res* **42**, 510-520.

Delpon E, Valenzuela C, Gay P, Franqueza L, Snyders DJ, & Tamargo J (1997). Block of human cardiac Kv1.5 channels by loratadine: voltage-, time- and use-dependent block at concentrations above therapeutic levels. *Cardiovasc Res* **35**, 341-350.

Dempsey EC, Newton AC, Mochly-Rosen D, Fields AP, Reyland ME, Insel PA, & Messing RO (2000). Protein kinase C isozymes and the regulation of diverse cell responses. *Am J Physiol Lung Cell Mol Physiol* **279**, L429-L438.

DiFrancesco D (2010). The role of the funny current in pacemaker activity. *Circ Res* **106**, 434-446.

Disatnik MH, Hernandez-Sotomayor SM, Jones G, Carpenter G, & Mochly-Rosen D (1994). Phospholipase C-gamma 1 binding to intracellular receptors for activated protein kinase C. *Proc Natl Acad Sci U S A* **91**, 559-563.

Dorn GW & Mochly-Rosen D (2002). Intracellular transport mechanisms of signal transducers. *Annu Rev Physiol* **64**, 407-429.

Doyle DA, Cabral JM, Pfuetzner RA, Kuo A, Gulbis JM, Cohen SL, Chait BT, & MacKinnon R (1998). The structure of the potassium channel: molecular basis of K^+ conduction and selectivity. *Science* **280**, 69-77.

Drolet B, Simard C, Mizoue L, & Roden DM (2005). Human cardiac potassium channel DNA polymorphism modulates access to drug-binding site and causes drug resistance. *J Clin Invest* **115**, 2209-2213.

Ellinor PT, Lunetta KL, Glazer NL, Pfeufer A, Alonso A, Chung MK, Sinner MF, de Bakker PI, Mueller M, Lubitz SA, Fox E, Darbar D, Smith NL, Smith JD, Schnabel RB, Soliman EZ, Rice KM, Van Wagoner DR, Beckmann BM, van NC, Wang K, Ehret GB, Rotter JI, Hazen SL, Steinbeck G, Smith AV, Launer LJ, Harris TB, Makino S, Nelis M, Milan DJ, Perz S, Esko T, Kottgen A, Moebus S, Newton-Cheh C, Li M, Mohlenkamp S, Wang TJ, Kao WH, Vasan RS, Nothen MM, MacRae CA, Stricker BH, Hofman A, Uitterlinden AG, Levy D, Boerwinkle E, Metspalu A, Topol EJ, Chakravarti A, Gudnason V, Psaty BM, Roden DM, Meitinger T, Wichmann HE, Witteman JC, Barnard J, Arking DE, Benjamin EJ, Heckbert SR, & Kaab S (2010). Common variants in KCNN3 are associated with lone atrial fibrillation. *Nat Genet* **42**, 240-244.

England SK, Uebele VN, Kodali J, Bennett PB, & Tamkun MM (1995a). A novel K^+ channel b-subunit (hKvb1.3) is produced via alternative mRNA splicing. *J Biol Chem* **270**, 28531-28534.

England SK, Uebele VN, Shear H, Kodali J, Bennett PB, & Tamkun MM (1995b). Characterization of a voltage-gated K^+ channel b subunit expressed in human heart. *Proc Natl Acad Sci U S A* **92**, 6309-6313.

Fan Z & Makielski JC (1997). Anionic phospholipids activate ATP-sensitive potassium channels. *J Biol Chem* **272**, 5388-5395.

Fedele F, Mancone M, Chilian WM, Severino P, Canali E, Logan S, De Marchis ML, Volterrani M, Palmirotta R, & Guadagni F (2013). Role of genetic polymorphisms of ion channels in the pathophysiology of coronary microvascular dysfunction and ischemic heart disease. *Basic Res Cardiol* **108**, 387.

Fedida D (1997). Gating charge and ionic currents associated with quinidine block of human Kv1.5 delayed rectifier channels. *J Physiol (Lond)* **499**, 661-675.

Fedida D, Wible B, Wang Z, Fermini B, Faust F, Nattel S, & Brown AM (1993). Identity of a novel delayed rectifier current from human heart with a cloned K^+ channel current. *Circ Res* **73**, 210-216.

Feng J, Wang Z, Li GR, & Nattel S (1997). Effects of class III antiarrhythmic drugs on transient outward and ultra-rapid delayed rectifier currents in human atrial myocytes. *J Pharmacol Exp Ther* **281**, 384-392.

Fernandez-Trillo J, Barros F, Machin A, Carretero L, Dominguez P, & de la Pena P (2011). Molecular determinants of interactions between the N-terminal domain and the transmembrane core that modulate hERG K+ channel gating. *PLoS One* **6**, e24674.

Ford JW & Milnes JT (2008). New drugs targeting the cardiac ultra-rapid delayed-rectifier current (I Kur): rationale, pharmacology and evidence for potential therapeutic value. *J Cardiovasc Pharmacol* **52**, 105-120.

Franqueza L, Longobardo M, Vicente J, Delpon E, Tamkun MM, Tamargo J, Snyders DJ, & Valenzuela C (1997). Molecular determinants of stereoselective bupivacaine block of hKv1.5 channels. *Circ Res* **81**, 1053-1064.

Franqueza L, Valenzuela C, Delpon E, Longobardo M, Caballero R, & Tamargo J (1998). Effects of propafenone and 5-hydroxy-propafenone on hKv1.5 channels. *Br J Pharmacol* **125**, 969-978.

Furukawa T, Yamane T, Terai T, Katayama Y, & Hiraoka M (1996). Functional linkage of the cardiac ATP-sensitive K+ channel to the actin cytoskeleton. *Pflugers Arch* **431**, 504-512.

Gabriel L, Lvov A, Orthodoxou D, Rittenhouse AR, Kobertz WR, & Melikian HE (2012). The acid-sensitive, anesthetic-activated potassium leak channel, KCNK3, is regulated by 14-3-3beta-dependent, protein kinase C (PKC)-mediated endocytic trafficking. *J Biol Chem* **287**, 32354-32366.

Gerges NZ, Backos DS, & Esteban JA (2004). Local control of AMPA receptor trafficking at the postsynaptic terminal by a small GTPase of the Rab family. *J Biol Chem* **279**, 43870-43878.

Gerrer T, Graumann P, Soufo HJD, & Wedlich-Söldner R. Super-resolution imaging of the bacterial cytoskeleton. 2013.
Ref Type: Online Source

Goldman DE (1943). Potential, impedance and rectification in membranes. *J Gen Physiol* **27**, 37-60.

Goldstein SA, Bockenhauer D, O'Kelly I, & Zilberberg N (2001). Potassium leak channels and the KCNK family of two-P-domain subunits. *Nat Rev Neurosci* **2**, 175-184.

Gonzalez T, David M, Moreno C, Macias A, & Valenzuela C (2010). Kv1.5-Kv beta interactions: molecular determinants and pharmacological consequences. *Mini Rev Med Chem* **10**, 635-642.

Gonzalez T, Navarro-Polanco R, Arias C, Caballero R, Moreno I, Delpon E, Tamargo J, Tamkun MM, & Valenzuela C (2002). Assembly with the Kvb1.3 subunit modulates drug block of hKv1.5 channels. *Mol Pharmacol* **62**, 1456-1463.

Grissmer S, Nguyen AN, Aiyar J, Hanson DC, Mather RJ, Gutman GA, Karmilowicz MJ, Auperin DD, & Chandy KG (1994). Pharmacological characterization of five cloned voltage-gated K^+ channels, types Kv1.1, 1.2, 1.3, 1.5, and 3.1, stably expressed in mammalian cell lines. *Mol Pharmacol* **45**, 1227-1234.

Grosshans BL, Ortiz D, & Novick P (2006). Rabs and their effectors: achieving specificity in membrane traffic. *Proc Natl Acad Sci U S A* **103**, 11821-11827.

Gu W, Wevers A, Schroder H, Grzeschik KH, Derst C, Brodtkorb E, de VR, & Steinlein OK (2002). The LGI1 gene involved in lateral temporal lobe epilepsy belongs to a new subfamily of leucine-rich repeat proteins. *FEBS Lett* **519**, 71-76.

Gudbjartsson DF, Arnar DO, Helgadottir A, Gretarsdottir S, Holm H, Sigurdsson A, Jonasdottir A, Baker A, Thorleifsson G, Kristjansson K, Palsson A, Blondal T, Sulem P, Backman VM, Hardarson GA, Palsdottir E, Helgason A, Sigurjonsdottir R, Sverrisson JT, Kostulas K, Ng MC, Baum L, So WY, Wong KS, Chan JC, Furie KL, Greenberg SM, Sale M, Kelly P, MacRae CA, Smith EE, Rosand J, Hillert J, Ma RC, Ellinor PT, Thorgeirsson G, Gulcher JR, Kong A, Thorsteinsdottir U, & Stefansson K (2007). Variants conferring risk of atrial fibrillation on chromosome 4q25. *Nature* **448**, 353-357.

Gulbis JM, Mann S, & MacKinnon R (1999). Structure of a voltage-dependent K+ channel beta subunit. *Cell* **97**, 943-952.

Gulbis JM, Zhou M, Mann S, & MacKinnon R (2000). Structure of the cytoplasmic beta subunit-T1 assembly of voltage- dependent K+ channels. *Science* **289**, 123-127.

Gutman GA, Chandy KG, Grissmer S, Lazdunski M, McKinnon D, Pardo LA, Robertson GA, Rudy B, Sanguinetti MC, Stuhmer W, & Wang X (2005). International Union of Pharmacology. LIII. Nomenclature and molecular relationships of voltage-gated potassium channels. *Pharmacol Rev* **57**, 473-508.

Hahn HS, Marreez Y, Odley A, Sterbling A, Yussman MG, Hilty KC, Bodi I, Liggett SB, Schwartz A, & Dorn GW (2003). Protein kinase Calpha negatively regulates systolic and diastolic function in pathological hypertrophy. *Circ Res* **93**, 1111-1119.

Hales CM, Vaerman JP, & Goldenring JR (2002). Rab11 family interacting protein 2 associates with Myosin Vb and regulates plasma membrane recycling. *J Biol Chem* **277**, 50415-50421.

Hayabuchi Y, Standen NB, & Davies NW (2001). Angiotensin II inhibits and alters kinetics of voltage-gated K(+) channels of rat arterial smooth muscle. *Am J Physiol Heart Circ Physiol* **281**, H2480-H2489.

Head K, Gong S, Joseph S, Wang C, Burkhardt T, Rossi MR, LaDuca J, Matsui S, Vaughan M, Hicks DG, Heintz N, & Cowell JK (2007). Defining the expression pattern of the LGI1 gene in BAC transgenic mice. *Mamm Genome* **18**, 328-337.

Heginbotham L, Abramson T, & MacKinnon R (1992). A functional connection between the pores of distantly related ion channels as revealed by mutant K^+ channels. *Science* **258**, 1152-1155.

Heinemann SH, Rettig J, Wunder F, & Pongs O (1995). Molecular and functional characterization of a rat brain Kvb3 potassium channel subunit. *FEBS Lett* **377**, 383-389.

Higuchi R, Krummel B, & Saiki RK (1988). A general method of in vitro preparation and specific mutagenesis of DNA fragments: study of protein and DNA interactions. *Nucleic Acids Res* **16**, 7351-7367.

Hilgemann DW & Ball R (1996). Regulation of cardiac Na+,Ca2+ exchange and KATP potassium channels by PIP2. *Science* **273**, 956-959.

Hille B (2001). *Ion channels of excitable membranes*, 3rd ed. Sinauer Associates, Inc., Sunderland.

Hille B, Armstrong CM, & MacKinnon R (1999). Ion channels: from idea to reality. *Nat Med* **5**, 1105-1109.

Hodgkin AL & Huxley AF (1952). A quantitative description of membrane current and its application to conduction and excitation in nerve. *J Physiol (Lond)* **117**, 500-544.

Hodgkin AL & Katz B (1949). The effect of sodium ions on the electrical activity of the giant axon of the squid. *J Physiol (Lond)* **108**, 37-77.

Hodgkin AL & Keynes RD (1955). The potassium permeability of a giant nerve fibre. *J Physiol* **128**, 61-88.

Holmes TC, Fadool DA, Ren R, & Levitan IB (1996). Association of Src tyrosine kinase with a human potassium channel mediated by SH3 domain. *Science* **274**, 2089-2091.

Horgan CP & McCaffrey MW (2009). The dynamic Rab11-FIPs. *Biochem Soc Trans* **37**, 1032-1036.

Hoshi T, Zagotta WN, & Aldrich RW (1990). Biophysical and molecular mechanisms of *Shaker* potassium channel inactivation. *Science* **250**, 533-538.

Hubbard MJ & Cohen P (1993). On target with a new mechanism for the regulation of protein phosphorylation. *Trends Biochem Sci* **18**, 172-177.

Idkowiak-Baldys J, Baldys A, Raymond JR, & Hannun YA (2009). Sustained receptor stimulation leads to sequestration of recycling endosomes in a classical protein kinase C- and phospholipase D-dependent manner. *J Biol Chem* **284**, 22322-22331.

Irani SR, Stagg CJ, Schott JM, Rosenthal CR, Schneider SA, Pettingill P, Pettingill R, Waters P, Thomas A, Voets NL, Cardoso MJ, Cash DM, Manning EN, Lang B, Smith SJ, Vincent A, & Johnson MR (2013). Faciobrachial dystonic seizures: the influence of immunotherapy on seizure control and prevention of cognitive impairment in a broadening phenotype. *Brain* **136**, 3151-3162.

Isacson CK, Lu Q, Karas RH, & Cox DH (2007). RACK1 is a BKCa channel binding protein. *Am J Physiol Cell Physiol* **292**, C1459-C1466.

Iwata K, Ikami K, Matsuno K, Yamashita T, Shiba D, Ibi M, Matsumoto M, Katsuyama M, Cui W, Zhang J, Zhu K, Takei N, Kokai Y, Ohneda O, Yokoyama T, & Yabe-Nishimura C (2014). Deficiency of NOX1/Nicotinamide Adenine Dinucleotide Phosphate, Reduced Form Oxidase Leads to Pulmonary Vascular Remodeling. *Arterioscler Thromb Vasc Biol* **34**, 110-119.

Jackson WF (2005). Potassium channels in the peripheral microcirculation. *Microcirculation* **12**, 113-127.

Jaken S & Parker PJ (2000). Protein kinase C binding partners. *Bioessays* **22**, 245-254.

Jiang Y, Ruta V, Chen J, Lee A, & MacKinnon R (2003). The principle of gating charge movement in a voltage-dependent K+ channel. *Nature* **423**, 42-48.

Joseph BK, Thakali KM, Moore CL, & Rhee SW (2013). Ion channel remodeling in vascular smooth muscle during hypertension: Implications for novel therapeutic approaches. *Pharmacol Res* **70**, 126-138.

Jou I, Pyo H, Chung S, Jung SY, Gwag BJ, & Joe EH (1998). Expression of Kv1.5 K+ channels in activated microglia in vivo. *GLIA* **24**, 408-414.

Kaab S, Darbar D, van NC, Dupuis J, Pfeufer A, Newton-Cheh C, Schnabel R, Makino S, Sinner MF, Kannankeril PJ, Beckmann BM, Choudry S, Donahue BS, Heeringa J, Perz S, Lunetta KL, Larson MG, Levy D, MacRae CA, Ruskin JN, Wacker A, Schomig A, Wichmann HE, Steinbeck G, Meitinger T, Uitterlinden AG, Witteman JC, Roden DM, Benjamin EJ, & Ellinor PT (2009). Large scale replication and meta-analysis of variants on chromosome 4q25 associated with atrial fibrillation. *Eur Heart J* **30**, 813-819.

Kerkela R, Ilves M, Pikkarainen S, Tokola H, Ronkainen J, Vuolteenaho O, Leppaluoto J, & Ruskoaho H (2002). Identification of PKCalpha isoform-specific effects in cardiac myocytes using antisense phosphorothioate oligonucleotides. *Mol Pharmacol* **62**, 1482-1491.

Knobloch K, Brendel J, Peukert S, Rosenstein B, Busch AE, & Wirth KJ (2002). Electrophysiological and antiarrhythmic effects of the novel I(Kur) channel blockers, S9947 and S20951, on left vs. right pig atrium in vivo in comparison with the I(Kr) blockers dofetilide, azimilide, d,l-sotalol and ibutilide. *Naunyn Schmiedebergs Arch Pharmacol* **366**, 482-487.

Kobayashi E, Nakano H, Morimoto M, & Tamaoki T (1989). Calphostin C (UCN-1028C), a novel microbial compound, is a highly potent and specific inhibitor of protein kinase C. *Biochem Biophys Res Commun* **159**, 548-553.

Korzick DH, Holiman DA, Boluyt MO, Laughlin MH, & Lakatta EG (2001). Diminished alpha1-adrenergic-mediated contraction and translocation of PKC in senescent rat heart. *Am J Physiol Heart Circ Physiol* **281**, H581-H589.

Kuhlkamp V, Schirdewan A, Stangl K, Homberg M, Ploch M, & Beck OA (2000). Use of metoprolol CR/XL to maintain sinus rhythm after conversion from persistent atrial fibrillation: a randomized, double-blind, placebo-controlled study. *J Am Coll Cardiol* **36**, 139-146.

Kunapuli P, Jang GF, Kazim L, & Cowell JK (2009). Mass spectrometry identifies LGI1-interacting proteins that are involved in synaptic vesicle function in the human brain. *J Mol Neurosci* **39**, 137-143.

Kunapuli P, Lo K, Hawthorn L, & Cowell JK (2010a). Reexpression of LGI1 in glioma cells results in dysregulation of genes implicated in the canonical axon guidance pathway. *Genomics* **95**, 93-100.

Kunapuli P, Lo K, Hawthorn L, & Cowell JK (2010b). Reexpression of LGI1 in glioma cells results in dysregulation of genes implicated in the canonical axon guidance pathway. *Genomics* **95**, 93-100.

Kurokawa J, Abriel H, & Kass RS (2001). Molecular basis of the delayed rectifier current I(ks)in heart. *J Mol Cell Cardiol* **33**, 873-882.

Kuryshev YA, Wible BA, Gudz TI, Ramirez AN, & Brown AM (2001). KChAP/Kvbeta1.2 interactions and their effects on cardiac Kv channel expression. *Am J Physiol Cell Physiol* **281**, C290-C299.

Kusuzawa S, Honda T, Fukata Y, Fukata M, Kanatani S, Tanaka DH, & Nakajima K (2012). Leucine-rich glioma inactivated 1 (Lgi1), an epilepsy-related secreted protein, has a nuclear localization signal and localizes to both the cytoplasm and the nucleus of the caudal ganglionic eminence neurons. *Eur J Neurosci* **36**, 2284-2292.

Kwak YG, Hu N, Wei J, George AL, Jr., Grobaski TD, Tamkun MM, & Murray KT (1999a). Protein kinase A phosphorylation alters Kvb1.3 subunit- mediated inactivation of the Kv1.5 potassium channel. *J Biol Chem* **274**, 13928-13932.

Kwak YG, Navarro-Polanco R, Grobaski T, Gallagher DJ, & Tamkun MM (1999b). Phosphorylation is required for alteration of Kv1.5 K^+ channel function by the Kvb1.3 subunit. *J Biol Chem* **274**, 25355-25361.

Leicher T, Roeper J, Weber k, Wang X, & Pongs O (1996). Structural and functional characterization of human potassium channel subunit beta 1 (KCNA1B). *Neuropharmacol* **35**, 787-795.

Lewis RS & Cahalan MD (1995). Potassium and calcium channels in lymphocytes. *Annu Rev Immunol* **13**, 623-653.

Li GR, Feng J, Wang Z, Fermini B, & Nattel S (1996). Adrenergic modulation of ultrarapid delayed rectifier K+ current in human atrial myocytes. *Circ Res* **78**, 903-915.

Li M, Jan YN, & Jan LY (1992). Specification of subunit assembly by the hydrophilic amino- terminal domain of the *Shaker* potassium channel. *Science* **257**, 1225-1230.

Lin Y, Jover-Mengual T, Wong J, Bennett MV, & Zukin RS (2006). PSD-95 and PKC converge in regulating NMDA receptor trafficking and gating. *Proc Natl Acad Sci U S A* **103**, 19902-19907.

Liu H, Shim AH, & He X (2009). Structural characterization of the ectodomain of a disintegrin and metalloproteinase-22 (ADAM22), a neural adhesion receptor instead of metalloproteinase: insights on ADAM function. *J Biol Chem* **284**, 29077-29086.

Logothetis DE, Petrou VI, Adney SK, & Mahajan R (2010). Channelopathies linked to plasma membrane phosphoinositides. *Pflugers Arch* **460**, 321-341.

Long SB, Campbell EB, & MacKinnon R (2005a). Crystal structure of a mammalian voltage-dependent Shaker family K+ channel. *Science* **309**, 897-903.

Long SB, Campbell EB, & MacKinnon R (2005b). Voltage sensor of Kv1.2: structural basis of electromechanical coupling. *Science* **309**, 903-908.

Longobardo M, Delpon E, Caballero R, Tamargo J, & Valenzuela C (1998). Structural determinants of potency and stereoselective block of hKv1.5 channels induced by local anesthetics. *Mol Pharmacol* **54**, 162-169.

Longobardo M, Gonzalez T, Caballero R, Delpon E, Tamargo J, & Valenzuela C (2001). Bupivacaine effects on hKv1.5 channels are dependent on extracellular pH. *Br J Pharmacol* **134**, 359-369.

Longobardo M, Gonzalez T, Navarro-Polanco R, Caballero R, Delpon E, Tamargo J, Snyders DJ, Tamkun MM, & Valenzuela C (2000). Effects of a quaternary bupivacaine derivative on delayed rectifier K^+ currents. *Br J Pharmacol* **130**, 391-401.

Lubitz SA, Yi BA, & Ellinor PT (2009). Genetics of atrial fibrillation. *Cardiol Clin* **27**, 25-33, vii.

MacDonald PE, Salapatek AM, & Wheeler MB (2003). Temperature and redox state dependence of native Kv2.1 currents in rat pancreatic beta-cells. *J Physiol* **546**, 647-653.

Macias A, Moreno C, Moral-Sanz J, Cogolludo A, David M, Alemanni M, Perez-Vizcaino F, Zaza A, Valenzuela C, & Gonzalez T (2010). Celecoxib blocks cardiac Kv1.5, Kv4.3 and Kv7.1 (KCNQ1) channels: effects on cardiac action potentials. *J Mol Cell Cardiol* **49**, 984-992.

MacKinnon R (1991). Determination of the subunit stoichiometry of a voltage- activated K channel. *Nature* **350**, 232-235.

MacKinnon R (2003). Potassium channels. *FEBS Lett* **555**, 62-65.

Majumder K, De Biasi M, Wang Z, & Wible BA (1995). Molecular cloning and functional expression of a novel potassium channel beta-subunit from human atrium. *FEBS Lett* **361**, 13-16.

Malmivuo J & Plonsey R (1995). Active Behavior of the Cell Membrane. In *Bioelectromagnetism. Principles and Applications of Bioelectric and Biomagnetic Fields.*

Manganas LN, Wang Q, Scannevin RH, Antonucci DE, Rhodes KJ, & Trimmer JS (2001). Identification of a trafficking determinant localized to the Kv1 potassium channel pore. *Proc Natl Acad Sci U S A* **98**, 14055-14059.

Manna I, Mumoli L, Labate A, Citrigno L, Ferlazzo E, Aguglia U, Quattrone A, & Gambardella A (2013). Autosomal dominant lateral temporal epilepsy (ADLTE): Absence of chromosomal rearrangements in LGI1 gene. *Epilepsy Res*.

Manna PT, Smith AJ, Taneja TK, Howell GJ, Lippiat JD, & Sivaprasadarao A (2010). Constitutive endocytic recycling and protein kinase C-mediated lysosomal degradation control K(ATP) channel surface density. *J Biol Chem* **285**, 5963-5973.

Mannuzzu LM, Moronne MM, & Isacoff EY (1996). Direct physical measure of conformational rearrangement underlying potassium channel gating. *Science* **271**, 213-216.

Martens JR, Kwak YG, & Tamkun MM (1999). Modulation of Kv channel alpha/beta subunit interactions. *Trends Cardiovasc Med* **9**, 253-258.

Mason HS, Latten MJ, Godoy LD, Horowitz B, & Kenyon JL (2002). Modulation of Kv1.5 currents by protein kinase A, tyrosine kinase, and protein tyrosine phosphatase requires an intact cytoskeleton. *Mol Pharmacol* **61**, 285-293.

Matsubara H, Liman ER, Hess P, & Koren G (1994). Pretranslational mechanisms determine the type of potassium channels expressed in the rat skeletal and cardiac muscles. *J Biol Chem* **266**, 13324-13328.

Matsuda T, Masumiya H, Tanaka N, Yamashita T, Tsuruzoe N, Tanaka Y, Tanaka H, & Shigenoba K (2001). Inhibition by a novel anti-arrhythmic agent, NIP-142, of cloned human cardiac K+ channel Kv1.5 current. *Life Sci* **68**, 2017-2024.

Mays DJ, Foose JM, Philipson LH, & Tamkun MM (1995). Localization of the Kv1.5 K^+ channel protein in explanted cardiac tissue. *J Clin Invest* **96**, 282-292.

McEwen DP, Schumacher SM, Li Q, Benson MD, Iniguez-Lluhi JA, Van Genderen KM, & Martens JR (2007). Rab-GTPase-dependent endocytic recycling of Kv1.5 in atrial myocytes. *J Biol Chem* **282**, 29612-29620.

Mia S, Munoz C, Pakladok T, Siraskar G, Voelkl J, Alesutan I, & Lang F (2012). Downregulation of Kv1.5 K channels by the AMP-activated protein kinase. *Cell Physiol Biochem* **30**, 1039-1050.

Michelakis ED, Rebeyka I, Wu X, Nsair A, Thebaud B, Hashimoto K, Dyck JR, Haromy A, Harry G, Barr A, & Archer SL (2002). O2 sensing in the human ductus arteriosus: regulation of voltage-gated K+ channels in smooth muscle cells by a mitochondrial redox sensor. *Circ Res* **91**, 478-486.

Michell RH (2009). First came the link between phosphoinositides and Ca2+ signalling, and then a deluge of other phosphoinositide functions. *Cell Calcium* **45**, 521-526.

Miranda P, Contreras JE, Plested AJ, Sigworth FJ, Holmgren M, & Giraldez T (2013). State-dependent FRET reports calcium- and voltage-dependent gating-ring motions in BK channels. *Proc Natl Acad Sci U S A* **110**, 5217-5222.

Miranda P, Manso DG, Barros F, Carretero L, Hughes TE, Alonso-Ron C, Dominguez P, & de la Pena P (2008). FRET with multiply labeled HERG K(+) channels as a reporter of the in vivo coarse architecture of the cytoplasmic domains. *Biochim Biophys Acta* **1783**, 1681-1699.

Mochly-Rosen D (1995). Localization of protein kinases by anchoring proteins: a theme in signal transduction. *Science* **268**, 247-251.

Mochly-Rosen D, Smith BL, Chen CH, Disatnik MH, & Ron D (1995). Interaction of protein kinase C with RACK1, a receptor for activated C-kinase: a role in beta protein kinase C mediated signal transduction. *Biochem Soc Trans* **23**, 596-600.

Mohamed BA, Barakat AZ, Zimmermann WH, Bittner RE, Muhlfeld C, Hunlich M, Engel W, Maier LS, & Adham IM (2012). Targeted disruption of Hspa4 gene leads to cardiac hypertrophy and fibrosis. *J Mol Cell Cardiol* **53**, 459-468.

Morais-Cabral JH, Zhou Y, & MacKinnon R (2001). Energetic optimization of ion conduction rate by the K+ selectivity filter. *Nature* **414**, 37-42.

Morales MJ, Castellino RC, Crews AL, Rasmusson RL, & Strauss HC (1995). A novel beta subunit increases rate of inactivation of specific voltage-gated potassium channel alpha subunits. *J Biol Chem* **270**, 6272-6277.

Moreno C. K(v) modulation by polyunsaturated fatty acids. Functional study of a new K(v)7.1 mutation associated to short QT syndrome. 2013.
Ref Type: Thesis/Dissertation

Moreno C, Prieto P, Macias A, Pimentel-Santillana M, de la Cruz A, Traves PG, Bosca L, & Valenzuela C (2013). Modulation of voltage-dependent and inward rectifier potassium channels by 15-epi-lipoxin-a4 in activated murine macrophages: implications in innate immunity. *J Immunol* **191**, 6136-6146.

Moreno I, Caballero R, Gonzalez T, Arias C, Valenzuela C, Iriepa I, Galvez E, Tamargo J, & Delpon E (2003). Effects of irbesartan on cloned potassium channels involved in human cardiac repolarization. *J Pharmacol Exp Ther* **304**, 862-873.

Murray KT, Fahrig SA, Deal KK, Po SS, Hu NN, Snyders DJ, Tamkun MM, & Bennett PB (1994). Modulation of an inactivating human cardiac K^+ channel by protein kinase C. *Circ Res* **75**, 999-1005.

Nagaya N & Papazian DM (1997). Potassium channel alpha and beta subunits assemble in the endoplasmic reticulum. *J Biol Chem* **272**, 3022-3027.

Need AC, Irvine EE, & Giese KP (2003). Learning and memory impairments in Kv beta 1.1-null mutants are rescued by environmental enrichment or ageing. *Eur J Neurosci* **18**, 1640-1644.

Neher E & Sakmann B (1976). Single-channel currents recorded from membrane of denervated frog muscle fibres. *Nature* **260**, 799-802.

Nelson MT & Quayle JM (1995). Physiological roles and properties of potassium channels in arterial smooth muscle. *Am J Physiol* **268**, C799-C822.

Nerbonne JM (2000). Molecular basis of functional voltage-gated K+ channel diversity in the mammalian myocardium. *J Physiol* **525 Pt 2**, 285-298.

Nerbonne JM & Kass RS (2005). Molecular physiology of cardiac repolarization. *Physiol Rev* **85**, 1205-1253.

Nesti E, Everill B, & Morielli AD (2004). Endocytosis as a mechanism for tyrosine kinase-dependent suppression of a voltage-gated potassium channel. *Mol Biol Cell* **15**, 4073-4088.

Nobile C, Michelucci R, Andreazza S, Pasini E, Tosatto SC, & Striano P (2009). LGI1 mutations in autosomal dominant and sporadic lateral temporal epilepsy. *Hum Mutat* **30**, 530-536.

Oliver D, Lien CC, Soom M, Baukrowitz T, Jonas P, & Fakler B (2004). Functional conversion between A-type and delayed rectifier K^+ channels by membrane lipids. *Science* **304**, 265-270.

Olson TM, Alekseev AE, Liu XK, Park S, Zingman LV, Bienengraeber M, Sattiraju S, Ballew JD, Jahangir A, & Terzic A (2006). Kv1.5 channelopathy due to KCNA5 loss-of-function mutation causes human atrial fibrillation. *Hum Mol Genet* **15**, 2185-2191.

Orlova EV, Papakosta M, Booy FP, van HM, & Dolly JO (2003). Voltage-gated K+ channel from mammalian brain: 3D structure at 18A of the complete (alpha)4(beta)4 complex. *J Mol Biol* **326**, 1005-1012.

Ottman R, Risch N, Hauser WA, Pedley TA, Lee JH, Barker-Cummings C, Lustenberger A, Nagle KJ, Lee KS, Scheuer ML, & . (1995). Localization of a gene for partial epilepsy to chromosome 10q. *Nat Genet* **10**, 56-60.

Pan Y, Weng J, Levin EJ, & Zhou M (2011). Oxidation of NADPH on Kvbeta1 inhibits ball-and-chain type inactivation by restraining the chain. *Proc Natl Acad Sci U S A* **108**, 5885-5890.

Papazian DM, Schwarz TL, Tempel BL, Jan YN, & Jan LY (1987). Cloning of genomic and complementary DNA from *Shaker*, a putative potassium channels gene from Drosophila. *Science* **237**, 749-753.

Papazian DM, Timpe LC, Jan YN, & Jan LY (1991). Alteration of voltage-dependence of Shaker potassium channel by mutations in the S4 sequence. *Nature* **349**, 305-310.

Pardo LA, del Camino D, Sanchez A, Alves F, Bruggemann A, Beckh S, & Stuhmer W (1999). Oncogenic potential of EAG K(+) channels. *EMBO J* **18**, 5540-5547.

Parker PJ, Kour G, Marais RM, Mitchell F, Pears C, Schaap D, Stabel S, & Webster C (1989). Protein kinase C--a family affair. *Mol Cell Endocrinol* **65**, 1-11.

Pass JM, Gao J, Jones WK, Wead WB, Wu X, Zhang J, Baines CP, Bolli R, Zheng YT, Joshua IG, & Ping P (2001). Enhanced PKC beta II translocation and PKC beta II-RACK1 interactions in PKC epsilon-induced heart failure: a role for RACK1. *Am J Physiol Heart Circ Physiol* **281**, H2500-H2510.

Pavarotti M, Capmany A, Vitale N, Colombo MI, & Damiani MT (2012). Rab11 is phosphorylated by classical and novel protein kinase C isoenzymes upon sustained phorbol ester activation. *Biol Cell* **104**, 102-115.

Pavri BB, Greenberg HE, Kraft WK, Lazarus N, Lynch JJ, Salata JJ, Bilodeau MT, Regan CP, Stump G, Fan L, Mehta A, Wagner JA, Gutstein DE, & Bloomfield D (2012). MK-0448, a specific Kv1.5 inhibitor: safety, pharmacokinetics, and pharmacodynamic electrophysiology in experimental animal models and humans. *Circ Arrhythm Electrophysiol* **5**, 1193-1201.

Pawson T & Nash P (2003). Assembly of cell regulatory systems through protein interaction domains. *Science* **300**, 445-452.

Peyser A & Nonner W (2012). Voltage sensing in ion channels: mesoscale simulations of biological devices. *Phys Rev E Stat Nonlin Soft Matter Phys* **86**, 011910.

Pongs O, Leicher T, Berger M, Roeper J, Bahring R, Wray D, Giese KP, Silva AJ, & Storm JF (1999). Functional and molecular aspects of voltage-gated K+ channel beta subunits. *Ann N Y Acad Sci* **868**, 344-355.

Pongs O & Schwarz JR (2010). Ancillary subunits associated with voltage-dependent K+ channels. *Physiol Rev* **90**, 755-796.

Pozeg ZI, Michelakis ED, McMurtry MS, Thebaud B, Wu XC, Dyck JR, Hashimoto K, Wang S, Moudgil R, Harry G, Sultanian R, Koshal A, & Archer SL (2003). In vivo gene transfer of the O2-sensitive potassium channel Kv1.5 reduces pulmonary hypertension and restores hypoxic pulmonary vasoconstriction in chronically hypoxic rats. *Circulation* **107**, 2037-2044.

Qatsha KA, Rudolph C, Marme D, Schachtele C, & May WS (1993). Go 6976, a selective inhibitor of protein kinase C, is a potent antagonist of human immunodeficiency virus 1 induction from latent/low-level-producing reservoir cells in vitro. *Proc Natl Acad Sci U S A* **90**, 4674-4678.

Qin M, Huang H, Wang T, Hu H, Liu Y, Cao H, Li H, & Huang C (2012). Absence of Rgs5 prolongs cardiac repolarization and predisposes to ventricular tachyarrhythmia in mice. *J Mol Cell Cardiol* **53**, 880-890.

Rangaraju S, Chi V, Pennington MW, & Chandy KG (2009). Kv1.3 potassium channels as a therapeutic target in multiple sclerosis. *Expert Opin Ther Targets* **13**, 909-924.

Ravens U (2010). Antiarrhythmic therapy in atrial fibrillation. *Pharmacol Ther* **128**, 129-145.

Ravens U & Cerbai E (2008). Role of potassium currents in cardiac arrhythmias. *Europace* **10**, 1133-1137.

Ravens U, Poulet C, Wettwer E, & Knaut M (2013). Atrial selectivity of antiarrhythmic drugs. *J Physiol*.

Ravens U & Wettwer E (2011). Ultra-rapid delayed rectifier channels: molecular basis and therapeutic implications. *Cardiovasc Res* **89**, 776-785.

Rettig J, Heinemann SH, Wunder F, Lorra C, Parcej DN, Dolly JO, & Pongs O (1994). Inactivation properties of voltage-gated K^+ channels altered by presence of b-subunit. *Nature* **369**, 289-294.

Rhodes KJ, Keilbaugh SA, Barrezueta NX, Lopez KL, & Trimmer JS (1995). Association and colocalization of K+ channel alpha- and beta- subunit polypeptides in rat brain. *J Neurosci* **15**, 5360-5371.

Roden DM & George AL, Jr. (1997). Structure and function of cardiac sodium and potassium channels. *Am J Physiol* **273**, H511-H525.

Rodriguez MM, Ron D, Touhara K, Chen CH, & Mochly-Rosen D (1999). RACK1, a protein kinase C anchoring protein, coordinates the binding of activated protein kinase C and select pleckstrin homology domains in vitro. *Biochem* **38**, 13787-13794.

Ron D, Adams DR, Baillie GS, Long A, O'Connor R, & Kiely PA (2013). RACK1 to the future--a historical perspective. *Cell Commun Signal* **11**, 53.

Ron D, Chen CH, Caldwell J, Jamieson L, Orr E, & Mochly-Rosen D (1994). Cloning of an intracellular receptor for protein kinase C: a homolog of the beta subunit of G proteins. *Proc Natl Acad Sci U S A* **91**, 839-843.

Ross ST, Schwarts S, Fellers TJ, & Davidson MW. Total Internal Reflection Fluorescence (TIRF) Microscopy. 2013.
Ref Type: Online Source

Roy R, Hohng S, & Ha T (2008). A practical guide to single-molecule FRET. *Nat Methods* **5**, 507-516.

Schechtman D & Mochly-Rosen D (2001). Adaptor proteins in protein kinase C-mediated signal transduction. *Oncogene* **20**, 6339-6347.

Schlaich MP, Kaye DM, Lambert E, Hastings J, Campbell DJ, Lambert G, & Esler MD (2005). Angiotensin II and norepinephrine release: interaction and effects on the heart. *J Hypertens* **23**, 1077-1082.

Schlaich MP, Kaye DM, Lambert E, Sommerville M, Socratous F, & Esler MD (2003). Relation between cardiac sympathetic activity and hypertensive left ventricular hypertrophy. *Circulation* **108**, 560-565.

Schulte U, Thumfart JO, Klocker N, Sailer CA, Bildl W, Biniossek M, Dehn D, Deller T, Eble S, Abbass K, Wangler T, Knaus HG, & Fakler B (2006). The epilepsy-linked Lgi1 protein assembles into presynaptic Kv1 channels and inhibits inactivation by Kvbeta1. *Neuron* **49**, 697-706.

Schumacher SM & Martens JR (2010). Ion channel trafficking: a new therapeutic horizon for atrial fibrillation. *Heart Rhythm* **7**, 1309-1315.

Schumacher SM, McEwen DP, Zhang L, Arendt KL, Van Genderen KM, & Martens JR (2009). Antiarrhythmic drug-induced internalization of the atrial-specific k+ channel kv1.5. *Circ Res* **104**, 1390-1398.

Scott VE, Rettig J, Parcej DN, Keen JN, Findlay JBC, Pongs O, & Dolly JO (1994). Primary structure of a b subunit of a-dendrotoxin-sensitive K^+ channels from bovine brain. *Proc Natl Acad Sci U S A* **91**, 1637-1641.

Senechal KR, Thaller C, & Noebels JL (2005). ADPEAF mutations reduce levels of secreted LGI1, a putative tumor suppressor protein linked to epilepsy. *Hum Mol Genet* **14**, 1613-1620.

Seoh SA, Sigg D, Papazian DM, & Bezanilla F (1996). Voltage-sensing residues in the S2 and S4 segments of the *Shaker* K^+ channel. *Neuron* **16**, 1159-1167.

Sewing S, Roeper J, & Pongs O (1996). Kvb1 subunit binding specific for *Shaker*-related potassium channel a subunits. *Neuron* **16**, 455-463.

Shamotienko OG, Parcej DN, & Dolly JO (1997). Subunit combinations defined for K+ channel Kv1 subtypes in synaptic membranes from bovine brain. *Biochem* **36**, 8195-8201.

Shen NV, Chen X, Boyer MM, & Pfaffinger PJ (1993). Deletion analysis of K^+ channel assembly. *Neuron* **11**, 67-76.

Shi G, Nakahira K, Hammond S, Rhodes KJ, Schechter LE, & Trimmer JS (1996). Beta subunits promote K+ channel surface expression through effects early in biosynthesis. *Neuron* **16**, 843-852.

Shimoda LA, Sylvester JT, & Sham JS (1998). Inhibition of voltage-gated K+ current in rat intrapulmonary arterial myocytes by endothelin-1. *Am J Physiol* **274**, L842-53.

Sigworth FJ (1994). Voltage gating of ion channels. *Quarterly Reviews of Biophysics* **27**, 1-40.

Sigworth FJ (2003). Structural biology: Life's transistors. *Nature* **423**, 21-22.

Simard C, Drolet B, Yang P, Kim RB, & Roden DM (2005). Polymorphism screening in the cardiac K+ channel gene KCNA5. *Clin Pharmacol Ther* **77**, 138-144.

Snyders DJ (1999). Structure and function of cardiac potassium channels. *Cardiovasc Res* **42**, 377-390.

Snyders DJ, Knoth KM, Roberds SL, & Tamkun MM (1992). Time-, voltage-, and state-dependent block by quinidine of a cloned human cardiac potassium channel. *Mol Pharmacol* **41**, 322-330.

Snyders DJ, Tamkun MM, & Bennett PB (1993). A rapidly activating and slowly inactivating potassium channel cloned from human heart. Functional analysis after stable mammalian cell culture expression. *J Gen Physiol* **101**, 513-543.

Sossin WS (1997). An autonomous kinase generated during long-term facilitation in Aplysia is related to the Ca(2+)-independent protein kinase C Apl II. *Learn Mem* **3**, 389-401.

Striano P, Busolin G, Santulli L, Leonardi E, Coppola A, Vitiello L, Rigon L, Michelucci R, Tosatto SC, Striano S, & Nobile C (2011). Familial temporal lobe epilepsy with psychic auras associated with a novel LGI1 mutation. *Neurology* **76**, 1173-1176.

Stuhmer W, Ruppersberg JP, Schroter KH, Sakmann B, Stocker M, Giese KP, Perschke A, Baumann A, & Pongs O (1989). Molecular basis of functional diversity of voltage-gated potassium channels in mammalian brain. *EMBO J* **8**, 3235-3244.

Svoboda LK, Reddie KG, Zhang L, Vesely ED, Williams ES, Schumacher SM, O'Connell RP, Shaw R, Day SM, Anumonwo JM, Carroll KS, & Martens JR (2012). Redox-sensitive sulfenic acid modification regulates surface expression of the cardiovascular voltage-gated potassium channel Kv1.5. *Circ Res* **111**, 842-853.

Swanson R, Marshall J, Smith JS, Williams JB, Boyle MB, Folander K, Luneau CJ, Antanavage J, Oliva C, Buhrow SA, Bennett C, Stein RB, & Kaczmarek LK (1990). Cloning and expression of cDNA and genomic clones encoding three delayed rectifier potassium channels in rat brain. *Neuron* **4**, 929-939.

Swartz KJ (2004). Towards a structural view of gating in potassium channels. *Nat Rev Neurosci* **5**, 905-916.

Takeishi Y, Jalili T, Ball NA, & Walsh RA (1999). Responses of cardiac protein kinase C isoforms to distinct pathological stimuli are differentially regulated. *Circ Res* **85**, 264-271.

Tamargo J, Caballero R, Gomez R, & Delpon E (2009). I(Kur)/Kv1.5 channel blockers for the treatment of atrial fibrillation. *Expert Opin Investig Drugs* **18**, 399-416.

Tamargo J, Caballero R, Gomez R, Valenzuela C, & Delpon E (2004). Pharmacology of cardiac potassium channels. *Cardiovasc Res* **62**, 9-33.

Tamkun MM, Knoth KM, Walbridge JA, Kroemer H, Roden DM, & Glover DM (1991). Molecular cloning and characterization of two voltage-gated K+ channel cDNAs from human ventricle. *FASEB J* **5**, 331-337.

Tao X, Lee A, Limapichat W, Dougherty DA, & MacKinnon R (2010). A gating charge transfer center in voltage sensors. *Science* **328**, 67-73.

Tessier S, Karczewski P, Krause EG, Pansard Y, Acar C, Lang-Lazdunski M, Mercadier JJ, & Hatem SN (1999). Regulation of the transient outward K(+) current by Ca(2+)/calmodulin-dependent protein kinases II in human atrial myocytes. *Circ Res* **85**, 810-819.

Thomas R, Favell K, Morante-Redolat J, Pool M, Kent C, Wright M, Daignault K, Ferraro GB, Montcalm S, Durocher Y, Fournier A, Perez-Tur J, & Barker PA (2010). LGI1 is a Nogo receptor 1 ligand that antagonizes myelin-based growth inhibition. *J Neurosci* **30**, 6607-6612.

Timpe LC & Fantl WJ (1994). Modulation of a voltage-activated potassium channel by peptide growth factor receptors. *J Neurosci* **14**, 1195-1201.

Tipparaju SM, Liu SQ, Barski OA, & Bhatnagar A (2007). NADPH binding to beta-subunit regulates inactivation of voltage-gated K(+) channels. *Biochem Biophys Res Commun* **359**, 269-276.

Tipparaju SM, Saxena N, Liu SQ, Kumar R, & Bhatnagar A (2005). Differential regulation of voltage-gated K+ channels by oxidized and reduced pyridine nucleotide coenzymes. *Am J Physiol Cell Physiol* **288**, C366-C376.

Tristani-Firouzi M, Chen J, & Sanguinetti MC (2002). Interactions between S4-S5 linker and S6 transmembrane domain modulate gating of HERG K+ channels. *J Biol Chem* **277**, 18994-19000.

Uebele VN, England SK, Gallagher DJ, Snyders DJ, Bennett PB, & Tamkun MM (1998). Distinct domains of the voltage-gated K^+ channel Kvb1.3 b-subunit affect voltage-dependent gating. *Am J Physiol* **274**, C1485-C1495.

Ullrich O, Reinsch S, Urbe S, Zerial M, & Parton RG (1996). Rab11 regulates recycling through the pericentriolar recycling endosome. *J Cell Biol* **135**, 913-924.

Valenzuela C (2003). Pharmacological electrical remodelling in human atria induced by chronic beta-blockade. *Cardiovasc Res* **58**, 498-500.

Valenzuela C, Delpon E, Franqueza L, Gay P, Perez O, Tamargo J, & Snyders DJ (1996). Class III antiarrhythmic effects of zatebradine. Time-, state-, use-, and voltage-dependent block of hKv1.5 channels. *Circulation* **94**, 562-570.

Valenzuela C, Delpon E, Franqueza L, Gay P, Snyders DJ, & Tamargo J (1997). Effects of ropivacaine on a potassium channel (hKv1.5) cloned from human ventricle. *Anesthesiol* **86**, 718-728.

Valenzuela C, Delpon E, Tamkun MM, Tamargo J, & Snyders DJ (1995a). Stereoselective block of a human cardiac potassium channel (Kv1.5) by bupivacaine enantiomers. *Biophys J* **69**, 418-427.

Valenzuela C, Snyders DJ, Bennett PB, Tamargo J, & Hondeghem LM (1995b). Stereoselective block of cardiac sodium channels by bupivacaine in guinea pig ventricular myocytes. *Circulation* **92**, 3014-3024.

Villalonga N, David M, Bielanska J, Gonzalez T, Parra D, Soler C, Comes N, Valenzuela C, & Felipe A (2010). Immunomodulatory effects of diclofenac in leukocytes through the targeting of Kv1.3 voltage-dependent potassium channels. *Biochem Pharmacol* **80**, 858-866.

Villalonga N, Martinez-Marmol R, Roura-Ferrer M, David M, Valenzuela C, Soler C, & Felipe A (2008). Cell cycle-dependent expression of Kv1.5 is involved in myoblast proliferation. *Biochim Biophys Acta* **1783**, 728-736.

Wadsworth SJ & Goldfine H (2002). Mobilization of protein kinase C in macrophages induced by Listeria monocytogenes affects its internalization and escape from the phagosome. *Infect Immun* **70**, 4650-4660.

Wang H, Zhang Y, Cao L, Han H, Wang J, Yang B, Nattel S, & Wang Z (2002). HERG K+ channel, a regulator of tumor cell apoptosis and proliferation. *Cancer Res* **62**, 4843-4848.

Wang J, Juhaszova M, Rubin LJ, & Yuan XJ (1997). Hypoxia inhibits gene expression of voltage-gated K+ channel alpha subunits in pulmonary artery smooth muscle cells. *J Clin Invest* **100**, 2347-2353.

Wang Z, Fermini B, & Nattel S (1993). Sustained depolarization-induced outward current in human atrial myocytes. Evidence for a novel delayed rectifier K^+ current similar to Kv1.5 cloned channel currents. *Circ Res* **73**, 1061-1076.

Wang Z, Fermini B, & Nattel S (1995). Effects of flecainide, quinidine, and 4-aminopyridine on transient outward and ultrarapid delayed rectifier currents in human atrial myocytes. *J Pharmacol Exp Ther* **272**, 184-196.

Wang Z, Kiehn J, Yang Q, Brown AM, & Wible BA (1996). Comparison of binding and block produced by alternatively spliced Kvbeta1 subunits. *J Biol Chem* **271**, 28311-28317.

Weng J, Cao Y, Moss N, & Zhou M (2006). Modulation of voltage-dependent Shaker family potassium channels by an aldo-keto reductase. *J Biol Chem* **281**, 15194-15200.

Wickenden A (2002a). K(+) channels as therapeutic drug targets. *Pharmacol Ther* **94**, 157-182.

Wickenden AD (2002b). Potassium channels as anti-epileptic drug targets. *Neuropharmacology* **43**, 1055-1060.

Williams CP, Hu N, Shen W, Mashburn AB, & Murray KT (2002). Modulation of the human Kv1.5 channel by protein kinase C activation: role of the Kvbeta1.2 subunit. *J Pharmacol Exp Ther* **302**, 545-550.

Woodard GE, Lopez JJ, Jardin I, Salido GM, & Rosado JA (2010). TRPC3 Regulates Agonist-stimulated Ca2 Mobilization by Mediating the Interaction between Type I Inositol 1,4,5-Trisphosphate Receptor, RACK1, and Orai1. *J Biol Chem* **285**, 8045-8053.

Workman AJ, Kane KA, Russell JA, Norrie J, & Rankin AC (2003). Chronic beta-adrenoceptor blockade and human atrial cell electrophysiology: evidence of pharmacological remodelling. *Cardiovasc Res* **58**, 518-525.

Wulff H, Calabresi PA, Allie R, Yun S, Pennington M, Beeton C, & Chandy KG (2003). The voltage-gated Kv1.3 K(+) channel in effector memory T cells as new target for MS. *J Clin Invest* **111**, 1703-1713.

Xu J, Yu W, Wright JM, Raab RW, & Li M (1998). Distinct functional stoichiometry of potassium channel beta subunits. *Proc Natl Acad Sci U S A* **95**, 1846-1851.

Yang Y, Li J, Lin X, Yang Y, Hong K, Wang L, Liu J, Li L, Yan D, Liang D, Xiao J, Jin H, Wu J, Zhang Y, & Chen YH (2009). Novel KCNA5 loss-of-function mutations responsible for atrial fibrillation. *J Hum Genet* **54**, 277-283.

Yellen G (2002). The voltage-gated potassium channels and their relatives. *Nature* **419**, 35-42.

Yeola SW, Rich TC, Uebele VN, Tamkun MM, & Snyders DJ (1996). Molecular analysis of a binding site for quinidine in a human cardiac delayed rectifier K^+ channel. Role of S6 in antiarrhythmic drug binding. *Circ Res* **78**, 1105-1114.

Young LH, Balin BJ, & Weis MT (2005). Go 6983: a fast acting protein kinase C inhibitor that attenuates myocardial ischemia/reperfusion injury. *Cardiovasc Drug Rev* **23**, 255-272.

Yu FH, Yarov-Yarovoy V, Gutman GA, & Catterall WA (2005). Overview of molecular relationships in the voltage-gated ion channel superfamily. *Pharmacol Rev* **57**, 387-395.

Yu W, Xu J, & Li M (1996). NAB domain is essential for the subunit assembly of both a-a and a-b complexes of shaker-like potassium channels. *Neuron* **16**, 441-453.

Zadeh AD, Xu H, Loewen ME, Noble GP, Steele DF, & Fedida D (2008). Internalized Kv1.5 traffics via Rab-dependent pathways. *J Physiol* **586**, 4793-4813.

Zadran S, Standley S, Wong K, Otiniano E, Amighi A, & Baudry M (2012). Fluorescence resonance energy transfer (FRET)-based biosensors: visualizing cellular dynamics and bioenergetics. *Appl Microbiol Biotechnol* **96**, 895-902.

Zagotta WN, Hoshi T, & Aldrich RW (1989). Gating of single Shaker potassium channels in Drosophila muscle and in Xenopus oocytes injected with Shaker mRNA. *Proc Natl Acad Sci U S A* **86**, 7243-7247.

Zhang L, Foster K, Li Q, & Martens JR (2007). S-acylation Regulates Kv1.5 Channel Surface Expression. *Am J Physiol Cell Physiol*.

Zhang X, Anderson JW, & Fedida D (1997). Characterization of nifedipine block of the human heart delayed rectifier, hKv1.5. *J Pharmacol Exp Ther* **281**, 1247-1256.

Zhang Y, Helm JS, Senatore A, Spafford JD, Kaczmarek LK, & Jonas EA (2008). PKC-induced intracellular trafficking of Ca(V)2 precedes its rapid recruitment to the plasma membrane. *J Neurosci* **28**, 2601-2612.

Zhao YJ, Wang J, Rubin LJ, & Yuan XJ (1997). Inhibition of K(V) and K(Ca) channels antagonizes NO-induced relaxation in pulmonary artery. *Am J Physiol* **272**, H904-12.

Zhou Y & MacKinnon R (2003). The occupancy of ions in the K+ selectivity filter: charge balance and coupling of ion binding to a protein conformational change underlie high conduction rates. *J Mol Biol* **333**, 965-975.

Zhou Y, Morais-Cabral JH, Kaufman A, & MacKinnon R (2001). Chemistry of ion coordination and hydration revealed by a K+ channel-Fab complex at 2.0 A resolution. *Nature* **414**, 43-48.

8. APPENDIX 1: SUPPLEMENTAL MATERIAL

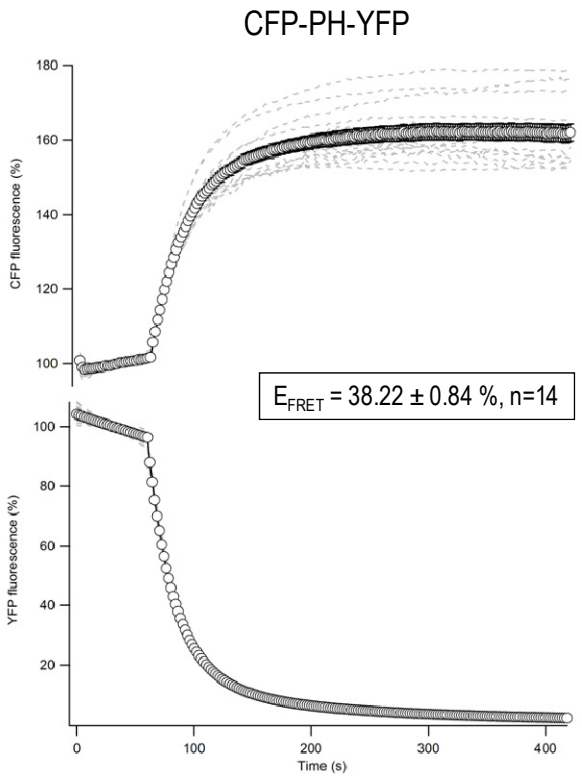

Figure S1: Determination of donor fluorescence recovery during disruption of energy transfer by selective acceptor photobleaching in the CFP-PH-YFP tandem construction. Transiently transfected HEK293 cells were imaged for CFP-PH-YFP tandem construction as indicated in Methods. Shown are the relative increases in CFP intensities (in percentages) over initial levels and the remaining fluorescence intensity of YFP. The symbols represent the calculated mean ± SEM, whereas the thin dotted lines correspond to single cell traces.

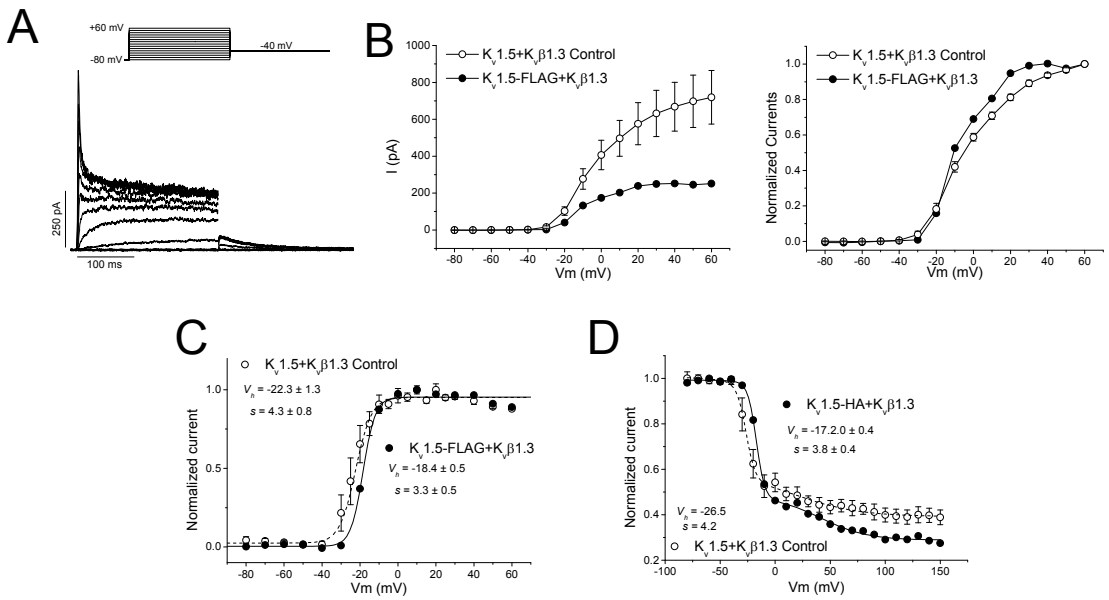

Figure S2: FLAG label in S1-S2 extracellular loop of the channel does not modify the electrophysiological properties of K_V1.5-K_Vβ1.3 construction. **A**, Representatives traces recorded after transfection of the K_V1.5-FLAG+K_Vβ1.3 construction and applying the pulse protocol showed at the top of the panel. **B,** IV relationship of the construction, in comparison with 'wild type' channels, before (*left side*) and after (*right side*) normalization by +60 mV value. **C,** Activation curves of 'wild type' channels and the construction. **D,** Inactivation curves of 'wild type' channels and the construction.

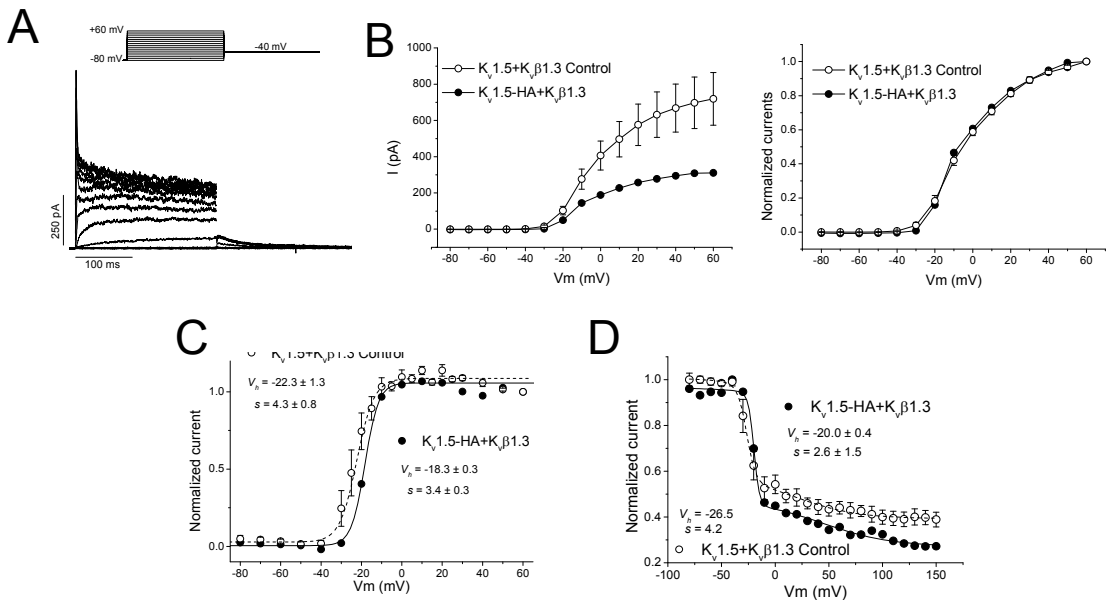

Figure S3: HA label in S1-S2 extracellular loop of the channel does not modify the electrophysiological properties of K_v1.5-K_vβ1.3 construction. **A,** Representatives traces recorded after transfection of the K_v1.5-HA+K_vβ1.3 construction and applying the pulse protocol showed at the top of the panel. **B,** IV relationship of the construction, in comparison with 'wild type' channels, before (*left side*) and after (*right side*) normalization by +60 mV value. **C,** Activation curves of 'wild type' channels and the construction. **D,** Inactivation curves of 'wild type' channels and the construction.

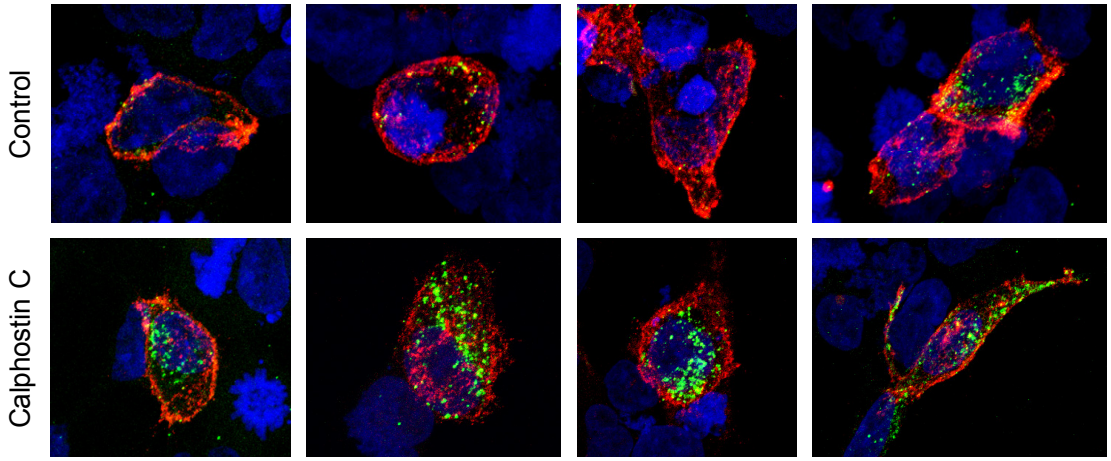

Figure S4: PKC inhibition increase the amount of cannel internalized in the inner part of the cell. Maximum Projections of the cells showed in Figure 28 in control conditions (*upper panels*) and after PKC inhibition by calphostin C treatment (*bottom panels*). It is important to highlight that in this particular case the difference in the intensity of signal in plasma membrane channels (red signal) is not so clear due to the process of the image formation. However, thanks to the 'reconstruction' of the cell, the difference between both conditions regarding the amount of channel internalized is more patent.

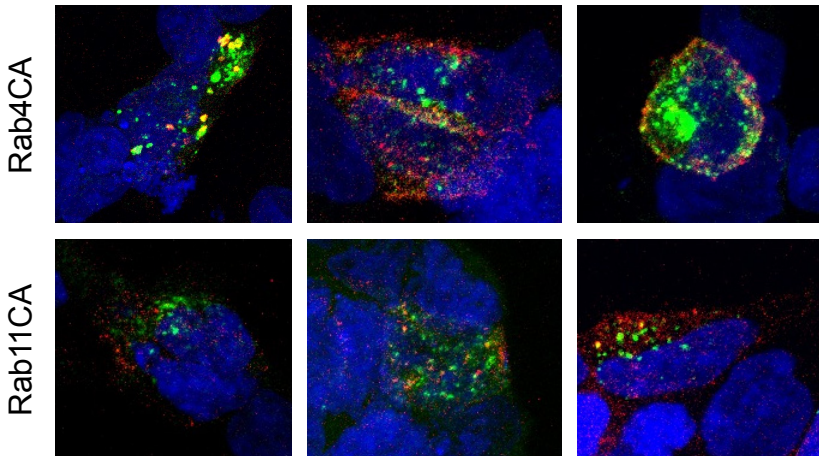

Figure S5: The cotransfection of K_v1.5-K_vβ1.3 with Rab11CA abolishes the increase of the internalization PKC inhibition-mediated. Maximum Projections of the cells showed in Figure 30 after cotransfection of K_v1.5-K_vβ1.3 channels with Rab4CA (*upper panels*) and with Rab11CA (*bottom panels*), after calphostin C treatment. Note that only in the presence of Rab11CA, the amount of channel internalized (green color) (*bottom*) after calphostin C treatment is decreased in comparison with that cell cotransfected with K_v1.5-HA+K_vβ1.3+Rab4CA (*top*) or those cotransfected with K_v1.5-HA+K_vβ1.3 channels (at *bottom of Figure 28*). The amount of channel present in plasma membrane is shown in red color.

9. APPENDIX 2: PUBLICATIONS

9.1 ORIGINAL PAPERS

Celecoxib blocks cardiac $K_v1.5$, $K_v4.3$ and $K_v7.1$ (KCNQ1) channels: effects on cardiac action potentials.

Macías A*, Moreno C*, Moral-Sanz J, Cogolludo A, David M, Alemanni M, Pérez-Vizcaíno F, Zaza A, Valenzuela C, González T. (*Both authors contributed equally to this work).

Abstract: Celecoxib is a COX-2 inhibitor that has been related to an increased cardiovascular risk and that exerts several actions on different targets. The aim of this study was to analyze the effects of this drug on human cardiac voltage-gated potassium channels (K_v) involved on cardiac repolarization $K_v1.5$ (I_{Kur}), $K_v4.3$+KChIP2 (I_{to1}) and $K_v7.1$+KCNE1 (I_{Ks}) and to compare with another COX-2 inhibitor, rofecoxib. Currents were recorded in transfected mammalian cells by whole-cell patch-clamp. Celecoxib blocked all the K_v channels analyzed and rofecoxib was always less potent, except on $K_v4.3$+KChIP2 channels. $K_v1.5$ block increased in the voltage range of channel activation, decreasing at potentials positive to 0 mV. The drug modified the activation curve of the channels that became biphasic. Block was frequency-dependent, increasing at fastest frequencies. Celecoxib effects were not altered by TEA_{out} in R487Y mutant $K_v1.5$ channels but the kinetics of block was slower and the degree of block was smaller with TEA_{in}, indicating that celecoxib acts from the cytosolic side. We confirmed the blocking properties of celecoxib on native K_v currents from rat vascular cells, where $K_v1.5$ are the main contributors ($IC_{50} \approx 7$ μM). Finally, we demonstrate that celecoxib prolongs the action potential duration in mouse cardiac myocytes and shortens it in guinea pig cardiac myocytes, suggesting that K_v block induced by celecoxib may be of clinical relevance. **J Mol Cell Cardiol.** 2010 Dec; 49(6):984-92.

Irvalec inserts into the plasma membrane causing rapid loss of integrity and necrotic cell death in tumor cells.

Molina-Guijarro JM, **Macías Á**, García C, Muñoz E, García-Fernández LF, David M, Núñez L, Martínez-Leal JF, Moneo V, Cuevas C, Lillo MP, Villalobos Jorge C, Valenzuela C, Galmarini CM.

Abstract: Irvalec is a marine-derived antitumor agent currently undergoing phase II clinical trials. In vitro, Irvalec induces a rapid loss of membrane integrity in tumor cells, accompanied of a significant Ca^{2+} influx, perturbations of membrane conductivity, severe swelling and the formation of giant membranous vesicles. All these effects are not observed in Irvalec-resistant cells, or are significantly delayed by pretreating the cells with Zn^{2+}. Using fluorescent derivatives of Irvalec it was demonstrated that the compound rapidly interacts with the plasma membrane of tumor cells promoting lipid bilayer restructuration. Also, FRET experiments demonstrated that Irvalec molecules localize in the cell membrane close enough to each other as to suggest that the compound could self-organize, forming supramolecular structures that likely

trigger cell death by necrosis through the disruption of membrane integrity. **PLoS One.** 2011 Apr 27;6(4):e19042.

Ceramide inhibits K_v currents and contributes to TP-receptor-induced vasoconstriction in rat and human pulmonary arteries.

Moral-Sanz J, Gonzalez T, Menendez C, David M, Moreno L, **Macías A**, Cortijo J, Valenzuela C, Perez-Vizcaino F, Cogolludo A.

Abstract: Neutral sphingomyelinase (nSMase)-derived ceramide has been proposed as a mediator of hypoxic pulmonary vasoconstriction (HPV), a specific response of the pulmonary circulation. Voltage-gated K(+) (K_v) channels are modulated by numerous vasoactive factors, including hypoxia, and their inhibition has been involved in HPV. Herein, we have analyzed the effects of ceramide on K_v currents and contractility in rat pulmonary arteries (PA) and in mesenteric arteries (MA). The ceramide analog C6-ceramide inhibited K_v currents in PA smooth muscle cells (PASMC). Similar effects were obtained after the addition of bacterial sphingomyelinase (SMase), indicating a role for endogenous ceramide in K_v channel regulation. K_v current was reduced by stromatoxin and diphenylphosphine oxide-1 (DPO-1), selective inhibitors of K_v2.1 and K_v1.5 channels, respectively. The inhibitory effect of ceramide was still present in the presence of stromatoxin or DPO-1, suggesting that this sphingolipid inhibited both components of the native K_v current. Accordingly, ceramide inhibited K_v1.5 and K_v2.1 channels expressed in Ltk^- cells. Ceramide-induced effects were reduced in human embryonic kidney 293 cells expressing K_v1.5 channels but not the regulatory subunit $K_v\beta$2.1. The nSMase inhibitor GW4869 reduced the thromboxane-endoperoxide receptor agonist U46619-induced, but not endothelin-1-induced pulmonary vasoconstriction that was partly restored after addition of exogenous ceramide. The PKC-ζ pseudosubstrate inhibitor (PKCζ-PI) inhibited the K_v inhibitory and contractile effects of ceramide. In MA ceramide had no effect on K_v currents and GW4869 did not affect U46619-induced contraction. The effects of SMase were also observed in human PA. These results suggest that ceramide represents a crucial signaling mediator in the pulmonary vasculature. **Am J Physiol Cell Physiol.** 2011 Jul; 301(1):C186-94.

Protein kinase C (PKC) activity regulates functional effects of $K_v\beta1.3$ subunit on $K_v1.5$ channels: identification of a cardiac $K_v1.5$ *channelosome*.

David M*, **Macías Á***, Moreno C, Prieto Á, Martínez-Mármol R, Vicente R, González T, Felipe A, Tamkun MM, Valenzuela C. (*Both authors contributed equally to this work).

Abstract: $K_v1.5$ channels are the primary channels contributing to the ultrarapid outward potassium current (I_{Kur}). The regulatory $K_v\beta1.3$ subunit converts $K_v1.5$ channels from delayed rectifiers with a modest degree of slow inactivation to channels with both fast and slow inactivation components. Previous studies have shown that inhibition of PKC with calphostin C abolishes the fast inactivation induced by $K_v\beta1.3$. In this study, we investigated the mechanisms underlying this phenomenon using electrophysiological, biochemical, and confocal microscopy approaches. To achieve this, we used HEK293 cells (which lack $K_v\beta$ subunits) transiently cotransfected with $K_v1.5$+ $K_v\beta1.3$ and also rat ventricular and atrial tissue to study native α-β subunit interactions. Immunocytochemistry assays demonstrated that these channel subunits colocalize in control conditions and after calphostin C treatment. Moreover, coimmunoprecipitation studies showed that $K_v1.5$ and $K_v\beta1.3$ remain associated after PKC inhibition. After knocking down all PKC isoforms by siRNA or inhibiting PKC with calphostin C, $K_v\beta1.3$-induced fast inactivation at +60 mV was abolished. However, depolarization to +100 mV revealed $K_v\beta1.3$-induced inactivation, indicating that PKC inhibition causes a dramatic positive shift of the inactivation curve. Our results demonstrate that calphostin C-mediated abolishment of fast inactivation is not due to the dissociation of $K_v1.5$ and $K_v\beta1.3$. Finally, immunoprecipitation and immunocytochemistry experiments revealed an association between $K_v1.5$, $K_v\beta1.3$, the receptor for activated C kinase (RACK1), PKCβI, PKCβII, and PKCθ in HEK293 cells. A very similar $K_v1.5$ *channelosome* was found in rat ventricular tissue but not in atrial tissue. **J Biol Chem.** 2012 Jun 15; 287(25):21416-28.

Modulation of Voltage-Dependent and Inward Rectifier Potassium Channels by 15-Epi-Lipoxin-A_4 in Activated Murine Macrophages: Implications in Innate Immunity.

Cristina Moreno*, Patricia Prieto*, Álvaro Macías*, María Pimentel-Santillana*, Alicia de la Cruz, Paqui G. Través, Lisardo Boscá, and Carmen Valenzuela.

Potassium channels modulate macrophage physiology. Blockade of voltage-dependent potassium channels (K_v) by specific antagonists decreases macrophage cytokine production and inhibits proliferation. In the presence of aspirin, acetylated cyclooxygenase-2 loses the activity required to synthesize PGs but maintains the oxygenase activity to produce 15R-HETE from arachidonate. This intermediate product is transformed via 5-LOX into epimeric lipoxins, termed 15-epi-lipoxins (15-epi-lipoxin A4 [e-LXA4]). K_v have

been proposed as anti-inflammatory targets. Therefore, we studied the effects of e-LXA4 on signaling and on K_v and inward rectifier potassium channels (Kir) in mice bone marrow–derived macrophages (BMDM). Electrophysiological recordings were performed in these cells by the whole-cell patch-clamp technique. Treatment of BMDM with e-LXA4 inhibited LPS-dependent activation of NF-kB and IkB kinase b activity, protected against LPS activation–dependent apoptosis, and enhanced the accumulation of the Nrf-2 transcription factor. Moreover, treatment of LPS-stimulated BMDM with e-LXA4 resulted in a rapid decrease of K_v currents, compatible with attenuation of the inflammatory response. Long-term treatment of LPS-stimulated BMDM with e-LXA4 significantly reverted LPS effects on K_v and Kir currents. Under these conditions, e-LXA4 decreased the calcium influx versus that observed in LPS-stimulated BMDM. These effects were partially mediated via the lipoxin receptor (ALX), because they were significantly reverted by a selective ALX receptor antagonist. We provide evidence for a new mechanism by which e-LXA4 contributes to inflammation resolution, consisting of the reversion of LPS effects on K_v and Kir currents in macrophages. **The Journal of Immunology**, 2013 Dec 15;191(12):6136-46.

9.2 REVIEWS

K_v1.5-K_v beta interactions: molecular determinants and pharmacological consequences.

González T, David M, Moreno C, **Macías A**, Valenzuela C.

Abstract: K_v1.5 channels are homotetramers of alpha-pore subunits mainly present in human atrium and pulmonary vasculature. Thus, K_v1.5 is a pharmacological target for cardiovascular diseases. K_v beta 1.3 assemblies with K_v alpha 1.5 and modifies its gating and pharmacology. A further knowledge of alpha-beta interactions and pharmacology will lead a better design of new drugs. **Mini Rev Med Chem.** 2010 Jun; 10(7):635-42.

Effects of n-3 polyunsaturated fatty acids on cardiac ion channels.

Moreno C, **Macías A**, Prieto A, de la Cruz A, González T, Valenzuela C.

Abstract: Dietary n-3 polyunsaturated fatty acids (PUFAs) have been reported to exhibit antiarrhythmic properties, and these effects have been attributed to their capability to modulate ion channels. In the present review, we will focus on the effects of PUFAs on a cardiac sodium channel (Na_v1.5) and two potassium channels involved in cardiac atrial and ventricular repolarization (K_v) (K_v1.5 and K_v11.1). n-3

PUFAs of marine (docosahexaenoic, DHA and eicosapentaenoic acid, EPA) and plant origin (alpha-linolenic acid, ALA) block $K_v1.5$ and $K_v11.1$ channels at physiological concentrations. Moreover, DHA and EPA decrease the expression levels of $K_v1.5$, whereas ALA does not. DHA and EPA also decrease the magnitude of the currents elicited by the activation of $Na_v1.5$ and calcium channels. These effects on sodium and calcium channels should theoretically shorten the cardiac action potential duration (APD), whereas the blocking actions of n-3 PUFAs on K_v channels would be expected to produce a lengthening of cardiac action potential. Indeed, the effects of n-3 PUFAs on the cardiac APD and, therefore, on cardiac arrhythmias vary depending on the method of application, the animal model, and the underlying cardiac pathology. **Front Physiol**. 2012 Jul 9; 3:245.

Polyunsaturated Fatty acids modify the gating of K_v channels.

Moreno C, **Macías A**, Prieto A, De La Cruz A, Valenzuela C.

Abstract: Polyunsaturated fatty acids (PUFAs) have been reported to exhibit antiarrhythmic properties, which are attributed to their capability to modulate ion channels. This PUFAs ability has been reported to be due to their effects on the gating properties of ion channels. In the present review, we will focus on the role of PUFAs on the gating of two K_v channels, $K_v1.5$ and $K_v11.1$. $K_v1.5$ channels are blocked by n-3 PUFAs of marine [docosahexaenoic acid (DHA) and eicosapentaenoic acid] and plant origin (alpha-linolenic acid, ALA) at physiological concentrations. The blockade of $K_v1.5$ channels by PUFAs steeply increased in the range of membrane potentials coinciding with those of $K_v1.5$ channel activation, suggesting that PUFAs-channel binding may derive a significant fraction of its voltage sensitivity through the coupling to channel gating. A similar shift in the activation voltage was noted for the effects of n-6 arachidonic acid (AA) and DHA on $K_v1.1$, $K_v1.2$, and $K_v11.1$ channels. PUFAs- $K_v1.5$ channel interaction is time-dependent, producing a fast decay of the current upon depolarization. Thus, $K_v1.5$ channel opening is a prerequisite for the PUFA-channel interaction. Similar to the $K_v1.5$ channels, the blockade of $K_v11.1$ channels by AA and DHA steeply increased in the range of membrane potentials that coincided with the range of $K_v11.1$ channel activation, suggesting that the PUFAs- K_v channel interactions are also coupled to channel gating. Furthermore, AA regulates the inactivation process in other K_v channels, introducing a fast voltage-dependent inactivation in non-inactivating K_v channels. These results have been explained within the framework that AA closes voltage-dependent potassium channels by inducing conformational changes in the selectivity filter, suggesting that K_v channel gating is lipid dependent. **Front Pharmacol.** 2012 Sep 10; 3:163.

Stereoselective interactions between local anesthetics and ion channels.

Valenzuela C, Moreno C, de la Cruz A, **Macías Á**, Prieto Á, González T.

Abstract: Local anesthetics are useful probes of ion channel function and structure. Stereoselective interactions are especially interesting because they can reveal three-dimensional relationships between drugs and channels with otherwise identical biophysical and physicochemical properties. Furthermore, stereoselectivity suggests direct and specific receptor-mediated action, and identification of such stereospecific interactions may have important clinical consequences. The fact that drug targets are able to discriminate between the enantiomers present in a racemic drug is the consequence of the ordered asymmetric macromolecular units that form living cells. However, almost 25% of the drugs used in the clinical practice are racemic mixtures, and their individual enantiomers frequently differ in both their pharmacodynamic and pharmacokinetic profiles. Moreover, their effects can be similar to or different from the pharmacological effect of the drug and may contribute to the undesired effects of the drug. In other cases, the pharmacological effects induced by the two enantiomers on the molecular target are opposite. In the present manuscript, we will review the stereoselective effects of bupivacaine-like local anesthetics on cardiac sodium and potassium channels. **Chirality.** 2012 Nov;24(11):944-50.

9.2 PUBLICATIONS IN PROGRESS

PKC inhibition results in a K_v1.5-K_vβ1.3 pharmacology closer to K_v1.5 channels.

A Macías, A de la Cruz, A Prieto, MM Tamkun, T González, C Valenzuela.

Abstract: **Background and purpose:** The K_vβ1.3 subunit modifies the gating and pharmacology of K_v1.5 channels in a protein kinase C (PKC)-dependent manner, decreasing their sensitivity to drug-mediated blockade. Cardiac K_v1.5 channels associate with RACK1, the K_vβ1.3 subunit and different PKC isoforms, resulting in the formation of a functional *channelosome*. The aim of the present study was to investigate the pharmacological consequences of PKC inhibition in K_v1.5-K_vβ1.3 channels analysing the effects of bupivacaine and quinidine. **Experimental approach**: HEK293 cells were transfected with K_v1.5-K_vβ1.3 channels, and currents were recorded using the whole-cell configuration of the patch-clamp technique. PKC inhibition was achieved by incubating the cells with calphostin C, and the effects of bupivacaine and quinidine were analysed. **Key results**: The effects on the voltage dependent inactivation of K_v1.5-K_vβ1.3 channels and their pharmacological behaviour after PKC inhibition were similar to that displayed by K_v1.5 channels alone. Indeed, the IC_{50} values for bupivacaine were similar in both cases (21.8 and 13.1 μM). Similar results were also observed in the presence of quinidine. **Conclusions and Implications:** These

results suggest that competition for a common binding site between the $K_v\beta1.3$ subunit and both drugs is phosphorylation dependent, which may have clinical relevance in diseases that are characterised by alterations in kinase activity. **British Journal of Pharmacology** (under review).

Tumor cells resistant to the marine-derived drug Irvalec present a distinctive pattern of lipid composition in their plasma membrane

José M. Molina-Guijarro, **Álvaro Macías**, Carolina García, Luis F. García-Fernández, Cristina Moreno, Juan F. Martínez-Leal, Carmen Cuevas, M. Pilar Lillo, Carmen Valenzuela and Carlos M. Galmarini.

Abstract: Irvalec is a marine derived synthetic depsipeptide showing cytotoxic activity against a wide diversity of tumor cells both *in vitro* and *in vivo*. The existing data on the mechanism of action of Irvalec indicate that the compound inserts and self-organize in the plasma membrane of tumor cells, rapidly inducing loss of membrane integrity and cell permeabilization, giving rise to a fast and dramatic necrotic death. By continuous exposure of human colon carcinoma HCT-116 cells to stepwise increasing concentrations of Irvalec, a resistant subclone of the cell line was established (HCT-116-Irv). In dose-response cytotoxicity assays, HCT-116-Irv cells showed an IC_{50} value >100 μM. The resistant cells did not show any of the morphological and physiological responses to Irvalec observed in parental cells. Due to the direct effect of Irvalec on the cell membrane, we searched for possible changes in the lipid composition of the resistant cells. After fractionation of the lipid extracts using thin layer cromatography (TLC), two differential fractions that were almost completely absent in the resistant cells as compared to wt cells, were identified and purified. Interestingly, one of these fractions was able to interact with a biotinylated derivative of Irvalec in a standard overlay assay. These results indicated that the lipid composition could be directly related to the sensitivity of tumor cells to Irvalec, suggesting that this selected lipid fraction exherts a crucial putative biological role mediating the cytotoxic response to Irvalec.

Protein kinase C inhibition reduces the slow K_v1.5 recycling Rab11-mediated.

A Macías, A de la Cruz, A Prieto, T González, C Valenzuela.

Abstract: The activation of voltage gated potassium channels K_v1.5 generates the Ikur current with slow inactivation. The regulatory K_vβ1.3 subunit converts K_v1.5 channels from delayed rectifiers with a modest degree of slow inactivation to channels with both fast and slow inactivation components in a protein kinase C (PKC)-dependent manner. Previous studies have shown that inhibition of PKC not only abolishes the fast inactivation induced by K_vβ1.3, but also decreases the magnitude of the current of K_v1.5-K_vβ1.3 channels. In this study we investigated the mechanisms underlying this last phenomenon using electrophysiological, biochemical, live cell imaging and confocal microscopy approaches. The PKC inhibition by calphostin C 3μM for 2 h. results in a decrease of 32.6±7.1% of the number of channels in the cell surface due to an increase of them in the inner part of the cell at the end of the treatment. Live cells imaging approaches suggest that after this treatment the mobility of the K_v1.5-K_vβ1.3 channels is completely abolished and this generates an accumulation of the channels into the cells because the channels are able to go in but not to go recycling to the plasma membrane. However, the electrophysiological experiments using Rab11CA increase the magnitude of the current with a similar degree of inactivation similar to that previously described. These results suggest that the slow trafficking regulation of K_v1.5-K_vβ1.3 channels is phosphorylation dependent, and along with its described effect in their pharmacology could results clinically relevant mainly in the diseases characterised by alterations in kinase activity.